

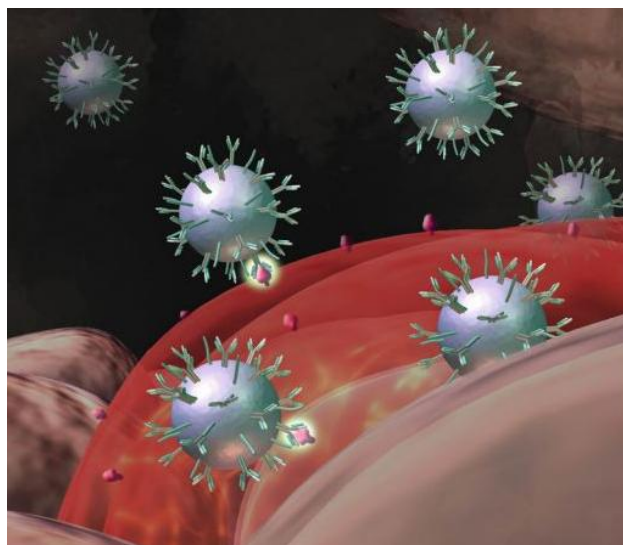
Università degli Studi del Piemonte Orientale
“Amedeo Avogadro”

Dipartimento di Scienze del Farmaco

Dottorato di Ricerca in Biotecnologie Farmaceutiche ed Alimentari

XXVII ciclo A.A. 2011-2014

**STUDY OF STRATEGIES FOR INCREASING
BIOCOMPATIBILITY AND EFFECTIVENESS OF
POLYETHYLENIMINE CARRIERS FOR GENE
THERAPY**



Elena Nicolì

Università degli Studi del Piemonte Orientale
“Amedeo Avogadro”

Dipartimento di Scienze del Farmaco

Dottorato di Ricerca in Biotecnologie Farmaceutiche ed Alimentari

XXVII ciclo A.A. 2011-2014

**STUDY OF STRATEGIES FOR INCREASING
BIOCOMPATIBILITY AND EFFECTIVENESS OF
POLYETHYLENIMINE CARRIER FOR GENE
THERAPY**

Elena Nicolì

Supervised by Prof. Michela Bosetti

Prof. V. Prasad Shastri

PhD program coordinator Prof Menico Rizzi

To my Family

Contents

1	Introduction	1
1.1	Nanomedicine	1
1.1.1	Definition and challenges	1
1.1.2	Nanomedicine for therapeutic application	2
1.1.3	Active and passive targeting.....	4
1.1.4	Nanomedicine in Tissue Engineering.....	6
1.2	Drug delivery strategies	9
1.2.1	Impact of physical properties of nanoparticles.....	10
1.3	Gene therapy	12
1.3.1	RNAi mechanism.	12
1.4	Gene delivery strategies.....	15
1.4.1	Viral delivery.....	15
1.4.2	Non-viral delivery	18
1.5	Non-viral delivery materials for gene therapy	20
1.5.1	Physical methods	20
1.5.2	Chemical methods	22
1.5.3	Challenges of non-viral gene delivery.....	25
1.5.4	Endocytosis mechanisms.....	27
1.6	Polyethylenimine and toxicity issues.....	29
1.7	Active targeting: the potential of albumin.	31
1.8	References.....	33
2	Outline of the Thesis	40
3	The genotoxicity of PEI-based nanoparticles is reduced by acetylation of PEI amines in human primary cells	44

Table of Contents

3.1	Summary.....	44
3.2	Introduction.....	45
3.3	Materials and Methods	47
3.4	Results.....	55
3.5	Discussion and conclusion.....	71
3.6	References.....	75
4	Enhanced gene silencing through human serum albumin-mediated delivery of polyethylenimine-siRNA polyplexes	79
4.1	Summary.....	79
4.2	Introduction.....	80
4.3	Materials and Methods	82
4.4	Results and discussion	88
4.5	Conclusion	105
4.6	References.....	106
5	Biocompatible cationic nanoparticles for gene delivery in bone tissue engineering: uptake trafficking, localization and activity in human primary osteoblasts.....	110
5.1	Summary.....	110
5.2	Introduction.....	111
5.3	Materials and methods.....	113
5.4	Results.....	122
5.5	References.....	137
6	Conclusions	140
	List of publications	147
	Acknowledgements.....	150

Table of Contents

1 Introduction

1.1 Nanomedicine

1.1.1 Definition and challenges

Nanotechnology is the branch of science that investigates the potential of materials in nanometre range of size. The specific definition was given in 2000 by the National Nanotechnology Initiative: “Nanotechnology is concerned with materials and systems whose structures and components exhibit novel and significantly improved physical, chemical and biological properties, phenomena and processes due to their nanoscale size” [1].

Nanotechnology applied for medical purposes takes the name of “Nanomedicine”. Nano-scale devices for treatment, diagnosis, monitoring and control of biological system have been referred as “Nanomedicine” by the National Institute of Health [2]. Nanomedicine aspires to develop nanoscale systems, from a few atoms to sub-cellular size (1-1000 nm), that can reach high level of cell targeting, with minimal impact on cell viability [1]. Applications of Nanomedicine are summarized in Figure 1.

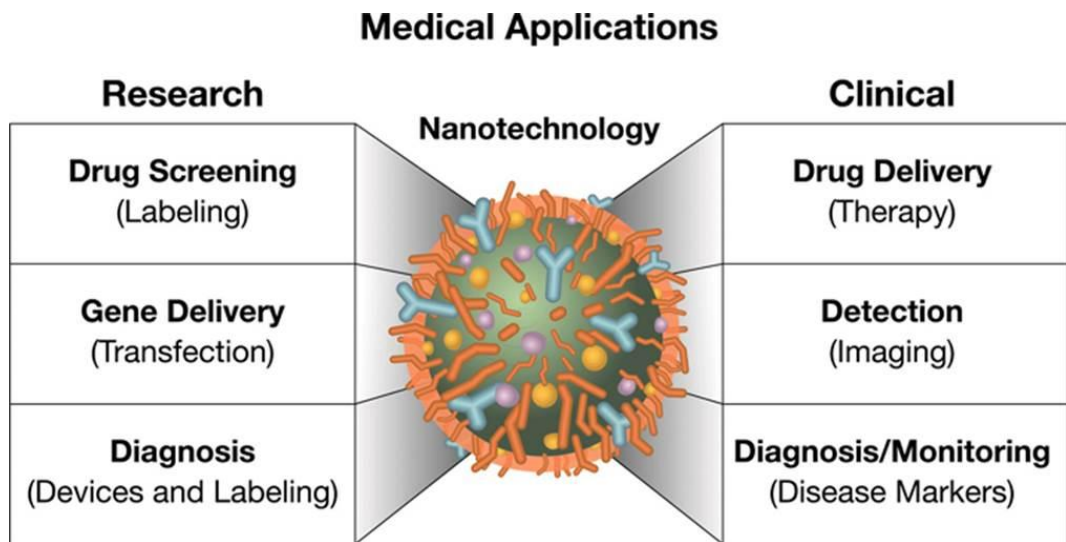


Figure 1. Research and clinical approaches of Nanomedicine.

1.1.2 Nanomedicine for therapeutic application

The successes of Nanomedicine are reported, for example, in the treatment of cancer. Cancer mortality counts more than 10 million new cases every year and in the past two years has decreased, owing to better understanding of tumor biology and improved diagnostic devices and treatments [3]. Ordinary cancer treatments include surgical intervention, radiation and chemotherapeutic drugs, and the higher limitations are due to low tumor specificity, low solubility and short circulation time of the drug. The concept of nanomedicine in therapeutic application is, thereby, closely related with drug-delivery. The design of an optimal nanocarrier, which ensures drug encapsulation, efficient cell targeting and intracellular drug release, has revolutionized the pharmaceutical field.

In the recent years a lot of efforts were employed to develop the perfect delivery carrier for individual therapeutic agents. Careful screening of the drug, interaction with the carrier, binding/dissociation properties and cell uptake/cytotoxicity are important issues to consider for obtaining a therapeutic effect. Furthermore, blood stability, tolerance from the immune system and extravasation to reach a target cell type are included in the multitask properties that a nanocarrier, for *in vivo* therapy, should possess (Figure 2).

Rational design of nanocarrier for cancer therapy	
What a nanocarrier should do	What a nanocarrier should be
Protect the drug from premature degradation	Be made from a material that is biocompatible, well characterized, and easily functionalized
Prevent drugs from prematurely interacting with the biological environment	Exhibit high differential uptake efficiency in the target cells over normal cells (or tissue)
Enhance absorption of the drugs into a selected tissue (for example, solid tumor)	Be either soluble or colloidal under aqueous conditions for increased effectiveness
Control the pharmacokinetic and drug tissue distribution profile	Have an extended circulating half-life
Improve intracellular penetration	Have a low rate of aggregation and a long shelf life

Figure 2. Physical and chemical properties for the design of an optimal drug-delivery agent [3].

1.1.3 Active and passive targeting

In cancer delivery, the specific drug accumulation is enhanced by the disorganized endothelial structure and increased permeability of the endothelial barrier, besides of the reduced lymphatic drainage. This passive tumor targeting has been defined as “Enhanced Permeability and Retention (EPR) effect”, discovered by Matsumura and Maeda [4]. Endothelial pores are reported to be in sizes varying from 10 to 1000 nm, depending on the type of tumor [5] and efficient vascular extravasation occurs with nanoparticles size profile lower than 400 nm [6].

Active targeting consists, instead, in conjugating the nanoparticles with a specific molecule able to target a specific tissue and cell type. Proteins, peptides, monoclonal antibodies, small molecules, aptamers can be used to target a specific cell type [7]. Most of tumors up-regulates the expression of specific receptors to cope with the higher proliferation of malignant cells. Nowadays, the more studied over-expressed surface molecules are transferrin receptor, folate receptor, specific glycoproteins and the epidermal growth factor receptor (EGFR). Transferrin transports iron to the cells and folic acid is important for nucleotides synthesis. Several lectins have been found to specifically interact with glycoproteins expressed on cancer cells, and EGF is involved in proliferation, angiogenesis and metastasis [6]. Targeting tumor vasculature, through specific endothelial receptors, it is also possible to inhibit tumor-induced angiogenesis. The vascular endothelial growth factor receptors VEGFR-1 and VEGFR-2 are over-expressed on tumor endothelium, like $\alpha v\beta 3$ integrin is highly expressed on neo-vascular endothelial cells [6][8].

Therefore, the possibility to target tumors based on the different pattern/expression of specific molecules on the cell surface is becoming extremely promising. PLGA nanoparticles, modified with isopropyl myristate moieties, showed increased delivery of chemotherapeutic Paclitaxel to the lung and superior in vitro effectiveness [9].

Furthermore, the development of nanoparticles carrying transferrin and/or transferrin antibodies [10][11] and nanoparticles linked with arginine-glycine-aspartic acid (RGD) sequence, to target the $\alpha v \beta 3$ integrin, demonstrated their efficiency *in vivo* [12][13]. Figure 3 represents passive and active targeting in tumor microenvironment.

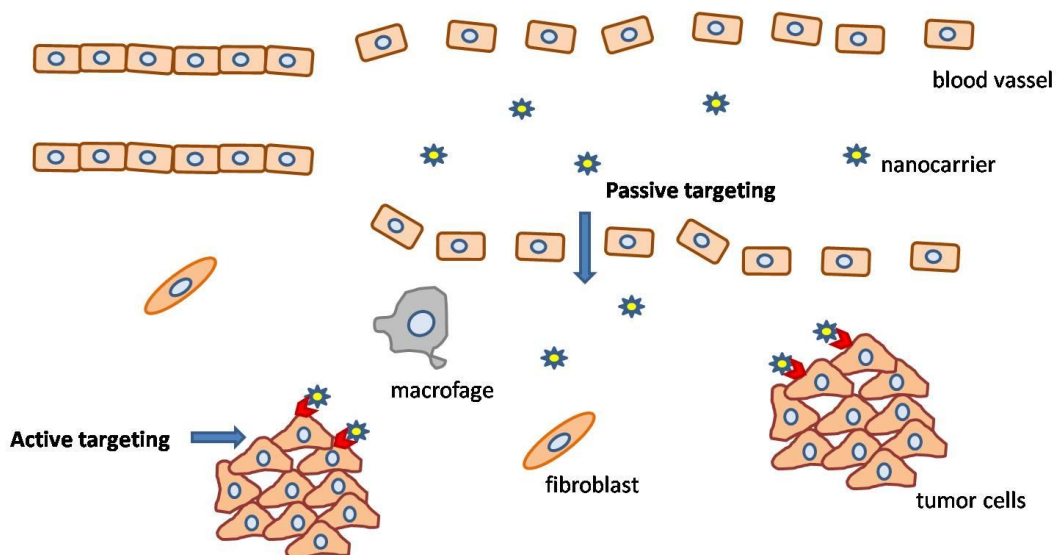


Figure 3. Representative chart of the role of endothelial fenestration in enhancing passive transportation in the tumor microenvironment and the role of tumor targeting molecules in developing selective nanocarriers.

1.1.4 Nanomedicine in Tissue Engineering

Nowadays, Nanomedicine is not only limited for therapeutic application, but offers also opportunities in regenerative medicine. The increased understanding of cell response to extracellular signals and the intracellular pathways involved in cell survival, proliferation and differentiation, inspired regenerative medicine strategies, with the aim to replicate biological instructions expressed during embryogenesis. Growth factors are the signaling molecules that instruct cells during tissue development, which can be studied to achieve tissue regeneration in adults. Encapsulation and controlled delivery of these factors may potentially activate specific proliferation/differentiation pathways to regenerate tissues [14][15].

Considering in details **bone regeneration**, traditional treatment methods for promoting bone healing include bone grafts or synthetic materials, to fill the defect and provide structural support. Bone autografts are considered the gold standard for treating bone defects, owing to the low risk of an adverse immune response, osteoinductive, osteoconductive, and osteogenic properties [16].

Recently, several growth factors have been discovered to play a role in bone regeneration, directly acting on osteoblasts, which produce mineralized bone matrix. Growth factors delivery by nanocarriers is promising for overcoming the actual disadvantages with conventional scaffold implantation, like immunogenicity, low growth factors expression and low cell proliferation. Furthermore, a nano-delivery system offer major control and longer-term release of the growth factor, compared to the direct adsorption on the surface of implanted scaffolds [17] [14].

Osteoblast commitment from pluripotent mesenchymal stem cells is mainly regulated by the growth factor family of TGF- β , with the demonstrated activity *in vitro* and *in vivo* of bone morphogenetic proteins (BMPs), especially BMP-2 and BMP-4, in

guiding the differentiation process [18][19]. Besides, a number of other growth factors are being investigated for their potential to regenerate bone, including platelet-rich plasma (PRP), platelet-derived growth factor (PDGF), vascular endothelial growth factor (VEGF), and fibroblast growth factor (FGF) [17].

Osteoblast commitment involves the expression of phase-specific genes, which are important to evaluate the response of an “osteogenic treatment”. Collagen type I (COL1) is expressed in the early stage of osteoblast differentiation and is the main structural component of bone matrix. Osteopontin (OPN), a non-collagenous matrix protein, and alkaline phosphatase (ALP) are important in stabilizing the matrix in formation, and are considered early markers of osteoblasts maturation. In the late stage of differentiation, osteocalcin (OC) expression is up-regulated [16][20].

Bone formation is a physiological balance between bone synthesis and bone resorption. Differentiated osteoblasts produce and release the cytokine RANKL, member of the Tumor Necrosis Factor (TNF) superfamily, that induce osteoclast differentiation and fusion of pre-osteoclasts [21] [22]. Therefore the activation of RANKL, in response to delivery agents, should be considered in order to induce effective osteogenesis.

The differentiation process of osteoblasts can be divided in four stages (Figure 4):

Proliferation phase: In this phase, genes required for proliferation (c-fos) and progression of the cell cycle (cyclins, histones) are expressed, together with genes associated with the biosynthesis of the extracellular matrix (COL1, TGF β) and cell adhesion proteins (fibronectin).

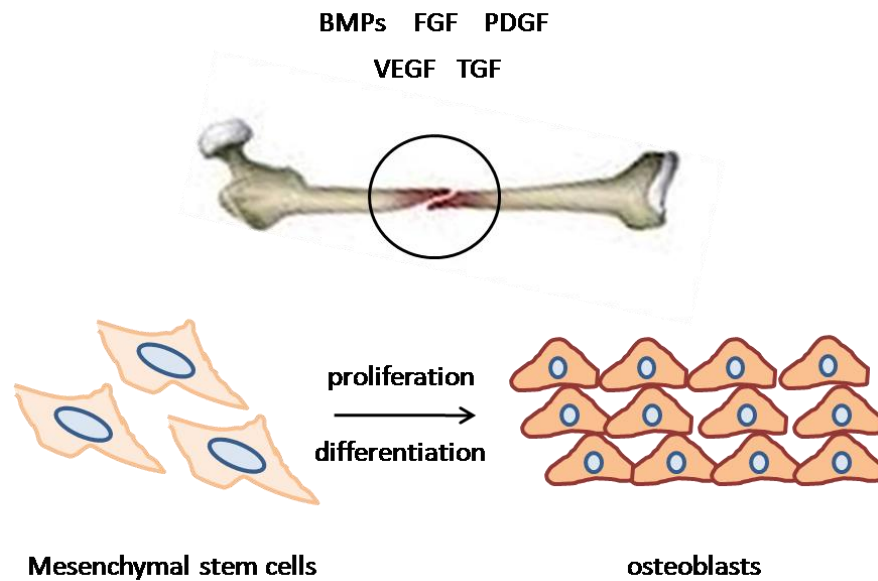
Matrix-maturation phase: In this phase the expression of genes involved in the maturation and organization of the bone extracellular matrix (alkaline phosphatase) are up-regulated. The role of alkaline phosphatase (ALP) is still uncertain, but since

this enzyme cleaves phosphate groups from monophosphate-ester substrates, it is assumed that the enzyme is involved in bone mineralization.

Mineralization phase. In this phase, the expression of genes associated with the organized deposition of hydroxyapatite (osteopontin and osteocalcin) is up-regulated.

Apoptosis phase. In this phase were observed an increased COL1 and collagenase gene expression, apoptotic cell death and compensatory proliferative activity [20].

A



B

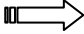
Proliferation	Differentiation	
Proliferation phase	Matrix maturation phase	Mineralization phase
↑ COL1 ↑ OPN	↑ ALP	↑ OP ↑ OC
 Days of culture		

Figure 4. Bone regeneration. A) Proliferation of mesenchymal stem cell (MSC) and differentiation to osteoblast lineage by the use of specific growth factors. B) Progressive stages of osteoblast differentiation with the increase in the expression or activity of phase specific markers.

1.2 Drug delivery strategies

Nowadays, the most used drug delivery strategies are lipids, inorganic materials, proteins and polymers, which can be strategically combined to obtain an optimal delivery agent.

Lipids, due to their dynamic nature are easily modifiable for cell targeting, because their dynamic nature allows clustering of peptides or other ligands. However, their dynamic nature reduces the stability of the system.

Inorganic materials (gold, carbon, and iron oxide) provide the advantage of stability; but the strength causes retention in the body and limited clinical application.

Polymers offer enhanced biocompatibility and major control of drug release. Biodegradable polymers, like poly(lactide-co-glycolide) (PLGA), poly(lactic acid)

(PLL-A), poly(ϵ -caprolactone) (PCL), chitosan, gradually release the therapeutic agent, with the degradation of the carrier, ensuring safe clearance of degraded products [12][23] (Figure 5).

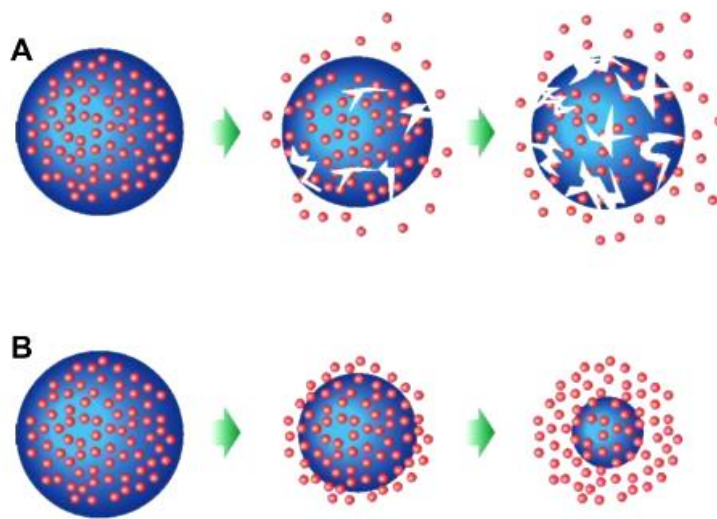


Figure 5. Degradation mechanisms of biodegradable polymeric nanoparticles: A) bulk erosion, B) surface erosion.

1.2.1 Impact of physical properties of nanoparticles

It is already known that the physics of the nanocarrier influences the delivery efficiency, and determinant parameters, independently from the specific material, are grouped under “physical targeting”:

Size - The size of the nanoparticles regulates uptake, clearance from the kidney and immune system activation [24]. Small particles inferior of 10 nm are easily excreted from the urinary system, while big particles or aggregation can cause vascular occlusion and immune response [25].

The size limitation for tumor targeting depends on the cut-off limit of the EPR effect on the endothelial barrier. Main pore size ranges between 380 and 780 nm in diameter, but change according with the type, location and cause of the tumor [26][27]. For tumor infiltration, usually small particles, around 20 nm or smaller, are facilitated in crossing the dense extracellular matrix [28].

Shape - The shape of the nanocarrier can be spherical, disk-like, rod-like, flexible [29] and can influence the rate of cellular uptake and body distribution [30].

Stiffness - A clear example of how stiffness can regulate efficiency of drug delivery, despite of the size of nanoparticles, is given by red blood cell physiology. Red blood cells (RBCs), biconcave microstructures of around 8 μm , are able to deform and pass through small blood vessels and have inspired the development of soft polymeric microparticles, with the aim to simulate the same deformability. Although only few studies have been done in this direction, stiffness seems to regulate uptake efficiency in different cell lines, for example, has been reported that cervical cancer Hela cells can take up soft particles better than hard ones [31].

Charge - The surface charge is another important factor to be considered in drug delivery. Positive charges improve non-specific cell uptake by electrostatic interaction with the cellular membrane, although hydrophobic nanoparticles can benefit of negative charges in promoting hydrophobic contacts [32]. Positive charges have the disadvantage to cause *in vivo* aggregation with serum proteins and erythrocytes and being rapidly excreted through the urinary system [33].

1.3 Gene therapy

Gene therapy is a scientific discipline that has been developed with the aim of correcting genetic diseases. Genes are the functional units of heredity and encode instructions to make proteins, which regulate most of the life functions. When the gene sequence is altered, proteins are unable to carry their normal function and result in genetic disorders. Genetic medicine is applicable in the treatment of monogenic hereditary disorders, cancer and viral infections, with the possibility to replace a defective gene or introducing a new gene to confer new properties to the cell [34][35]. In tissue regeneration growth factors gene delivery resulted being more effective than protein delivery, for the possibility to overcome the unstable biological activity, short half-life and low tissue penetration of the growth factors [17]. The strategies of gene therapy include gene encapsulation in inactivated viral carrier or alternatively into non-viral delivery, with the incorporation of the gene sequence in a bacterial plasmid. Recently the discovery of RNA-modification therapy opened the possibility to modify the gene expression through the activation of an endogenous pathway, RNA interference (RNAi), which specifically blocks the translation of a target mRNA, through antisense oligonucleotides [36].

1.3.1 RNAi mechanism.

Since 1998, when the researchers Fire, Mello and colleagues discovered the ability of double strand antisense RNA to silence the expression of a target protein, a new approach for gene therapy gained international attention. Synthetic double strand RNA sequences opened the possibility to specifically regulate the expression of a protein in cells and potentially reach any part of the genome. We can distinguish two

main pathways of the RNAi mechanism (Figure 6). The first mechanism is physiologically activated as anti-viral response, where long double strand RNA sequences (dsRNA), are interpreted as pathogens by cells and degraded in the cytoplasm. The enzyme Dicer processes dsRNA into small interfering RNAs (siRNAs), which are then recognized and incorporated into the RNA-induced-silencing complex (RISC). Argonaute2, a multifunctional protein part of the RISC complex, unwinds the siRNA, and mediates the degradation of the sense strand. The activated RISC works binding the antisense strand, using this sequence as a template to perfectly match the sequence of a target messenger RNA (mRNA) in the cell cytoplasm. RISC mediates cleavage and degradation of the target, inhibiting protein translation.

The synthetic sequences, to mimic this process, are formulated to be around 21-25 bp, skipping the Dicer functional cleavage, in order to reduce the inflammatory response mediated by interferon- γ (IFN- γ) [37] [36].

The second pathway is mediated by endogenous microRNAs (miRNAs), codified by the cell genome. They have been discovered to finely regulate the gene expression in cells, especially during embryogenesis and development [38]. miRNAs often reside into introns or polycistronic units in the genome and are processed in the cytoplasm with nearly the same mechanism of siRNAs. Different Argonaute proteins are involved (1-4) and the main difference in the process is the imperfect match with the target mRNA in sites within the 3'untranslated regions (UTRs), steric inhibition of mRNA translation or destabilization of mRNA by deadenylation of the poly-A tail [39].

For therapeutic application the use of siRNA is more practical and specific than miRNA, since miRNA can regulate the expression of multiple genes and one gene can be regulated by multiple miRNA.

The gene silencing through endogenous siRNAs ensure its therapeutic effect for 3-7 days in high proliferating cells and for several weeks in non-dividing cells [40]. Considering the limitations of siRNA therapeutics, siRNAs, like pDNA, do not cross the cellular membrane spontaneously, because of their high negative charge. The development of a delivery strategy is also required in order to reduce the high extracellular degradation and to counteract the poor targeting and high clearance by the urinary system [37].

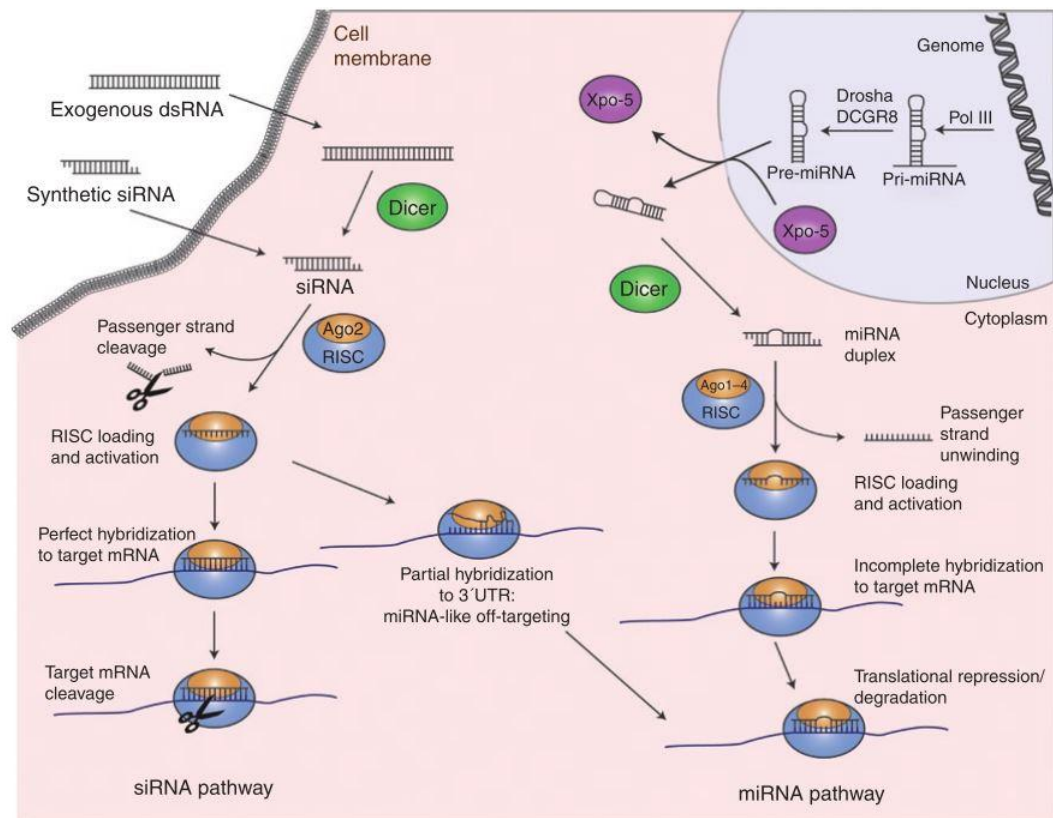


Figure 6. RNAi endogenous mechanisms for protein silencing: similarity and differences in siRNA and miRNA mechanism [36].

1.4 Gene delivery strategies

Nowadays, a lot of efforts are directed to develop an efficient carrier for nucleic acids, to be applicable for gene and siRNA therapeutics. The two main strategies involve 1) engineered viruses, deprived of the genes responsible for pathogenesis, carrying the gene of interest and the proteins important for the transfection; 2) Non-viral carriers, that create Van der Waals or electrostatic interactions with pDNA or siRNA sequences. Viral systems ensure high transfection efficiency, but they have the disadvantage to provoke immune response, toxicity and mutagenesis [41]. Non-viral carriers are preferred for the possibility to increase the safety of the gene delivery system for *in vivo* application, the possibility to insert targeting molecules, simple preparation and low production costs [42].

1.4.1 Viral delivery

Viral-mediated gene delivery consists in the utilization of viruses deprived of the capacity to replicate, but engineered to deliver exogenous genes. The most common viral systems involve functional modification of adenoviruses, adeno-associated virus vectors, retroviruses and lentiviruses (Figure 7). These systems provide high delivery efficiency and a constant expression of the therapeutic gene. The major limitations that restrict the *in vivo* utilization are immunogenicity, toxicity, mutagenesis and limited size of DNA encapsulation [42][35].

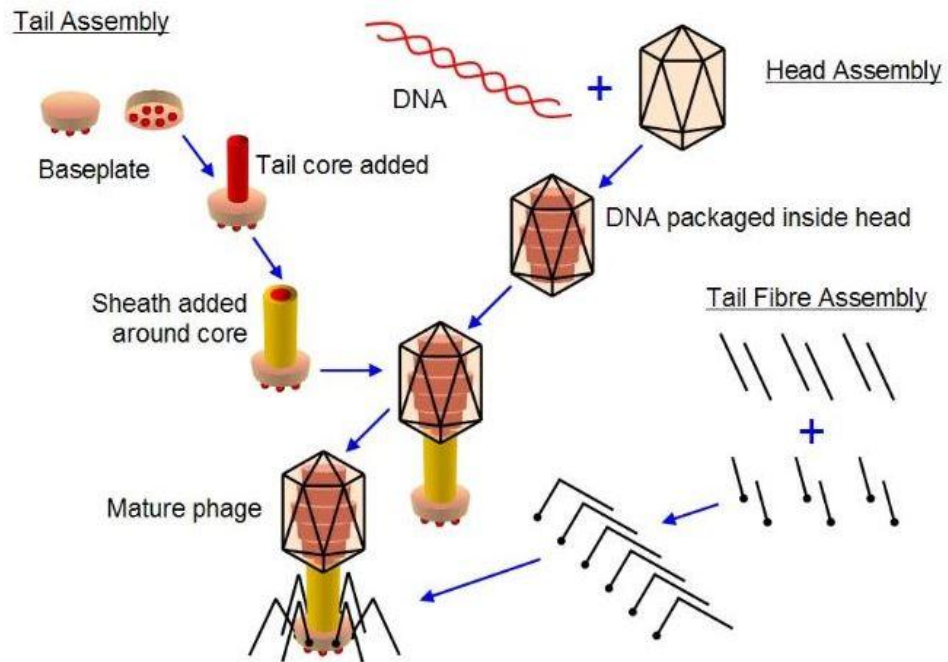


Figure 7. Representative T4 Phage assembly for gene delivery.

Adenovirus vectors - Adenoviruses are double strand DNA viruses, they do not contain lipid or membrane, and the genetic material is encapsulated in icosahedral particles, containing a complex combination of structural proteins. Adenovirus vectors can contain a relatively large amount of DNA, up of 36 kb; they cause receptor mediated endocytosis and do not integrate in the host genome, remaining as episomes in the infected cells. Therefore, the expression of the exogenous gene is transient. The main disadvantage of this system is the strong immune and inflammatory response [43].

Adeno-associated virus vectors - Adeno-associated viruses are small single strand DNA viruses, with a simple protein coat. The absence of a complex envelope structure induces a less problematic immunogenicity compared to adenoviruses. They can infect cells with good efficiency and they can be engineered to persist in

cells in an extra-chromosomal state, without integration in the host genome. The major limitation of these vectors is the low packaging capacity (4.5 kb)[43] [35].

Retroviral vectors - Retroviruses are circular-enveloped RNA viruses and they have the capacity to be integrated in the host genome. The infection of retroviruses is not cell specific and it is mediated by glycoproteins on the viral surface. Viral RNA is injected into cells.

Retroviral vectors require three important genes that should be conserved in the engineered viral vector: *ENV*, *POL* and *GAG*. *ENV* codifies for the viral envelop, *GAG* for the viral matrix, capsid and glycoproteins and *POL* for the reverse transcriptase (RT) and the integrase enzyme (IN). RT is a viral DNA polymerase that converts the viral RNA in single strand DNA in the cell cytoplasm, which in the nucleus will be transformed in double strand DNA and integrated in the host genome by the integrase. The casual insertion in the genome, mediated by LTR sequences, causes a high risk of mutagenesis. Retroviral vectors show high transfection efficiency, with the capacity to deliver DNA up to 8 kb, although the transgene expression ceases in a range of days or weeks. The reason of the silencing is not well known, although the methylation of DNA into condensed chromatin seems to be involved [43][35][42].

Lentiviruses - Lentiviruses belong to the family of *Retroviridae*. Lentivirus vectors are mostly based on components of HIV1. HIV is the lentivirus responsible to cause chronic immune deficiency, known as acquired immune disorder syndrome (AIDS). Lentiviruses have a good capacity to transfect non dividing cells, as monocyte/macrophage lineage and neurons, with potential use for gene delivery in the central nervous system (CNS). Compared to retroviruses, they have a more complex structure, with additional regulatory genes like *TAT*, *REV*, *VIF*, *VPR*, *NEF* and *VPU*, to effective transfection to host cells [42].

1.4.2 Non-viral delivery

The development of non-viral gene delivery carriers aims to minimize immunogenicity, toxicity and mutagenesis of the viral delivery system. The potential of non-viral delivery systems, beyond the lower toxicity for *in vivo* applications, is the possibility to link antibodies, proteins, aptamers and ligands that can confer specificity for a target cell type [41]. In this case the genetic material is not compacted into the viral nucleus, but it is incorporated in bacterial plasmids, commonly isolated from the bacteria *Escherichia Coli*. In nature, plasmids are small molecules that codify for some additional survival characteristics, like resistance to antibiotics. They consist in extra-chromosomal DNA and they can be transmitted from one bacteria to another one. The plasmid can replicate independently in the nucleus of a suitable host, exploiting the replication and transcription machinery of the cell. Important features, for constructing a plasmid able to replicate in bacterial/eukaryotic cells and express the gene of interest, are: *the origin of replication (ORI)*, *an antibiotic resistance gene*, which allows the selection of the transfected cell population, a *promoter* and a *multiple cloning site*, a short region rich in several commonly used restriction sites, to insert the foreign gene (Figure 8).

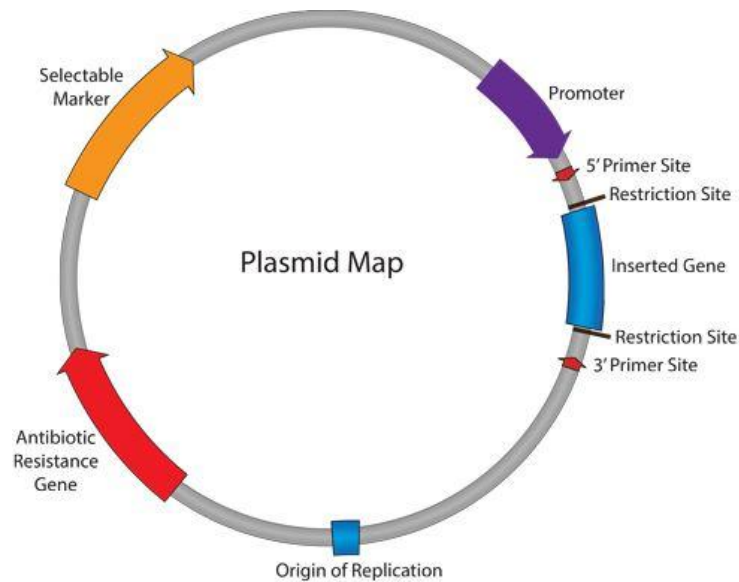


Figure 8. Representation of key characteristics of plasmids used for gene delivery.

Cell delivery of genetic material, as pDNA or siRNAs, requires a non-viral delivery system able to promote gene transfection. Native nucleic acids are large molecules with negative charge, that result in poor cellular uptake and immune stimulation through *Toll-like receptors* activation [36]. Therefore, nucleic acids need to be compacted in small particles, which reduce the electrostatic repulsion with the cellular membrane, promoting cell internalization and masking the immunogenic nature. In the recent years, a lot of efforts have been made to improve non-viral gene delivery. Non-viral delivery mainly involves the formulation of cationic lipids and cationic polymers. The electrostatic-based condensation allows the formation of lipoplexes or polyplexes, in nano-scale, to be easily internalized by non-specific endocytosis [44].

1.5 Non-viral delivery materials for gene therapy

In order to efficiently describe the current strategies of non-viral gene therapy, the delivery methods have been divided in physical and chemical systems.

Physical methods based their efficiency in creating transitory permeability in the cellular membrane. The applicability in vivo is limited for the lack of specificity, toxicity, for tissue damage and in most of the cases low transfection efficiency [41][42].

Chemical methods group the non-viral carriers for gene delivery, commonly cationic lipids (Liposomes) or cationic polymers. Electrostatic interactions with pDNA/siRNA regulate the condensation in lipoplexes and polyplexes and the cell internalization exploits the physiological cell uptake mechanisms. Chemical methods have higher prospective for in vivo application, focusing the research efforts in reducing the cytotoxicity and improving selective targeting.

1.5.1 Physical methods

Microinjection - consists in the use of a micropipette to inject the genetic material through the cell membrane of a single cell and if necessary, through the nuclear envelop. This technique limits the transfection to few cells, with manipulation of each single cell, although allows to transfect large amount of genetic material without toxicity.

Gene Gun - The DNA is encapsulated in heavy metal particles, which are accelerated with pressurized gas at high speed, to penetrate the cell membrane. Usually gold, tungsten and silver have been used. This method allows the penetration of few

millimetres into the tissue, but tissue damage and activation of the immune response are the main disadvantages.

Electroporation - uses high voltage to create transitory nanometric pores into the cellular membrane. This method, if optimized can reach high transfection efficiency that is comparable with viral systems. The major disadvantage for *in vivo* application is the large area of tissue that is subjected to the high voltage and the necessity of surgical operation to position the electrodes.

Sonoporation - exploits ultrasound waves to facilitate passive gene transfection. A contrast agent, often air-filled microbubbles stabilized with polymers or phospholipids, is used to increase the permeability of the membrane of surrounding cells. The advantage, compared to electroporation is the safety of the method that does not require surgical procedures, but the transfection efficiency is low.

Needle injection - applies the direct injection of naked DNA to tissues, organs and bloodstream. The method could reach high efficiency when the genetic material is complexed with a chemical non-viral vector, to reduce the level of extracellular degradation and increase the transfection efficiency.

Jet injection: high-speed delivery of DNA, through the use of pressurized gas, facilitates cell penetration into a target tissue, compared to needle-injection. The high-speed contact with the cell membrane creates pores that increase the transfection capability.

Hydrodynamic gene transfer: hydrodynamic pressure is the driving force for DNA/RNA delivery into target organs. The volume of the injected solution is the main problem that limits the applicability *in vivo*, since humans cannot tolerate solutions equivalent to 8% of the body weight.

1.5.2 Chemical methods

Recently chemical non-viral vectors have been extensively studied. Condensation with various formulations of cationic lipids or cationic polymers has been tested, with particular regard to pDNA/siRNA protection, transfection efficiency, *in vivo* application and toxicity issues.

Liposomes - are spherical vesicles composed of a single lipid bilayer, where the hydrophilic head groups are in contact with the aqueous environment and the hydrophobic tails face each other. The association with highly hydrophilic molecules, as pDNA and siRNA, increases with the utilization of cationic lipids, which contain one or more amines in the head group (Figure 9). The positive charge of the amino groups head group is not only necessary to incorporate the genetic material, but also for efficient binding to the cellular membrane.

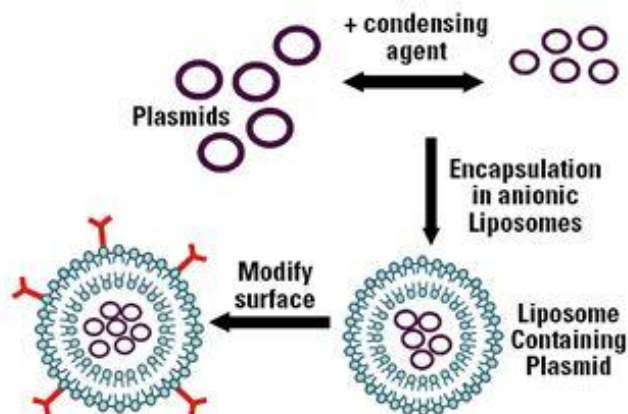


Figure 9. Schematic incorporation of plasmids in liposomes, forming lipoplexes that can be modified with surface molecules for specific targeting.

Typical reagents for cationic lipid transfection are N-[1-(2,3-dioleoyloxy)propyl]-N,N,N-trimethyl ammonium chloride (DOTMA), [1,2-bis(oleoyloxy)-3-(trimethylammonio)-propane] (DOTAP), 3 β [N-(N', N'-dimethylaminoethane)-carbamoyl] cholesterol (DC-Chol), and dioctadecylamidoglycylspermine (DOGS) [45]. Dioleoylphosphatidylethanolamine (DOPE) is often used, as neutral lipid, to improve the transfection efficiency, probably due to the conformational shift to an inverted hexagonal structure [45][41]. Besides, the use of cholesterol has been shown to increase the stability of liposomes, decreasing the probability of gene release by exposure to serum proteins [46]. However, the clinical application of liposomes is hindered by toxic-side effects, large size of the complexes and high surface charge, which lead to rapid renal clearance [46]. PEGylated-liposomes, with absorption or covalent attachment of polyethylene glycol (PEG), improve gene transfection in presence of serum, *in vivo* half-life of lipoplexes and reduced macrophage phagocytosis [45][46]. The property of phospholipids to fuse with the cellular membrane is one possibility of cell internalization, although endocytosis seems the major mechanism involved [41].

Cationic polymers - can be divided in natural and synthetic and biodegradable and non-biodegradable [42]. Natural and biodegradable polymers like polyamides, polypeptides as poly-lysine (PLL), dextran and chitosan showed comparatively low transfection efficiency than synthetic polymers, like branched and linear polyethylenimine (PEI), and PAMAM dendrimers [47][41][48]. The biodegradability, if in one hand ensures the safety of the delivery system, can on the other hand undergo through degradation in biological environment, before reaching the target tissue.

Cationic polymers have the capacity to interact with nucleic acids for the high density of amino groups, which are protonable at neutral pH, but the high transfection efficiency mostly correlates with high cytotoxicity [48][49]. PEI is one of the most efficient cationic polymers in pDNA/siRNA delivery, but the high molecular weight and the high nitrogen/phosphate ratio (N/P) necessary for efficient transfection, cause cytotoxicity with limited application *in vivo*. PAMAM dendrimers have also shown good interaction with siRNA, with efficient ability to escape from endosomes, due to the internal tertiary amino groups [50]. The higher efficiency of PEI, compared with the other polymers, has been attributed to the higher capacity to escape from endosomes [41][48]. At intracellular level the ability to release pDNA/siRNA in the cytoplasm is of critical importance to avoid lysosomal degradation and has been found that endosomal escape is proportional to the protonable amines of the delivery agent. PLL has been demonstrated to have, at physiological pH, almost all the *N*-atoms protonated and the low transfection efficiency is attributed to the low capacity of activating the proton-sponge effect [47]. The proton-sponge effect assumes that amino group protonation delays the acidification that occurs during the maturation of endosomes. The ATPase proton pumps continue to actively translocate protons into the endosomes, which resist to acidification. The endosomal accumulation of protons is followed by passive entry of chloride ions and the ionic concentration leads to water influx. The osmotic pressure cause endosome swelling and wall rupture, causing pDNA/siRNA release in the cytoplasm [51][47].

PEI is partially protonated at physiological pH and the remaining amino-groups can be protonated in the acidic environment of endosomes, resulting more efficient in activating the proton-sponge effect. The importance of the phenomenon is demonstrated by the fact that most of the polyplexes showing low transfection

efficiency increase their delivery capacity after co-transfection with chloroquine, a lysomotropic compound [47].

For *in vivo* application the main concern about cationic polymers is the cytotoxicity and the poor circulation time, due to serum proteins and erythrocytes aggregation [44]. Davis *et al.* have recently developed the first polymer-based nanoparticle formulation for siRNA delivery entered in clinical trial and systemically administered to humans [52]. The formulation CALAA-01 is a four component system for siRNA therapeutics to be administered in cancer patients: a cyclic oligosaccharide (β -cyclodextrin) was incorporated into the backbone of linear polycation chains to condense the siRNA, amantane polyethylene glycol (AD-PEG) was used to stabilize the nanoparticles in biological fluids and human transferrin was adsorbed to the surface to target tumors [52][48].

1.5.3 Challenges of non-viral gene delivery.

Biological barriers and physical/chemical properties of the delivery system need to be considered for a therapeutic application. First, whether we consider, *in vitro* or *in vivo* application, the genetic material needs to be protected by extracellular nucleases. This point is particularly critical for siRNA delivery, because RNA is highly susceptible to RNase degradation [41].

Secondly, the material should not aggregate with serum proteins in the bloodstream, it should possess a high circulation time, avoid the activation of the immune system, and finally cross the endothelial barrier. As discussed before, this operation is facilitated in case of tumor treatment, by EPR effect, but crossing the endothelium in presence of a healthy intima structure requires a specific uptake mechanism. The molecules known to be transported through endothelial cells are mainly plasma

proteins with bloodstream transport function, like low density lipoproteins (LDL), very low density lipoproteins (VLDL), albumin, insulin and the iron transporter transferrin [53].

Once the gene delivery system reaches the target tissue it should be able to penetrate into the target cell and efficiently disassemble. Important difference to be considered between pDNA and siRNA delivery is the intracellular site where the mechanism takes place: RNAi pathway entirely plays in the cytoplasm, while pDNA needs to further penetrate the nuclear membrane to be expressed (Figure 10). Considering that endocytosis is the major uptake mechanism involved in the internalization of nanoparticles, the delivery system requires the ability to activate endosome escape and intracellular release of free pDNA/siRNA molecules [54].

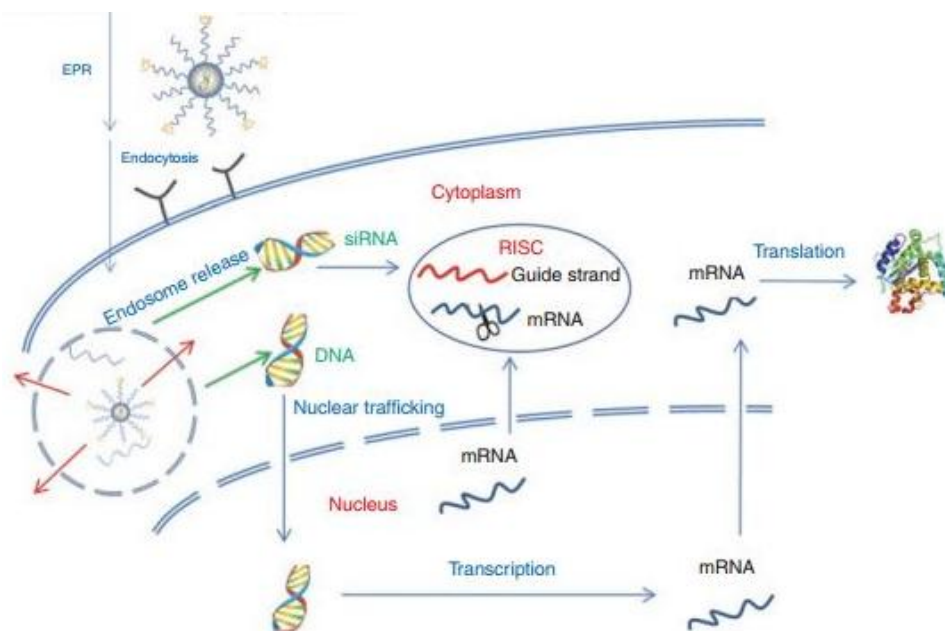


Figure 10. Intracellular trafficking of nanoparticles for gene therapy. Endosome escape allows nuclear trafficking of DNA for gene expression and siRNA incorporation in the RISC complex for gene silencing.

1.5.4 Endocytosis mechanisms

Cell membrane is impermeable to most of the macromolecules and particles and non-viral delivery systems have to follow specific pathways to be up-taken by cells. The knowledge of the uptake mechanisms and how they vary between the cell types is recognised, but not yet completely understood [49][55]. A part from certain types of liposomes, which have the capacity to fuse with the cellular membrane for their hydrophobic nature, most of the nanoparticles require a specific energy-dependent internalization mechanism [41]. Physical properties (nanoparticles size, charge, stiffness) and active targeting, through molecules that activate a receptor-mediated endocytosis, mainly regulate the uptake direction.

Phagocytosis is an uptake mechanism mostly activated by phagocytes, like monocytes and macrophages, which, being part of the immune system, are specialized in the internalization of viruses and bacteria [49]. The other mechanisms are grouped under the term of pinocytosis and are distinguished in: macropinocytosis, clathrin-mediated pathway, caveolae-mediated pathway and lipid raft-mediated pathway (Figure 11). The size of the nanoparticles firstly give an idea of the possible internalization mechanism, although the rigid classification into size parameters is under discussion [47]. Clathrin-coated pits are generally large 100-150 nm, caveolin-1 flask-shaped invagination around 50-80 nm, while macropinocytosis can cover big sizes of 500-2000 nm [48]. The abundance of caveolae, despite clathrin pits, depends on the cell type in consideration [56]. Recent studies have shown the ability of “caveosomes”, derived from multiple association of caveolae, to internalize big particles [57]. Microspheres with a diameter superior of 500 nm were selectively inhibited by cholesterol depletors, which block the internalization mediated by lipid rafts. Serum albumin, viruses like cholera toxin and bacteria are known to be internalized by caveolae-mediated endocytosis [58][59][60]. The knowledge about

uptake mechanisms is nowadays limited and other pathways might be involved in regulating the uptake of macromolecules. Besides, the uptake mechanism regulates the intracellular trafficking of nanoparticles: clathrin-based pits are transported through early and late endosomes directly to lysosome to be degraded, while caveolae-mediated endocytosis seems to transport molecules to the Golgi apparatus, convenient route for pathogens to avoid lysosomal degradation [60]. The capacity of the gene delivery carrier to escape from endosomes is particularly important to ensure the release of the therapeutic agent in the cytoplasm.

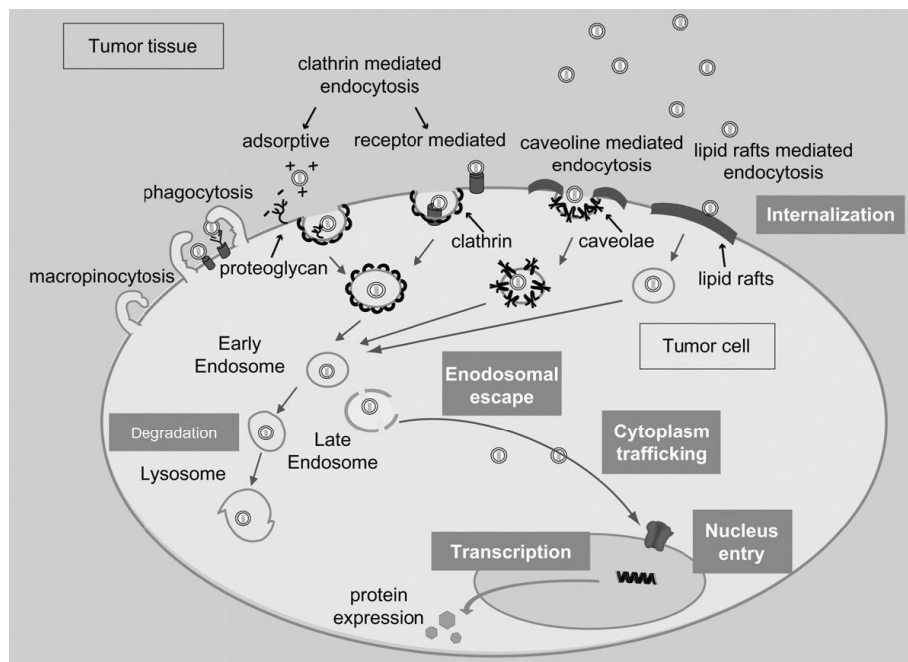


Figure 11. Schematic representation of the known intracellular trafficking pathways involved in the uptake mediated by endocytosis.

1.6 Polyethylenimine and toxicity issues.

PEI, in linear and branched form, resulted, as described before, one of the best pDNA/siRNA delivery carrier, but the efficiency is critically correlated with high molecular weight (25kDa) and high N/P ratio required for efficient transfection, with toxicity issues for systemic administration [41]. PEI has been demonstrated to induce cell membrane damage (necrosis post-treatment) and mitochondrial-mediated apoptosis in a later stage, 24 hours post-treatment. Furthermore, the high positive charge of the polyplexes lead to nanoparticles aggregation with serum proteins and erythrocytes *in vivo* [48].

Linear and branched PEI showed different ability to complex pDNA or siRNAs. In particular, linear polyethylenimine (lPEI) resulted more efficient to complex pDNA than siRNA; contrarily, branched polyethylenimine (bPEI) showed good ability to transport siRNA, probably due to the three-dimensional structure that allows multiple folding options for the siRNA [51].

Research efforts are, nowadays, focused in reducing PEI cytotoxicity, improving at the same time pDNA/siRNA delivery: modifications of PEI backbone and conjugation with neutral charged polymers or proteins are the most considered options for improving biocompatibility, bloodstream circulation and cell targeting [50]. Modification of the PEI backbone with poly-ethylene glycol (PEG) has been already demonstrated to reduce non-specific localization in liver, spleen and lung, compared to the PEI polyplexes. However, the uptake efficiency by cells resulted low for the dramatic reduction of the surface charge [61].

A lot of efforts are nowadays directed to functionalize PEI structure: amino groups acetylation, succinylation, alkylation are proposed for improving siRNA-therapeutics, reducing toxic side effects [50] (Figure 12). Moreover, the oxidation of

the amino groups of PEI with hydrogen peroxide (H_2O_2) showed reduced cytotoxicity of PEI-DNA polyplexes, without compromising, although increasing green fluorescent protein (GFP) expression [62].

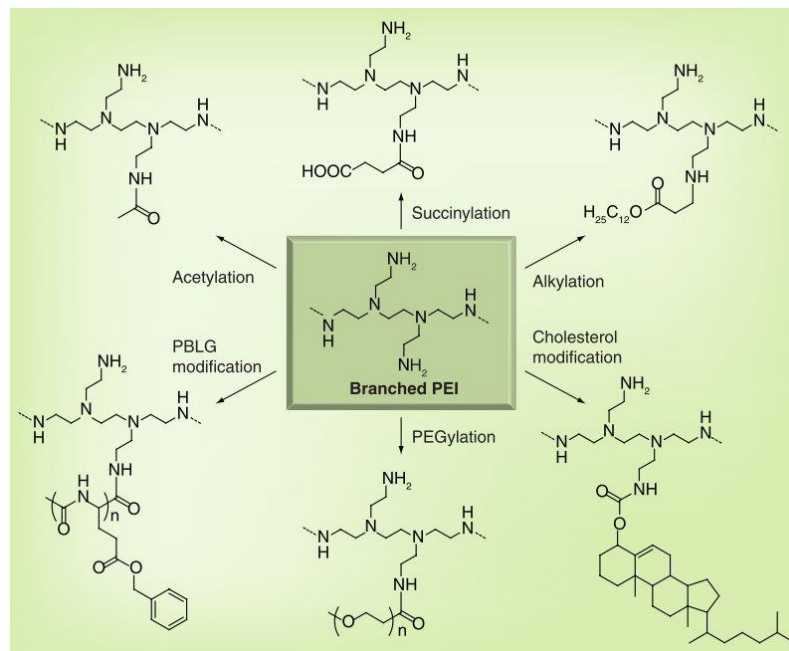


Figure 12. Functionalization of bPEI by acetylation, succinylation, PEGylation and modification with hydrophobic cholesterol, long alkyl chains and PBLG chains for decreasing the cytotoxicity, increasing the stability of polycation complexes and prolonged blood circulation time [50].

Besides the structural modifications, the conjugation of PEI with “cell-targeting ligands”, as serum proteins or macromolecules, have been tested. The conjugation with cholesterol and long alkyl groups, for example, can increase the possibility to target the liver by interacting *in vivo* with the high-density lipoprotein (HDL) and low-density lipoprotein (LDL) receptors [37]. More recently, the conjugation of PEI

with galactose has been investigated to increase a receptor-mediated endocytosis in hepatocytes [48].

PEI conjugation with transferrin (Tf), epithelial growth factor (EGF) and folic acid was studied for the possibility to target cancer, considering that tumor cells over-express their receptors. Ogris *et al.*, have demonstrated that PEI conjugated with transferrin, improves gene transfection in human erythromyeloid leukemia cells, compared to unmodified PEI polyplexes [63].

1.7 Active targeting: the potential of albumin.

Serum proteins have been recently discovered to serve as endogenous targeting ligands and for increasing nanoparticles circulation, after injection [44][53]. In Kim *et al.*, have reported that apolipoprotein A-I, a component of the high density lipoprotein (HDL), can be assembled with liposomes to address siRNA delivery to the liver, through specific receptor-mediated internalization in hepatocytes [64]. Transferrin, the iron transporter in the bloodstream, in the recent years has been largely employed for non-viral gene therapy, as the cited CALAA-01 siRNA-therapeutic agent and PEI-Tf-DNA complexes. The future direction of genetic medicine is, therefore, direct the therapeutic agent to the target cells, ensuring a good transfection efficiency, which translates in high therapeutic effect.

Nowadays, plasma proteins are gaining attention for the possibility to increase the half-life of a therapeutic agent and the possibility to target tumors, due to the EPR effect. Serum proteins, as transferrin, albumin, LDL are promising as anti-neoplastic agents [53].

Human serum albumin (HSA) is the most abundant protein in human plasma and it transports a broad range of molecules in the bloodstream: fatty acids, therapeutic

drugs (aspirin, penicillins, benzodiazepines), metabolites and metal ions (copper II, nickel II, calcium II, zinc II) [53].

HSA has been discovered to accumulate in malignant tumors and inflamed tissues and the therapeutic application as drug delivery carrier has been validated with the commercialized agent Abraxane (ABI-007) [65]. Abraxane consists in paclitaxel albumin-loaded nanoparticles, which improves the anticancer therapeutic efficiency of paclitaxel in the treatment of metastatic breast cancer. Other types of malignant tumors have been tested for the therapeutic efficiency of Abraxane, for example head and neck cancer [66].

A recent study has demonstrated the role of albumin in preventing non-specific protein absorption to nanoparticles in presence of serum, with potential to enhance nanoparticles circulation time [67]. Moreover, it is known that albumin, further being transported to tumors by EPR effect, possesses the ability to actively cross the endothelial membrane by gp60 receptor-mediated transcytosis [56][68][69]. The internalization of HSA has been demonstrated to involve caveolae-mediated endocytosis in endothelial cells [56].

In the intra-tumor environment the secreted protein acidic and rich in cysteine (SPARC) has been shown to have a role in binding albumin, facilitating the transportation in tumor cells, to probably being used as source of amino-acids and energy [70]. SPARC and gp60 share a region of structural homology, which is associated with the common albumin binding activity [71]. The over-expression of SPARC and caveolae in many malignant tumors have been correlated with high tumor invasion and metastasis [66][72].

Therefore, many advantages could derive from the use of albumin as gene delivery carrier, including high circulation time in the bloodstream, tolerance from the immune system and tumor targeting.

1.8 References

- [1] K. Riehemann, S. W. Schneider, T. a Luger, B. Godin, M. Ferrari, and H. Fuchs, "Nanomedicine--challenge and perspectives.," *Angew. Chem. Int. Ed. Engl.*, vol. 48, no. 5, pp. 872–97, Jan. 2009.
- [2] S. M. Moghimi, a C. Hunter, and J. C. Murray, "Nanomedicine: current status and future prospects.," *FASEB J.*, vol. 19, no. 3, pp. 311–30, Mar. 2005.
- [3] D. Peer, J. M. Karp, S. Hong, O. C. Farokhzad, R. Margalit, and R. Langer, "Nanocarriers as an emerging platform for cancer therapy.," *Nat. Nanotechnol.*, vol. 2, no. 12, pp. 751–60, Dec. 2007.
- [4] H. Maeda, J. Wu, T. Sawa, Y. Matsumura, and K. Hori, "Tumor vascular permeability and the EPR effect in macromolecular therapeutics: a review," *J. Control. Release*, vol. 65, no. 1–2, pp. 271–284, Mar. 2000.
- [5] V. P. Torchilin, "Drug targeting," *Eur. J. Pharm. Sci.*, vol. 11, pp. S81–S91, Oct. 2000.
- [6] F. Danhier, O. Feron, and V. Préat, "To exploit the tumor microenvironment: Passive and active tumor targeting of nanocarriers for anti-cancer drug delivery.," *J. Control. Release*, vol. 148, no. 2, pp. 135–46, Dec. 2010.
- [7] S. Nie, "Understanding and overcoming major barriers in cancer nanomedicine.," *Nanomedicine (Lond)*, vol. 5, no. 4, pp. 523–8, Jun. 2010.
- [8] J. S. Desgrosellier and D. a Cheresch, "Integrins in cancer: biological implications and therapeutic opportunities.," *Nat. Rev. Cancer*, vol. 10, no. 1, pp. 9–22, Jan. 2010.
- [9] Y. Mo and L.-Y. Lim, "Preparation and in vitro anticancer activity of wheat germ agglutinin (WGA)-conjugated PLGA nanoparticles loaded with paclitaxel and isopropyl myristate.," *J. Control. Release*, vol. 107, no. 1, pp. 30–42, Sep. 2005.
- [10] J. D. Byrne, T. Betancourt, and L. Brannon-Peppas, "Active targeting schemes for nanoparticle systems in cancer therapeutics.," *Adv. Drug Deliv. Rev.*, vol. 60, no. 15, pp. 1615–26, Dec. 2008.
- [11] J. Y. Yhee, S. J. Lee, S. Lee, S. Song, H. S. Min, S.-W. Kang, S. Son, S. Y. Jeong, I. C. Kwon, S. H. Kim, and K. Kim, "Tumor-targeting transferrin nanoparticles for systemic polymerized siRNA delivery in tumor-bearing mice.," *Bioconjug. Chem.*, vol. 24, no. 11, pp. 1850–60, Nov. 2013.

- [12] J. M. Morachis, E. a Mahmoud, and A. Almutairi, "Physical and chemical strategies for therapeutic delivery by using polymeric nanoparticles.," *Pharmacol. Rev.*, vol. 64, no. 3, pp. 505–19, Jul. 2012.
- [13] R.-Y. Lin, K. Dayananda, T.-J. Chen, C.-Y. Chen, G.-C. Liu, K.-L. Lin, and Y.-M. Wang, "Targeted RGD nanoparticles for highly sensitive in vivo integrin receptor imaging.," *Contrast Media Mol. Imaging*, vol. 7, no. 1, pp. 7–18, 2012.
- [14] K. Lee, E. a Silva, and D. J. Mooney, "Growth factor delivery-based tissue engineering: general approaches and a review of recent developments.," *J. R. Soc. Interface*, vol. 8, no. 55, pp. 153–70, Feb. 2011.
- [15] E. Engel, A. Michiardi, M. Navarro, D. Lacroix, and J. a Planell, "Nanotechnology in regenerative medicine: the materials side.," *Trends Biotechnol.*, vol. 26, no. 1, pp. 39–47, Jan. 2008.
- [16] B. Munksgaard, "Regeneration of vascularized bone," vol. 41, pp. 109–122, 2006.
- [17] K. Kim and J. P. Fisher, "Nanoparticle technology in bone tissue engineering.," *J. Drug Target.*, vol. 15, no. 4, pp. 241–52, May 2007.
- [18] H. G. Schmoekel, F. E. Weber, J. C. Schense, K. W. Grätz, P. Schawalder, and J. a Hubbell, "Bone repair with a form of BMP-2 engineered for incorporation into fibrin cell ingrowth matrices.," *Biotechnol. Bioeng.*, vol. 89, no. 3, pp. 253–62, Feb. 2005.
- [19] T. N. Vo, F. K. Kasper, and A. G. Mikos, "Strategies for controlled delivery of growth factors and cells for bone regeneration.," *Adv. Drug Deliv. Rev.*, vol. 64, no. 12, pp. 1292–309, Sep. 2012.
- [20] H. C. S. Der, L. Kurz, W. E. G. M, and B. Lorenz, "Polyphosphate in Bone," vol. 65, no. 3, pp. 296–303, 2000.
- [21] J. Caetano-lobes, H. Canhão, and F. J. Eurico, "Osteoblasts and bone formation," pp. 103–110.
- [22] Y. L. C.S. Soltanoff, W.Chen, S. Yang, "Signaling Networks that Control the Lineage Commitment and Differentiation of Bone Cells," *Crit Rev Eukaryot Gene Expr*, vol. 19, no. 1, pp. 1–46, 2009.
- [23] R. Dinarvand, N. Sepehri, S. Manoochehri, H. Rouhani, and F. Atyabi, "Polylactide-co-glycolide nanoparticles for controlled delivery of anticancer agents.," *Int. J. Nanomedicine*, vol. 6, pp. 877–95, Jan. 2011.

- [24] H. S. Choi, W. Liu, P. Misra, E. Tanaka, J. P. Zimmer, B. Itty Ipe, M. G. Bawendi, and J. V. Frangioni, "Renal clearance of quantum dots.," *Nat. Biotechnol.*, vol. 25, no. 10, pp. 1165–70, Oct. 2007.
- [25] C. Wong, T. Stylianopoulos, J. Cui, J. Martin, V. P. Chauhan, W. Jiang, Z. Popovic, R. K. Jain, M. G. Bawendi, and D. Fukumura, "Multistage nanoparticle delivery system for deep penetration into tumor tissue.," *Proc. Natl. Acad. Sci. U. S. A.*, vol. 108, no. 6, pp. 2426–31, Mar. 2011.
- [26] R. K. Jain, "Understanding Barriers to Drug Delivery : High Resolution in Vivo Imaging Is Key Understanding Barriers to Drug Delivery : High Resolution in Vivo Imaging Is Key," pp. 1605–1606, 1999.
- [27] H. Hashizume, P. Baluk, S. Morikawa, J. W. McLean, G. Thurston, S. Roberge, R. K. Jain, and D. M. McDonald, "Openings between defective endothelial cells explain tumor vessel leakiness.," *Am. J. Pathol.*, vol. 156, no. 4, pp. 1363–80, Apr. 2000.
- [28] a Pluen, Y. Boucher, S. Ramanujan, T. D. McKee, T. Gohongi, E. di Tomaso, E. B. Brown, Y. Izumi, R. B. Campbell, D. a Berk, and R. K. Jain, "Role of tumor-host interactions in interstitial diffusion of macromolecules: cranial vs. subcutaneous tumors.," *Proc. Natl. Acad. Sci. U. S. A.*, vol. 98, no. 8, pp. 4628–33, Apr. 2001.
- [29] R. a Petros and J. M. DeSimone, "Strategies in the design of nanoparticles for therapeutic applications.," *Nat. Rev. Drug Discov.*, vol. 9, no. 8, pp. 615–27, Aug. 2010.
- [30] H.-C. Huang, S. Barua, G. Sharma, S. K. Dey, and K. Rege, "Inorganic nanoparticles for cancer imaging and therapy.," *J. Control. Release*, vol. 155, no. 3, pp. 344–57, Nov. 2011.
- [31] J.-O. You and D. T. Auguste, "Nanocarrier cross-linking density and pH sensitivity regulate intracellular gene transfer.," *Nano Lett.*, vol. 9, no. 12, pp. 4467–73, Dec. 2009.
- [32] J. Voigt, J. Christensen, and V. P. Shastri, "Differential uptake of nanoparticles by endothelial cells through polyelectrolytes with affinity for caveolae.," *Proc. Natl. Acad. Sci. U. S. A.*, vol. 111, no. 8, pp. 2942–7, Feb. 2014.
- [33] M. Lundqvist, J. Stigler, G. Elia, I. Lynch, T. Cedervall, and K. a Dawson, "Nanoparticle size and surface properties determine the protein corona with possible implications for biological impacts.," *Proc. Natl. Acad. Sci. U. S. A.*, vol. 105, no. 38, pp. 14265–70, Sep. 2008.
- [34] S. Misra, "Human gene therapy: a brief overview of the genetic revolution.," *J. Assoc. Physicians India*, vol. 61, no. 2, pp. 127–33, Feb. 2013.
- [35] T. P. O'Connor and R. G. Crystal, "Genetic medicines: treatment strategies for hereditary disorders.," *Nat. Rev. Genet.*, vol. 7, no. 4, pp. 261–76, Apr. 2006.

- [36] R. L. Kanasty, K. a Whitehead, A. J. Vegas, and D. G. Anderson, "Action and reaction: the biological response to siRNA and its delivery vehicles.," *Mol. Ther.*, vol. 20, no. 3, pp. 513–24, Mar. 2012.
- [37] K. a Whitehead, R. Langer, and D. G. Anderson, "Knocking down barriers: advances in siRNA delivery.," *Nat. Rev. Drug Discov.*, vol. 8, no. 2, pp. 129–38, Feb. 2009.
- [38] A. Pauli, J. L. Rinn, and A. F. Schier, "Non-coding RNAs as regulators of embryogenesis.," *Nat. Rev. Genet.*, vol. 12, no. 2, pp. 136–49, Feb. 2011.
- [39] T. G. McDanel, "MicroRNA: mechanism of gene regulation and application to livestock.," *J. Anim. Sci.*, vol. 87, no. 14 Suppl, pp. E21–8, Apr. 2009.
- [40] D. W. Bartlett and M. E. Davis, "Insights into the kinetics of siRNA-mediated gene silencing from live-cell and live-animal bioluminescent imaging.," *Nucleic Acids Res.*, vol. 34, no. 1, pp. 322–33, Jan. 2006.
- [41] W. Wang, W. Li, N. Ma, and G. Steinhoff, "Non-Viral Gene Delivery Methods," *Curr. Pharm. Biotechnol.*, vol. 14, no. 1, pp. 46–60, Jan. 2013.
- [42] E. Cevher, A. D. Sezer, and E. Ş. Çağlar, "Gene Delivery Systems : Recent Progress in Viral and Non-Viral Therapy," 2012.
- [43] L. S. Young, P. F. Searle, D. Onion, and V. Mautner, "Viral gene therapy strategies: from basic science to clinical application.," *J. Pathol.*, vol. 208, no. 2, pp. 299–318, Jan. 2006.
- [44] R. Kanasty, J. R. Dorkin, A. Vegas, and D. Anderson, "Delivery materials for siRNA therapeutics.," *Nat. Mater.*, vol. 12, no. 11, pp. 967–77, Nov. 2013.
- [45] D. a Balazs and W. Godbey, "Liposomes for use in gene delivery.," *J. Drug Deliv.*, vol. 2011, p. 326497, Jan. 2011.
- [46] T. M. Allen and P. R. Cullis, "Liposomal drug delivery systems: from concept to clinical applications.," *Adv. Drug Deliv. Rev.*, vol. 65, no. 1, pp. 36–48, Jan. 2013.
- [47] S. C. De Smedt, J. Demeester, and W. E. Hennink, "Cationic Polymer Based Gene Delivery Systems," vol. 17, no. 2, 2000.
- [48] Y. Yue and C. Wu, "Progress and perspectives in developing polymeric vectors for in vitro gene delivery," *Biomater. Sci.*, vol. 1, no. 2, p. 152, 2013.
- [49] L. Parhamifar, A. K. Larsen, a. C. Hunter, T. L. Andresen, and S. M. Moghimi, "Polycation cytotoxicity: a delicate matter for nucleic acid therapy—focus on polyethylenimine," *Soft Matter*, vol. 6, no. 17, p. 4001, 2010.

- [50] A. Tamura and Y. Nagasaki, "Smart siRNA delivery systems based on polymeric nanoassemblies and nanoparticles.," *Nanomedicine (Lond)*, vol. 5, no. 7, pp. 1089–102, Sep. 2010.
- [51] W. Liang and J. K. W. Lam, "Endosomal Escape Pathways for Non-Viral Nucleic Acid Delivery Systems," 2012.
- [52] J. E. Zuckerman, I. Gritli, a. Tolcher, J. D. Heidel, D. Lim, R. Morgan, B. Chmielowski, a. Ribas, M. E. Davis, and Y. Yen, "Correlating animal and human phase Ia/Ib clinical data with CALAA-01, a targeted, polymer-based nanoparticle containing siRNA," *Proc. Natl. Acad. Sci.*, vol. 111, no. 31, Jul. 2014.
- [53] F. Kratz and U. Beyer, "Serum Proteins as Drug Carriers of Anticancer Agents : A Review," *Inf. Heathcare*, vol. 5, no. 4, pp. 281–299, 1998.
- [54] C. Scholz and E. Wagner, "Therapeutic plasmid DNA versus siRNA delivery: common and different tasks for synthetic carriers.," *J. Control. Release*, vol. 161, no. 2, pp. 554–65, Jul. 2012.
- [55] M. Morille, C. Passirani, A. Vonarbourg, A. Clavreul, and J.-P. Benoit, "Progress in developing cationic vectors for non-viral systemic gene therapy against cancer.," *Biomaterials*, vol. 29, no. 24–25, pp. 3477–96, 2008.
- [56] R. D. Minshall, C. Tiruppathi, S. M. Vogel, W. D. Niles, a Gilchrist, H. E. Hamm, and a B. Malik, "Endothelial cell-surface gp60 activates vesicle formation and trafficking via G(i)-coupled Src kinase signaling pathway.," *J. Cell Biol.*, vol. 150, no. 5, pp. 1057–70, Sep. 2000.
- [57] A. Manuscript and L. E. Cells, "NIH Public Access," vol. 3, no. 12, pp. 4110–4116, 2013.
- [58] J. Rejman, A. Bragonzi, and M. Conese, "Role of clathrin- and caveolae-mediated endocytosis in gene transfer mediated by lipo- and polyplexes.," *Mol. Ther.*, vol. 12, no. 3, pp. 468–74, Oct. 2005.
- [59] J. Rejman, V. Oberle, I. S. Zuhorn, and D. Hoekstra, "Size-dependent internalization of particles via the pathways of clathrin- and caveolae-mediated endocytosis.," *Biochem. J.*, vol. 377, no. Pt 1, pp. 159–69, Jan. 2004.
- [60] I. A. Khalil, K. Kogure, H. Akita, and H. Harashima, "Uptake Pathways and Subsequent Intracellular Trafficking in Nonviral Gene Delivery," vol. 58, no. 1, pp. 32–45, 2006.
- [61] M. Neu, D. Fischer, and T. Kissel, "Recent advances in rational gene transfer vector design based on poly(ethylene imine) and its derivatives.," *J. Gene Med.*, vol. 7, no. 8, pp. 992–1009, Aug. 2005.

- [62] W. Y. Seow, K. Liang, M. Kurisawa, and C. a E. Hauser, "Oxidation as a facile strategy to reduce the surface charge and toxicity of polyethyleneimine gene carriers.," *Biomacromolecules*, vol. 14, no. 7, pp. 2340–6, Jul. 2013.
- [63] M. Ogris, P. Steinlein, S. Carotta, S. Brunner, and E. Wagner, "DNA/polyethylenimine transfection particles: influence of ligands, polymer size, and PEGylation on internalization and gene expression.," *AAPS PharmSci*, vol. 3, no. 3, p. E21, Jan. 2001.
- [64] S. I. Kim, D. Shin, H. Lee, B.-Y. Ahn, Y. Yoon, and M. Kim, "Targeted delivery of siRNA against hepatitis C virus by apolipoprotein A-I-bound cationic liposomes.," *J. Hepatol.*, vol. 50, no. 3, pp. 479–88, Mar. 2009.
- [65] F. Kratz, "Albumin as a drug carrier: design of prodrugs, drug conjugates and nanoparticles.," *J. Control. Release*, vol. 132, no. 3, pp. 171–83, Dec. 2008.
- [66] N. Desai, V. Trieu, B. Damascelli, and P. Soon-shiong, "SPARC Expression Correlates with Tumor Response to Albumin-Bound Paclitaxel in Head and Neck Cancer Patients," *Transl. Oncol.*, vol. 2, no. 2, pp. 59–64, 2009.
- [67] C. M. Kummitha, A. S. Malamas, and Z.-R. Lu, "Albumin pre-coating enhances intracellular siRNA delivery of multifunctional amphiphile/siRNA nanoparticles.," *Int. J. Nanomedicine*, vol. 7, pp. 5205–14, Jan. 2012.
- [68] C. Tiruppathi, "Gp60 Activation Mediates Albumin Transcytosis in Endothelial Cells by Tyrosine Kinase-dependent Pathway," *J. Biol. Chem.*, vol. 272, no. 41, pp. 25968–25975, Oct. 1997.
- [69] W. Schubert, P. G. Frank, B. Razani, D. S. Park, C. W. Chow, and M. P. Lisanti, "Caveolae-deficient endothelial cells show defects in the uptake and transport of albumin in vivo.," *J. Biol. Chem.*, vol. 276, no. 52, pp. 48619–22, Dec. 2001.
- [70] E. Frei, "Albumin binding ligands and albumin conjugate uptake by cancer cells.," *Diabetol. Metab. Syndr.*, vol. 3, no. 1, p. 11, Jan. 2011.
- [71] J. A. N. E. Schnitzer, "Antibodies to SPARC inhibit albumin binding endothelium to SPARC , gp60 , and microvascular," 1992.
- [72] Y. Lavie, G. Fiucci, and M. Liscovitch, "Upregulation of caveolin in multidrug resistant cancer cells: functional implications.," *Adv. Drug Deliv. Rev.*, vol. 49, no. 3, pp. 317–23, Jul. 2001.

2 Outline of the Thesis

The overall aim of this thesis is to improve branched polyethylenimine (bPEI) delivery system for gene therapy application. As previously discussed in the introduction, despite the good efficiency in condensing nucleic acids and promoting cell transfection, the major limitation of PEI for *in vivo* application is the high cytotoxicity, due to the high positive charged amino groups density.

The effect of amino groups acetylation on bPEI backbone and the incorporation of human serum albumin (HSA) in bPEI-siRNA polyplexes have been investigated to improve cell transfection efficiency and reduce the toxicity that accompanies the delivery efficiency.

Firstly, my project was focused in investigating the effect of partial acetylation of primary amino groups, along PEI backbone, in the capacity to form nanoparticles (NPs) with poly(lactic-co-glycolic acid) (PLGA), the influence of acetylated PEI (AcPEI) in nanoparticles size and surface charge and the ability of NPs to deliver genetic material. Particular attention was paid in testing cell cytotoxicity, genotoxicity and immunotoxicity, following transfection of both PEI-PLGA (PEI-NPs) and AcPEI NPs, with the aim to increase the biocompatibility of the system for *in vivo* applications. Nanotoxicity is often underestimated, but it is of fundamental importance for therapeutic use. Considering the application of NPs as medical devices, collateral effects as inflammation, immunoreaction, or cancer, can emerge due to NPs toxicity. Free oxygen radicals production, following cell stress and immune system activation, can contribute in the risk of DNA mutation and cancer. Therefore we concentrated our work in studying PEI-NPs capability of promoting

DNA damage and intracellular ROS release, investigating the potential of AcPEI-NPs, with 50% of acetylated amino groups, in reducing the toxicity of PEI, without compromising the transfection efficiency.

After having demonstrated the effectiveness of AcPEI gene delivery system in human umbelical vein endothelial cells (HUVEC), we focused our study on the possibility to use acetylated PEI nanoparticles as gene delivery carrier in tissue engineering. In this study, the internalization efficiency, the mechanism of uptake involved and the endosome escape efficiency were investigated in human primary osteoblasts (hOBs), isolated from human trabecular bone. The cytotoxicity was evaluated in terms of membrane damage (necrosis) or activation of apoptosis, while the effect of the nanoparticles on hOB activity and differentiation was studied quantifying alkaline phosphatase (ALP) activity, collagen type I production (COL1), mineralization and gene expression of markers of differentiated osteoblasts. The results will be used for future application of these nanoparticles in gene delivery to promote osteogenesis and in siRNA delivery to inhibit bone formation in blood vessel walls.

The project, developed at the University of Freiburg, involved the incorporation of human serum albumin (HSA) into pre-formed bPEI-siRNA polyplexes, with the aim to improve transfection efficiency in the tumor microenvironment, since HSA has been demonstrated to accumulate in inflamed tissues and tumors [65]. The ternary complex, formed by electrostatic interactions, was characterized in terms of size and surface charge. The intracellular delivery efficiency, mechanism of uptake and silencing efficiency were evaluated with *in vitro* studies, investigating a direct role of HSA in promoting cell uptake and gene silencing, compared to bPEI-siRNA complexes. Further studies will be focused in investigating a possible HSA receptor

mediated endocytosis of the complexes, for HSA utilization as a tumor targeting molecule.

3 The genotoxicity of PEI-based nanoparticles is reduced by acetylation of polyethylenimine amines in human primary cells

Anna Calarco^{a,1}, Michela Bosetti^{b,1}, Sabrina Margarucci^a, Luca Fusaro^c, Elena Nicoli^b, Orsolina Petillo^a, Mario Cannas^c, Umberto Galderisi^d, Gianfranco Peluso^a,

a Institute of Protein Biochemistry, CNR, Naples, Italy, b School of Pharmacy, University of Eastern Piedmont, Novara, Italy, c Department of Clinical and Experimental Medicine, University Eastern Piedmont, Novara, Italy, d Department of Experimental Medicine, Second University of Naples, Naples, Italy

Toxicol. Lett., vol. 218, no. 1, pp. 10–7, Mar. 2013.

3.1 Summary

The ultrasmall size and unique properties of polymeric nanoparticles (NPs) have led to raising concerns about their potential cyto- and genotoxicity on biological systems. Polyethylenimine (PEI) is a highly positive charged polymer and is known to have varying degree of toxic effect to cells based on its chemical structure (i.e., amount of primary and secondary amine).

Herein, drug delivery carriers such as PEI-PLGA nanoparticles (PEI-NPs) and acetylated PEI-PLGA nanoparticles (AcPEI-NPs) were utilized to examine the effect of acetylation on NPs biocompatibility and genotoxicity, using human primary cells as in vitro model.

Cell uptake of NPs was characterized along with their effects on cellular viability. The results indicate that both NPs showed an equivalent behavior in terms of uptake and biocompatibility. In depth analysis of NP uptake on cell biology evidenced that these nanoparticles induced dose dependant genotoxic effects. This phenomenon was significantly reduced by PEI acetylation. Endocytosed PEI-NPs trigger an oxidative stress on cells by inducing the production of reactive oxygen species (ROS), which cause DNA damage without apparently affecting cell viability. Thus, the genotoxicity of nanoparticles that could be used as non-viral drug carriers, should be evaluated based on the intracellular level of ROS generation and DNA damage even in absence of a significant cell death.

3.2 Introduction

In the last decades it is increased the interest in the development of drug delivery systems, with special emphasis on the design and fabrication of delivery platform for cancer treatment and regenerative medicine. In general, these delivery systems are engineered to minimize drug degradation upon administration, prevent undesirable side effects, and sustain and/or increase drug's bioavailability in the targeted area. More recently, several studies took advantage from basic chemistry to obtain structurally simple materials, where the topography and nanoscale dimensions are crucial to promote cell interactions mediating intracellular drug delivery [1][2]. Indeed, engineered nanomaterials possess distinct physicochemical properties as a result of their nanometre-scale size, increased surface area, variable chemical composition, surface structure, and shape [3]. Although impressive from an applicative point of view, the novel properties of nanomaterials can generate adverse effects on biological systems, since their size increases the possible interactions at

the cellular, subcellular, and protein levels [4]. In addition, some conventional nanomaterials that are used in biomedical and pharmaceutical applications have also exhibited considerable toxicogenomic effects. A study of DNA delivery systems comprised of common transfection agents (i.e., lipofectamine and oligofectamine), revealed marked changes in the expression of several genes in epithelial cells [5]. In another study, it was shown that the polycationic polyethylenimine (PEI), formulated with plasmid DNA and administered to mouse lungs, activated p38 pathway involved in endocytosis, phagocytosis and hydrogen peroxide production [6]. The considerable toxicity of such PEI polyplex formulations observed in vitro and in vivo was, therefore, linked to a general oxidative stress reaction leading to inflammatory responses, cell cycle dysregulation and DNA damage.

Clearly, analysis of toxicogenomic responses of new polymers and nanomaterials along with conventional assessment of their toxicity in animal models is now becoming essential for development of safe pharmaceutical formulations with wide therapeutic index and low toxicity profiles [3]. It is therefore imperative that direct effects on DNA must be examined to provide preliminary information on the potential genotoxicity of nanomaterials.

However, while the cytotoxicity of specific nanoparticles (NPs) traditionally evaluated by determining the extent of cell survival after exposing NPs to cells, has shown reproducible results, there are only some conflicting evidences about the genotoxicity of the same NPs. Since the genotoxicity behavior of NPs is quite distinguished from bulk materials, there is an urgent call for the establishment of principles and test procedures to ensure the safety of NPs. Taking into account that the cytotoxic and genotoxic potential of a nanomaterial is most likely dependent on chemical properties, we have synthesized and biologically tested PEI-based

copolymers modified or not by the addition of acetyl groups to amines in the PEI backbone [7].

Bearing in mind that in vitro tests involving nanoparticulate systems represent a key aspect of current investigations on clinical applications of nanomaterials, we evaluated the genotoxicity of PEI-NPs using human primary cells as targetable cellular models. We evaluated also if acetylated PEI-NPs may represent an effective alternative to classical PEI-NPs for intracellular DNA delivery.

3.3 Materials and Methods

Cell culture and materials

Human umbilical vein endothelial cells (HUVEC) were from Life Technologies (Italy) and cultured in accordance with the manufacturer's instructions. Branched polyethylenimine (PEI, MW: 25 kDa), poly(vinylalcohol) (PVA), acetic anhydride, 5,5-dimethyl-pyrrolidine N-oxide (DMPO), phenyl N-tert-butyl nitrene (POBN), dicyclohexylcarbodiimide (DCC), N-hydroxysuccinimide (NHS), 2,4,6-trinitrobenzenesulfonic acid (TNBS), D₂O, coumarin-6, etoposide, dimethyl sulfoxide (DMSO), phytohemagglutinin (PHA), bromodeoxyuridine were obtained from Sigma Aldrich (Italy). Dialysis membranes (molecular weight cut off 3500 Da) were from Spectrum Laboratories. d,l-Lactide/glycolide copolymer (PLGA, PURASORB® , inherent viscosity 0.20 dl/g) was a generous gift from PURAC (Gorinchem, The Netherlands). Endonuclease III (Endo III) and formamidopyrimidine-DNA glycosylase (Fpg) were from New England Bio-Labs (United Kingdom). Lactate dehydrogenase (LDH) Release Assay and WST-1 reagent

were from Roche Applied Science (Milan, Italy). pHMGFP plasmid, PureYield™ Plasmid Maxiprep System, 1-kb DNA ladder and 6× DNA loading buffer (30% glycerol, 125 mM EDTA, 0.25% bromophenol blue and 0.25% xylene cyanol) were from Promega (Milan, Italy).

Preparation of nanoparticles

Polyethylenimine 25 kDa was acylated using acetic anhydride as reported earlier [8][9]. The modified polymers were characterized by ¹H-NMR in D₂O and FTIR. IR (KBr) ν (cm⁻¹): 3437 (amino stretching), 2932, 1638 (carbonyl stretching). The extent of acetylation was determined through quantification of the free amino groups remaining on the polymer following 2,4,6-trinitrobenzenesulfonic acid (TNBS) method [10]. The extent of acetylation of PEI was also confirmed by ¹H NMR [9].

Copolymer composed of branched PEI or acetylated PEI (AcPEI) and PLGA were prepared using a two-step procedure. First, PLGA was activated by DCC and NHS, then PEI or AcPEI were reacted with activated PLGA at a PLGA:PEI molar ratio of 3:1. Nanoparticles of PEI-PLGA and AcPEI-PLGA copolymer were prepared directly from the reaction solution by using emulsion-solvent-evaporation method. Briefly, the reaction was stopped after 3 h by ice cooling, and a mixed solution of acetone and dichloromethane was added to 100 ml of 1.0% (w/v) PVA aqueous solution, and emulsified using a probe sonicator (Digital Sonifier S-250D, BRANSON) at 200 W of energy output for 5 min on ice bath. The emulsion was stirred overnight on a magnetic stir plate to allow organic solvents to be evaporated and then dialyzed against distilled water for 2 days. PEI-PLGA or AcPEI-PLGA

nanoparticles (PEI-NPs and AcPEI-NPs) were obtained after lyophilization on a speed vac.

Coumarin-6-loaded nanoparticles were prepared with the same procedure except that 0.01% (w/v) of coumarin-6 was added to the dichloromethane/acetone mixture before emulsification. In addition, the coumarin-6 loaded nanoparticles were subjected to a 1.5 cm × 20 cm sepharose CL-4B column (Pharmacia Biotech) eluted with 0.05 M HEPES buffer (containing 0.15 M NaCl, pH 7.0) to remove the non conjugated coumarin-6 [11].

Nanoparticles characterization

Dynamic light scattering (DLS) with a Zetasizer Nano ZS90 instrument (Malvern Instruments, Worcestershire, UK) was used to measure the diameter and zeta potential of the nanoparticles. The hydrodynamic diameter of the freshly prepared PEI-NPs and AcPEI-NPs was measured at 25 °C with a scattering angle of 90° (10 mW He–Ne laser, 633 nm), and the zeta potential was determined by the standard capillary electrophoresis cell of Zetasizer Nano ZS at position 17.0 and at 25 °C. Polystyrene nanospheres (220 ± 6 nm and –50 mV) were used to verify the performance of the instrument. All the average values were performed with the data from six separate measurements. Arithmetic mean and standard deviation were calculated from six consecutive runs, and samples were analyzed using Malvern PCS software. To evaluate if a fluorescence probe remained associated with the particles during a 24 h incubation period, the in vitro release of coumarin-6 from the nanoparticles was investigated under sink condition. Coumarin-6-loaded PEI-NPs and AcPEI-NPs were incubated at 37 °C in pH 4 and pH 7.4 in PBS, which represented the pH in the endo-lysosomal compartment and physiologic pH,

respectively, at a coumarin-6 concentration of 50 ng/ml with a shaking rate at 100 rpm. Periodic samples were subject to centrifugation at $21,000 \times g$ for 45 min and the supernatant was further diluted with methanol and analyzed for the released coumarin-6 by HPLC assay [12].

Cytotoxicity assays

All assays were carefully established to avoid nanoparticle-induced interferences. Cells were seeded in 96-well format and then treated with nanoparticles (PEI-NPs and AcPEI-NPs) in concentrations of 5–300 $\mu\text{g/ml}$ for 24 h of incubation. The stable tetrazolium salt WST-1 is cleaved to a soluble formazan by a cellular mechanism that occurs primarily at the cell surface. This bio-reduction is largely dependent on the glycolytic production of NAD(P)H in viable cells. Therefore, the amount of formazan dye formed directly correlates to the number of metabolically active cells in the culture. For the WST-1 assay, WST-1 tetrazolium salt reagent (Roche, Italy) was added and after 3 h of incubation, supernatants were transferred into vials, and centrifuged with maximum speed at room temperature in a table-top centrifuge (Eppendorf, Italy) to remove interfering particles ($16,800 \times g$). After centrifugation, spectrophotometric readout was performed. Two positive chemical controls were included (1 mM hydrogen peroxide and 200 μM glutamate).

LDH assay is based on the measurement of lactate dehydrogenase (LDH) released into the growth media when the integrity of the cell membrane is lost. For this assay, the supernatant was removed, centrifuged, and analyzed with LDH assay kit (Roche, Italy). As a positive control, cells were completely lysed with Triton X-100 according to the manufacturer's instructions [13]. Proliferation of the cells treated with nanoparticles was determined by trypan blue exclusion. Briefly, a 0.5 ml aliquot

of cell suspension was mixed with 0.5 ml of 0.4% trypan blue dye and left for 5 min at room temperature. Cell number was counted on a hemocytometer and the proliferation indexes (N/N_0 , where N is the total number of cells at $T = 24$ or 48 h and N_0 is the number at $T = 0$) was determined.

Quantitative uptake of coumarin-6-loaded PEI-NP and AcPEI-NP

HUVEC cells were seeded at a density of 105 cells/cm² onto 24-well plates. On the second day, the cells were pre-incubated with Hank's buffered salt solution (Hyclone, Italy) for 15 min, and the medium was replaced with the suspension of nanoparticles (5–300 µg/ml) and incubated for 1 h at 4 °C and 37 °C, respectively, to study the effect of incubation temperature on nanoparticle uptake. In a separate experiment, to study the effect of incubation time on nanoparticle uptake, the medium was replaced with 1 ml (50 µg/ml) suspension of nanoparticles in HBSS per well and the plate was incubated for 15 min, 30 min, 1 h, 2 h and 4 h at 37 °C, respectively. Then the cells were washed with ice-cold PBS for 5 times and solubilized in 400 µl 1% Triton X-100. Cell lysates were subjected to BCA protein assay, lyophilized and used for HPLC analysis of coumarin-6 after methanol extraction. A standard curve of nanoparticles was constructed by suspending different concentrations of nanoparticles (6–1200 ng/ml) in 1% Triton X-100 followed by lyophilization and extraction of coumarin-6 in methanol. The uptake of nanoparticles by HUVEC cells was calculated from the standard curve and expressed as the amount of nanoparticles (µg) uptaken per mg cell protein [12].

Transfection in vitro

We carried out experiment on HUVEC cells, since they are among the hard to transfect cell types [14]. In order to evaluate the transfection efficiency of the NPs in vitro, complexes of nanoparticles and plasmid DNA (1 μ g of pHMGFP encoding green fluorescent protein, Promega, Italy) were formed by first diluting plasmid and the appropriate amount of nanoparticles separately with 150 mM NaCl, pH 7.4, to equal volumes. The nanoparticles suspension was then added to the pHMGFP plasmid solution, vortexed immediately at room temperature and allowed to stand for 30 min to attain complexes (PEI-NPs/DNA and AcPEI-NPs/DNA).

For pHMGFP transfection, cells were seeded in 24-well plate at a density of 1×10^5 per well in medium with 10% FBS. The day after, cells reached 50–70% confluence and the medium in each well was replaced with 0.4 ml of fresh serum-free medium, and 0.1 ml serum-free medium containing naked plasmid DNA, PEI- NPs/DNA or AcPEI-NPs/DNA complex at different nanoparticles/DNA weight ratios and incubated for 4 h under standard incubator conditions. After 4 h, the medium was replaced with 0.5 ml of complete medium and incubated until 24 h post transfection. The analysis of transfection efficiency was performed using a flow cytometer (FACS, BD Biosciences, USA). The percentage of cells expressing the green fluorescent protein (GFP) was then determined from 10,000 events, and reported as a mean \pm standard deviation of at least four samples.

Comet assay

HUVECs were suspended in low melting point agarose in PBS, pH 7.4 and the cell-agarose suspension was pipetted onto a frosted glass microscope slide pre-coated with a layer of normal melting point agarose. Subsequently, each slide was lysed for 1 h at 4 °C in lysis solution (2.5 M NaCl, 0.1 M EDTA, 10 mM Tris, 1% N-

lauroylsarcosine, 1% Triton X-100 and 10% DMSO added prior to use, pH 10.0). The slides were then placed in an electrophoresis tank containing 0.3 M NaOH and 1 mM sodium EDTA pH > 13.0 for 40 min of alkali denaturation, before electrophoresis at 20 V for 30 min at 4 °C. The slides were neutralized by rinsing in neutralizing buffer (0.4 M Tris–chloride, pH 7.5) for 20 min at 4 °C. The slides were finally stained with ethidium bromide (20 µg/ml) for the visualization. Dimethyl sulfoxide (DMSO, 1%) was used as negative control and etoposide (0.5 µg/ml) as positive control. One hundred images were randomly selected from each sample and the comet tail DNA (tail DNA %) was measured. Each experiment was repeated two times. The percentage tail DNA is positively correlated with the level of DNA breakage or/and the number of alkali-labile sites and is negatively correlated with the level of DNA cross-links in the alkaline version of the comet assay [15]. The mean value of the tail DNA % in a particular sample was taken as an index of the DNA damage in this sample.

Oxidative modifications to the DNA bases

We carried out a modified Comet assay to detect oxidized purines and pyrimidines [16]. The cell-agarose suspension slides were prepared as described above for the standard comet assay. After lysing, the slides were incubated at 37 °C for 30 min with (i) endonuclease III (Endo III, 1:1000, 30 min), (ii) formamidopyrimidine-DNA glycosylase (Fpg, 1:1000, 45 min) and (iii) with enzyme buffer (control). Endo III recognizes oxidized pyrimidines while FPG recognizes oxidized purines, specifically 8-oxo-guanine. The slides were electrophoresed and analyzed as above reported.

Reactive oxygen species (ROS) detection

Intracellular ROS levels were investigated by measuring the oxidative conversion of 2',7'-dichlorofluorescein diacetate (DCFH-DA) to the fluorescent compound dichlorofluorescein (DCF, Molecular Probes, Milan, Italy) as published elsewhere [17]. Cells were exposed to increased concentration of nanoparticles (5–300 µg/ml) for 24 h, washed twice with PBS, and incubated 30 min at 37 °C with 80 µM H₂O₂ - DCF-DA. They were then harvested by scraping, centrifuged, and resuspended in PBS. High DMEM culture medium was used as a negative control. Hydrogen peroxide was used as a positive control to validate the protocol. The fluorescence intensity of cell suspensions was measured with excitation at 480 nm and emission at 530 nm (Molecular Devices, Gemini X fluorescence spectrophotometer, USA).

Effects of nanoparticles on cytokine production in peripheral blood cells

Peripheral blood mononuclear cells (PBMCs) were obtained from healthy volunteers. Peripheral human blood samples, containing sodium citrate 3.8% solution as anticoagulant agent, were centrifuged in Lymphoprep gradient at 2000 × g for 20 min. The obtained PBMCs were diluted in PBS and centrifuged at 1200 × g for 10 min. The isolated cells were resuspended in PBS, plated at 7 × 10⁴ cells/well in a 96-well plate and used to test NPs effect on cytokine production. PBMCs activation was evaluated using a sandwich ELISA kit that allows to perceive and semiquantify the released proteins (Human Cytokine Antibody Array-Panomics, Affymetrics, USA). Briefly, the media of PBMCs cultured with the 300 µg/ml NPs, were incubated with

the array membrane where capture antibodies, specific to particular cytokine proteins, are immobilized.

Then a detection biotin-conjugated antibody binds to a second epitope on the protein, creating an antibody “sandwich” around the cytokine. After streptavidin–HRP incubation, membranes were analyzed using a VersaDoc Imaging System Model 3000 (BioRad, Italy).

Statistical analysis

A statistical analysis of data was carried out using the SPSS for Windows software. Multiple comparison of data was performed using one-way analysis of variance (ANOVA), Bonferroni’s t-test was applied to evaluate differences in the trend of the measured parameters. P-value was obtained from the ANOVA table and the conventional 0.05 level was considered to reflect statistical significance.

3.4 Results

Synthesis and characterization of nanoparticles

To investigate the effects of acetylation on the polymer toxicity, we modified commercially available high molecular weight branched 25 kDa PEI through the addition of acetyl groups to amines in the polymer backbone. To determine the extent of acetylation, PEI and AcPEI were dissolved in D₂O and H-NMR spectra were acquired (Suppl. Figure 1). The extent of primary and secondary amine acetylation was determined by peak integration as reported by Gabrielson and Pack [18]. The reactions produced PEI with $35.6 \pm 0.5\%$ and $52 \pm 1.4\%$ (AcPEI₃₆ and

AcPEI52), respectively of their primary amines acetylated as confirmed by TNBS method. The reduction in concentration of primary amines decreases the concentration of protonable nitrogens of PEI, which might affect DNA binding and hence, toxicity and transfection. Supplementary data associated with this article can be found, in the online version, at <http://dx.doi.org/10.1016/j.toxlet.2012.12.019>.

Particle size and zeta potential have been demonstrated to play important roles in determining the effect on the cell toxicity. Moreover, the measures of size, polydispersion and zeta potential of particles are parameters indicative of their stability in suspension. Size distribution of nanoparticles was assessed using dynamic light scattering (DLS) after dispersion in deionized water (Table 1). The size of the nanoparticles was not affected by PEI acetylation since it was between 90 and 105 nm for all PEI-NPs and AcPEI-NPs preparations examined, with a polydispersion index lower than 0.2. The zeta potential values were found to decrease with the increase in the degree of acetylation, which is consistent with the decreased percentage of available amino functions in the nanoparticles (Table 1).

Table 1. Size distribution and zeta potential of the nanoparticles

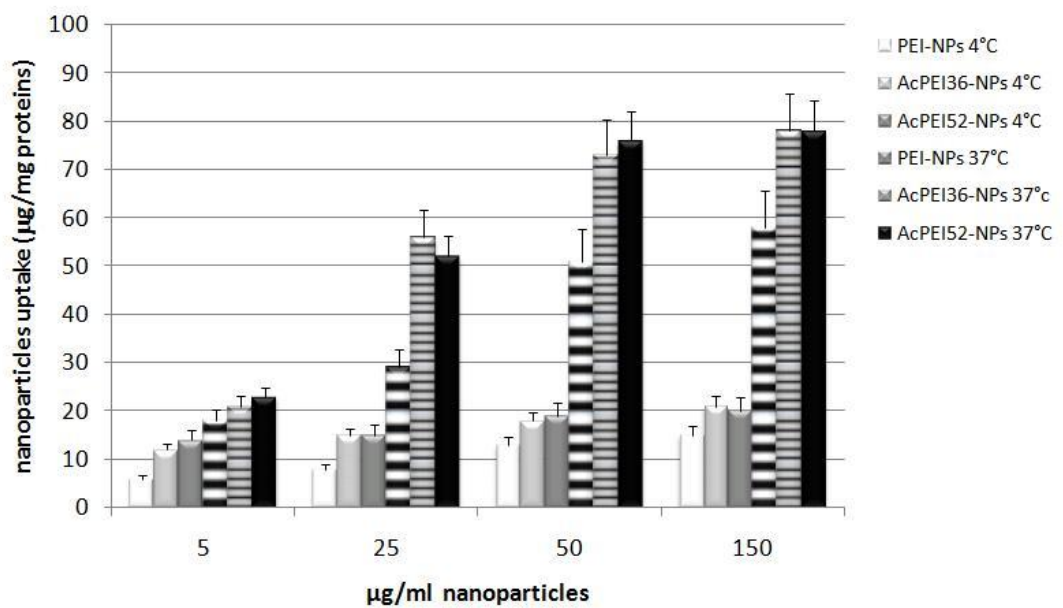
Type of formulation	Average size (nm)	Polydispersity index (PDI)	Zeta potential (MV)
PLGA	62 ± 1.7	0.12 ± 1	-20.5 ± 0.3
PLGA-PEI (PEI/NPs)	90 ± 1.6	0.15 ± 1.6	26.5 ± 1.6
PLGA-AcPEI36 (AcPEI36 -NPs)	105 ± 1.5	0.18 ± 0.4	24.1 ± 1.5
PLGA-AcPEI52 (AcPEI52 -NPs)	110 ± 2.8	0.16 ± 1.2	18.1 ± 1.9

Values represent nanoparticles population range. The subscript of AcPEI indicates the percentage of acetylated primary amines.

Nanoparticles cellular uptake

To evaluate quantitatively the cellular uptake and kinetic internalization of the PEI-NPs and AcPEI-NPs further, the effects of various concentrations of coumarin-6-labeled nanoparticles and different incubation times were investigated in HUVEC cells (Figure 1). As reported in Figure 1A, a concentration-dependent increase in the cell-associated fluorescence intensity was observed in cell after 4 h of incubation, showing almost a first order kinetics. It can be clearly observed that the efficiency of nanoparticles uptake by cells was higher at lower nanoparticles concentration, while it decreased at greater concentration, which indicates the saturated and limited capability of cellular uptake of the nanoparticles (Figure 1A). There were no

statistically significant differences in cell-associated fluorescence between AcPEI36-NPs and AcPEI52-NPs ($p > 0.05$). The nanoparticle uptake was also dependent on the incubation time. The uptake was seen as early as at 15 min, which increased gradually with the incubation time (Figure 1B)



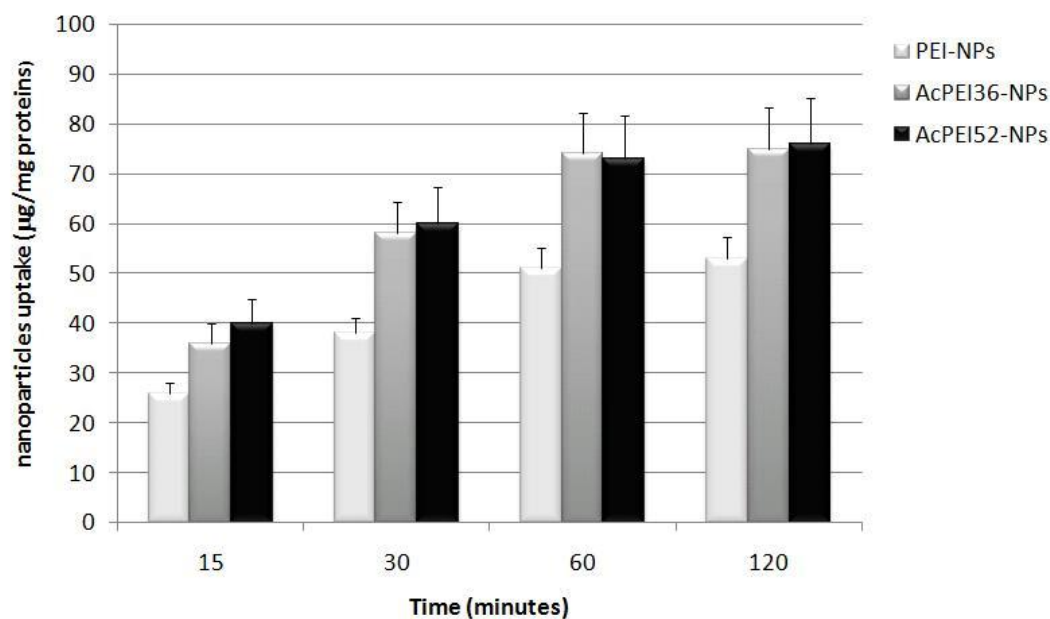


Figure 1. Cellular uptake of coumarin-6-loaded PEI/NPs and AcPEI/NPs at (A) different concentrations incubated at 37 °C and 4 °C for 4 h, and (B) for different incubation periods of time at 50 µg/ml. Cell-associated fluorescence was calculated from the standard curve and expressed as the amount of nanoparticles (µg) uptaken per mg cell protein. Results are expressed as the mean of three independent experiments ± standard deviation (n = 3–4).

Recent papers have demonstrated that less than 0.6% of the incorporated coumarin-6 could leach out from the nanoparticles over 48 h under in vitro sink conditions, and that the raw coumarin-6 cannot be directly internalized by the cells. Thus, the fluorescence measured from our uptake experiments reflects the fluorescent nanoparticles taken up by the cells but not the released.

In vitro gene expression assay

The uptake experiments evidenced that acetylation of PEI did not modify the internalization of NPs, then we decided to evaluate the effect of acetylation on the PEI's ability to promote cellular DNA uptake. It is clear that cell transfection is dependent on DNA/vector uptake efficiency. HUVEC cells were transfected in vitro with 1 μ g of plasmid DNA complexed with polymer at different nanoparticles/DNA weight ratios (w/w) ranging from 5 to 30. Gene transfer efficiency was measured and evaluated for their transfection efficiency in cells by using FACS in absence (Figure 2A) or presence (Figure 2B) of serum. AcPEI-NPs showed transfection efficiency in a dose dependent manner while PEI-NPs reached optimum at PEI-NPs/DNA weight ratio 10 and further decreased till PEI-NPs/DNA weight ratio 20. This is undoubtedly because of the toxicity of PEI-NPs at high concentrations where AcPEI-NPs remained much efficient because of their significant low toxicity.

These data strongly suggest that the transfection efficiency of AcPEI-NPs is superior to that of PEI-NPs. Based on these results, we decided to use AcPEI52-NPs in all the following experiments, unless otherwise specified.

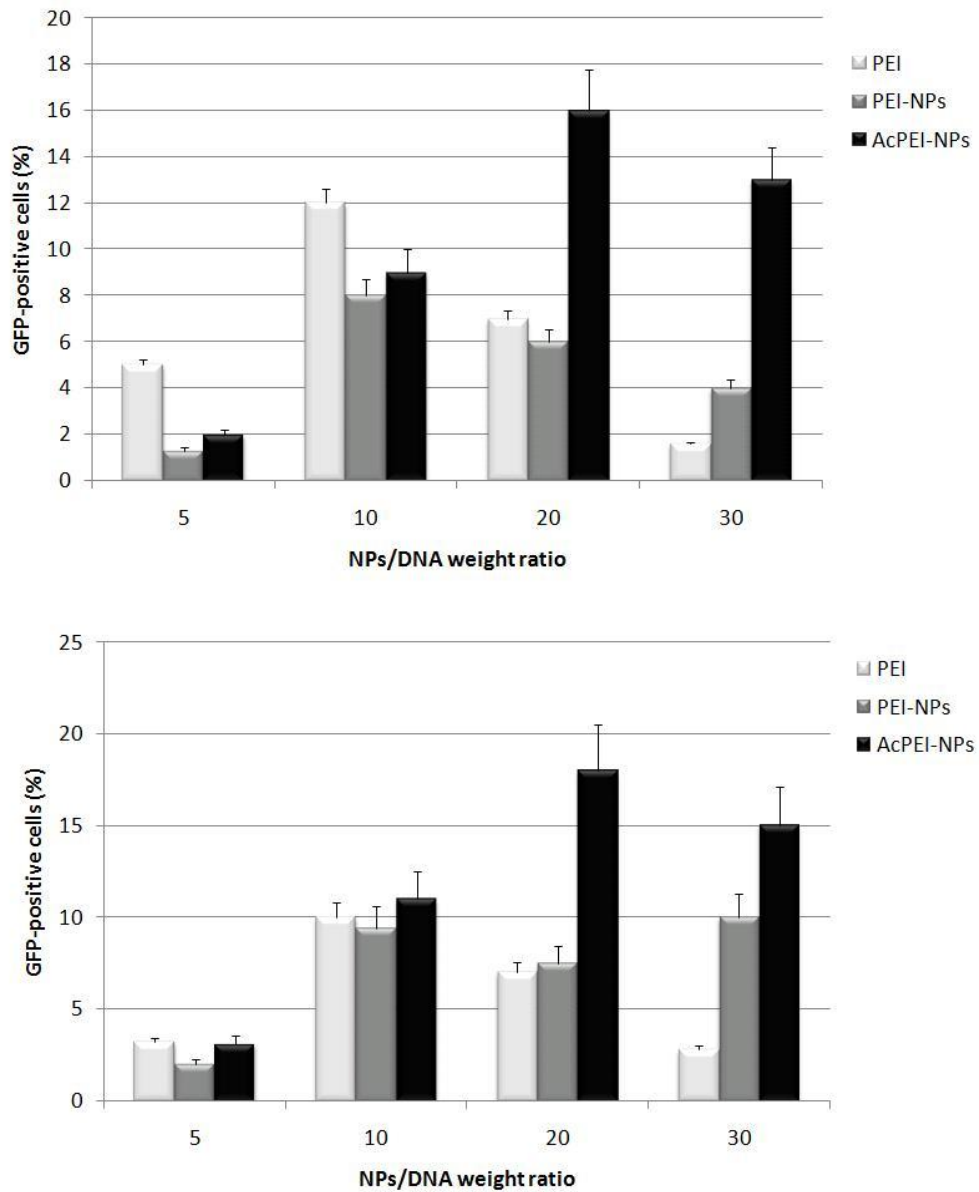


Figure 2. In vitro gene transfection efficiency of PEI/NPs and AcPEI/NPs at various nanoparticles/DNA weight ratios in absence (A) and in presence (B) of serum. Data are the mean \pm SD of four separate experiments. As control we used PEI without PLGA copolymerization (PEI). * $p < 0.05$ compared with PEI.

Cellular nanoparticles toxicity: in vitro assessment

The uptake and transfection experiments suggested that AcPEI- NPs were more effective as DNA transfection agent than PEI-NPs. So, we decided to carry out in depth analysis on cyto- and genotoxicity of such compounds to evaluate if they could be considered a valid alternative as drug carrier. NP-dependent effects on cell viability and cytotoxicity were assessed after 24, 48 and 72 h of incubation by applying the WST-1 and the LDH assays in parallel. Both toxicity assays were optimized to reduce potential particle interferences and both produced similar results (Figure 3A and B). No decrease of cell viability was observed on the cells tested after 24, 48 and 72 h of incubation with AcPEI-NPs added at 5, 50, and 300 $\mu\text{g/ml}$. Then, we examined the effect of various concentrations of PEI-NPs and AcPEI-NPs on cell proliferation. Cell proliferation indexes (N/N0) were assessed by cell counting and trypan blue exclusion assays [19]. In control conditions, cell number increased at 24 h ($N/N0 = 1.1 \pm 0.03$) and 48 h ($N/N0 = 2.3 \pm 0.19$). When cells were cultured with PEI-NPs and AcPEI-NPs, no significant change in the proliferation rate was observed even when very high PEI-NPs concentrations were added to culture medium (300 $\mu\text{g/ml}$).

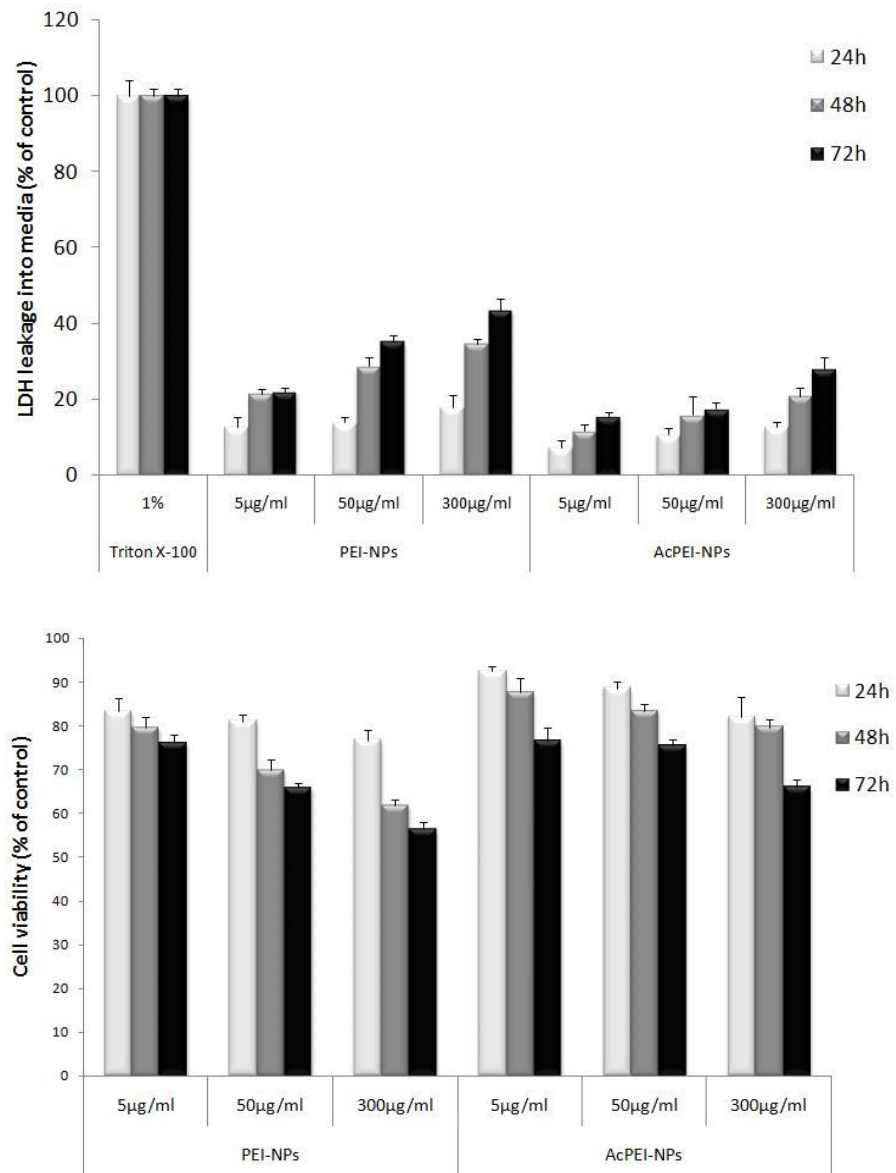


Figure 3. Cytotoxicity of the nanoparticles tested via LDH (A) and WST-1 (B) assays after 24, 48 and 72 h of incubation. In each experiment, four replicates per concentration were tested. The experiment was repeated three times. The data shown are mean values of three independent experiments (\pm SEM).

The genotoxicity of nanoparticles prepared with PEI (and its formulation components) have been little studied, although this polymer is one of the most widely used in the preparation of polymer nanoparticles. Studies of the impacts of these nanostructures on living organisms and on the environment are therefore needed so that the safety of these nanosystems can be assessed before they become even more widely commercialized. The literature describes several assays that can be used to determine genotoxicity in polymeric nanostructured systems, including assays involving plants such as the *Allium cepa* chromosome aberration test [20][21] single- and double-strand breaks (SSB and DSB), and alkalilabile sites (ALS). The general trend was that PEI-NPs caused a concentration-dependent increase in the percentage of tail DNA in the alkaline version of the comet assay. The increase was three times for the highest PEI-NPs concentration (300 µg/ml, $p < 0.05$). No changes in the percent tail DNA was observed with AcPEI-NPs at the same PEI-NPs concentration, which indicates that AcPEI-NPs did not introduce DNA-strand breaks in HUVEC cells.

We carried out also an alkaline Comet assay using lesion-specific enzymes to detect oxidized pyrimidine and purine to evaluate if the observed DNA damage induced by PEI-NPs treatment is related to oxidative events. In order to identify the oxidative damage, two repair-specific enzymes (ENDO III and Fpg) that recognize and cut oxidized DNA bases were employed. Figure 5 shows DNA damage of HUVEC exposed to PEI-NPs or AcPEI-NPs followed by post-treatment with Endo III and Fpg for 1 h, compared with cells without treatment with these enzymes. DNA from HUVEC incubated with the highest concentration of PEI-NPs and treated with Endo III or Fpg showed a significantly ($p < 0.05$) increased DNA damage compared with that in cells treated with AcPEI-NPs or not treated with enzymes. The increase observed for Fpg was not significantly different from that for Endo III. These results

demonstrate that ROS induced by PEI-NPs enhanced the oxidative damage of DNA, including oxidation of purines and pyrimidines.

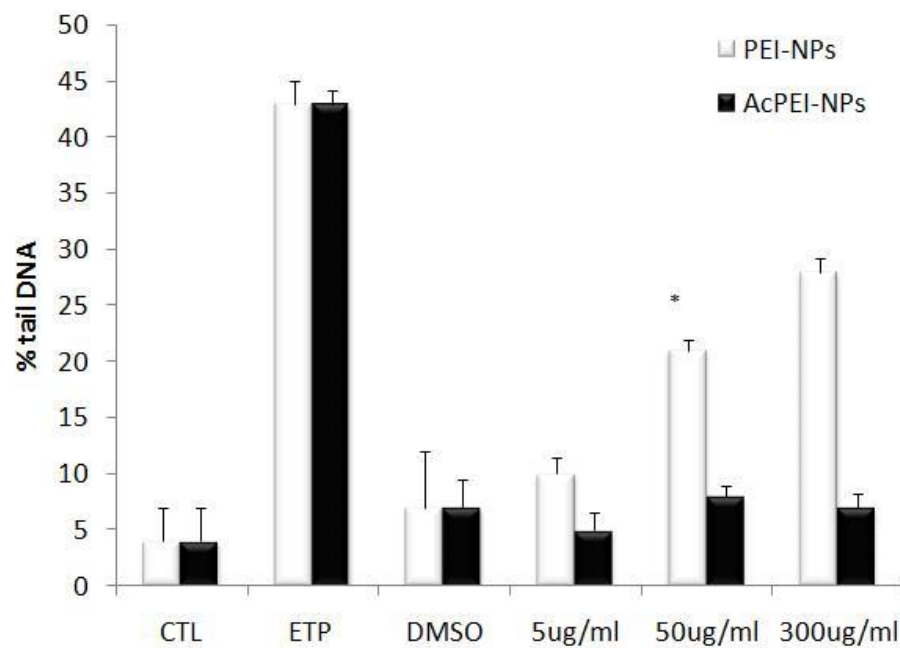


Figure 4. DNA damage (% tail DNA measured using the comet assay) in HUVEC cells exposed to various concentrations (5, 50 and 300 $\mu\text{g/ml}$) of PEI/NPs or AcPEI/NPs. ETP (etoposide, 0.5 $\mu\text{g/ml}$) and DMSO (dimethyl-sulfoxide 1%) were used as positive and negative control, respectively. The results are expressed as the mean \pm SD of three separate experiments for each data point of the olive tail moment (% DNA in tail \times distance between centres of mass). Values are significantly different from control: * $p < 0.05$ compared with PEI/NPs.

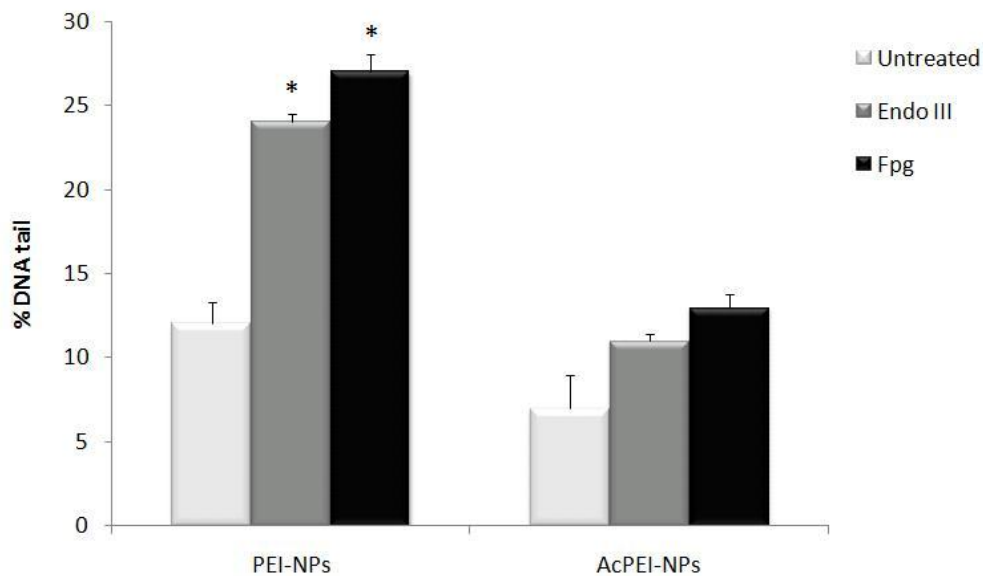


Figure 5. Oxidative modifications to the DNA bases evoked by nanoparticles. DNA damage in HUVEC cells exposed to PEI/NPs or AcPEI/NPs at 300 $\mu\text{g/ml}$ and measured as percentage of DNA in the tail in the alkaline comet assay as probed by endonuclease III and formamidopyrimidine-DNA glycosylase at 1 $\mu\text{g/ml}$. The number of cells scored for each treatment was 100. The results are expressed as the mean \pm SD of three separate experiments for each data point. * $p < 0.05$ compared with untreated.

Supplementary information (S1) reports the contribute of PEI-NPs in causing sister chromatide exchanges and the formation of micronuclei in peripheral lymphocytes, effect that was not induced after transfection with AcPEI-NPs.

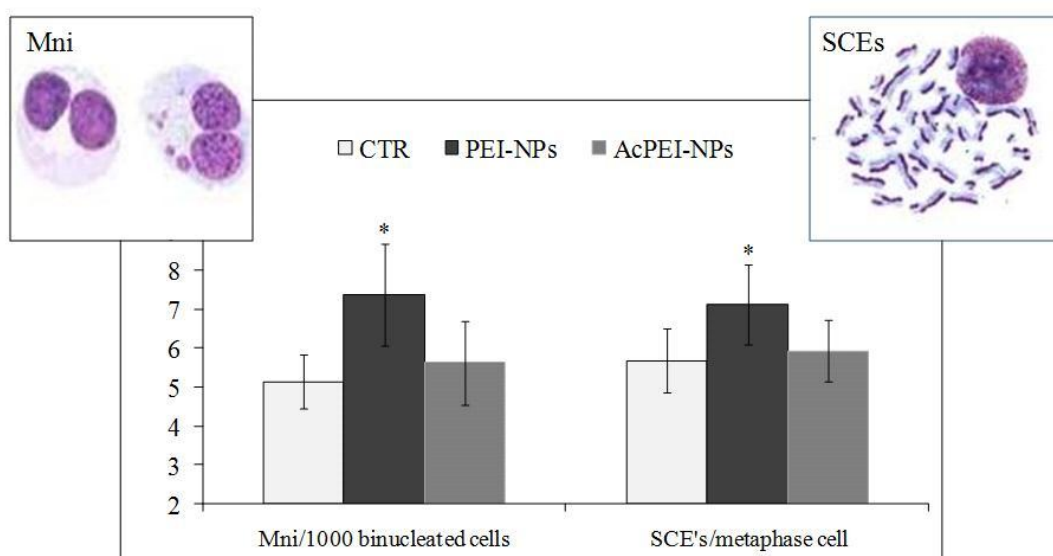


Figure S1. Quantitative evaluation of the formation of micronuclei (Mni) and sister chromatid exchanges (SCEs), after cell exposure to PEI-NPs and AcPEI-NPs.

Intracellular ROS production

The presence of oxidized DNA base following incubation of cells with NPs and literature data showing that nanoparticles may elicit production of reactive oxygen/nitrogen species [3][23] prompted us to evaluate the level of intracellular ROS following incubation with NPs.

The potential for our nanoparticles to induce oxidative stress was tested by evaluating intracellular ROS using the DCFH-DA assay. ROS generation in HUVEC cells following 24 h of exposure to PEI-NPs and AcPEI-NPs at different concentrations is shown in Fig. 6. Fluorescence intensity, indicative of oxidative stress (OS) in the cells, increase in a dose-dependent manner after treatment with PEI-NPs, and assumed values statistically relevant if compared to controls and AcPEI-NPs. No increase of ROS production was demonstrated after addition of

AcPEI-NPs to cell culture both at low (50 $\mu\text{g/ml}$) and high (300 $\mu\text{g/ml}$) nanoparticle concentration. The same trend line was obtained testing ROS production in peripheral monocytes, isolated from peripheral blood of volunteers (Figure S2).

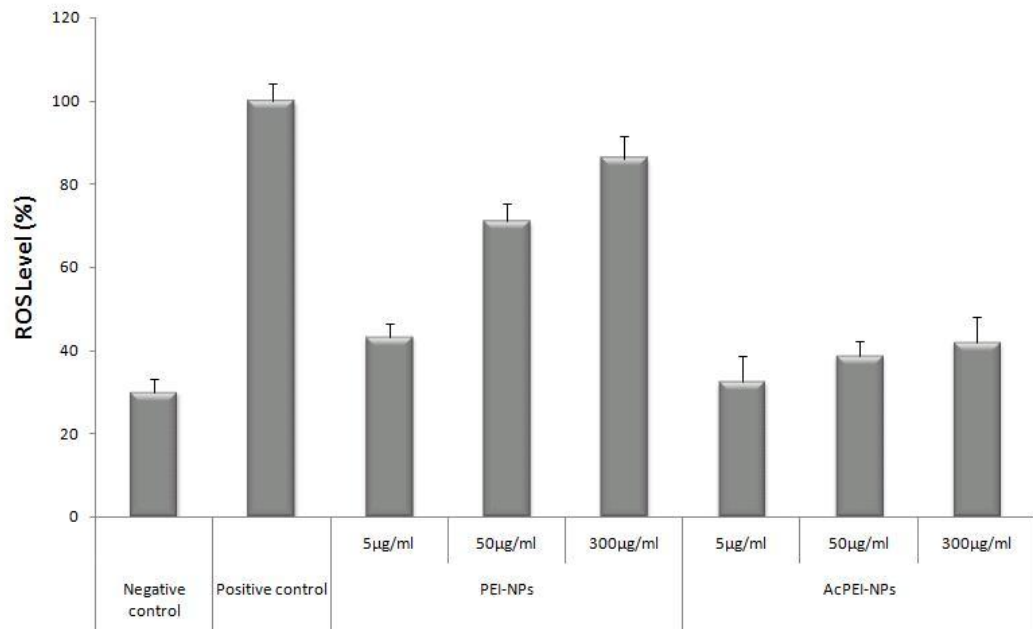


Figure 6. Intracellular ROS generation of PEI- and AcPEI-nanoparticles. HUVEC cells were treated with different concentrations of nanoparticles for 24 h. The ROS level of the positive control was set at 100%. The negative control was high DMEM culture medium, and the positive control was hydrogen peroxide. Values are represented as the mean \pm the standard error of the mean (n = 6). *p < 0.05 compared with negative control.

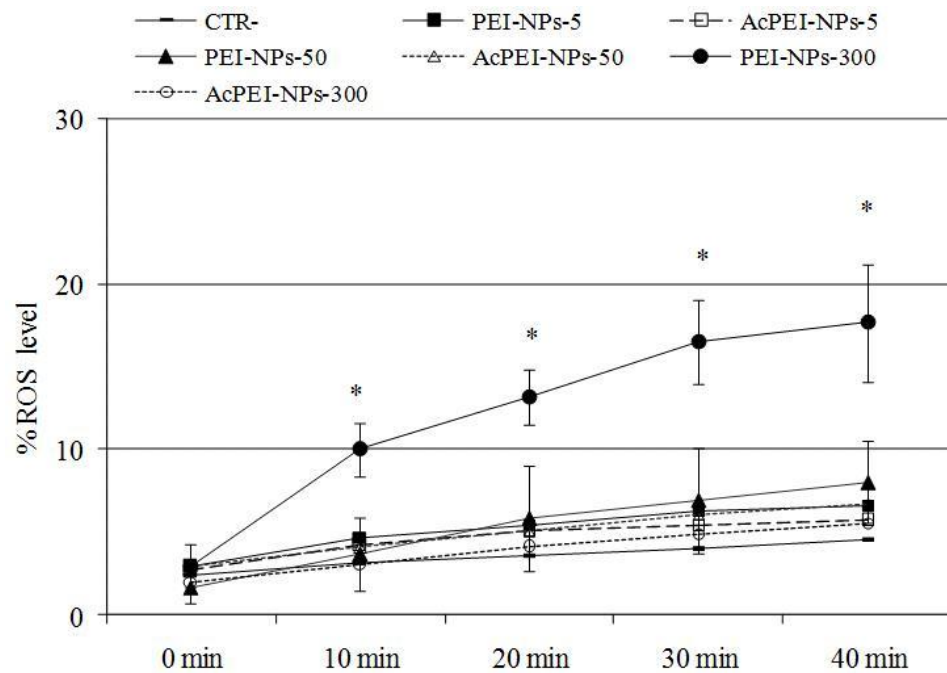


Figure S2. Intracellular ROS generation of PEI- and AcPEI-nanoparticles. Peripheral human monocytes cells were treated with different concentrations of nanoparticles for 40 minutes, with intervals of 10 minutes. The ROS level of the positive control was set at 100%. The negative control was high DMEM culture medium, and the positive control was phorbol-12-myristate-13-acetate (PMA). Values are represented as the mean \pm the standard error of the mean (n = 6). *p < 0.05 compared with negative control.

Effects of nanoparticles on cytokine activation in peripheral blood immune cells

Our results suggest that ROS production by PEI-NP and AcPEI- NP treatment should be a cell autonomous phenomenon, since we use an in vitro cell system. Others demonstrated that nanoparticles may also elicit an inflammatory response that in turn contributes to intracellular ROS production [23]. We decided to carry a preliminary experiment to evaluate whether the nanoparticles might induce an activation of immune-competent cells. To this end the conditioned media of peripheral human lymphocytes and monocytes cultured for 24 h in the presence of 300 μ g/ml of both

PEI-NPs and AcPEI-NPs were analyzed for cytokine secretion. The human cytokine array quantification (Figure 7) did not show any inflammatory cytokine production in cell cultures exposed to nanoparticles compared to control unstimulated cells. This may suggest that, at least in our experimental conditions, the contribution of inflammation response on cyto/genotoxicity of NPs is negligible.

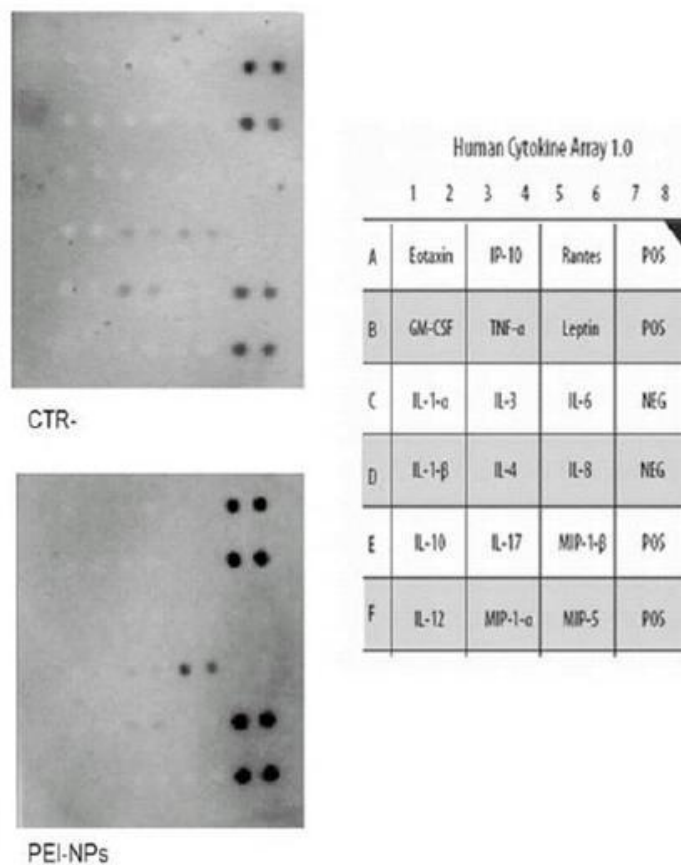


Figure 7. Effects of nanoparticles on cytokine activation in peripheral blood immune cells. Nanoparticles did not induce inflammatory cytokine production in primary human peripheral blood cells cultured 24 h. Cytokine production was evaluated by ELISA and data are expressed as percentage of activation values obtained from control cells treated with an immunotoxic agent (PMA) and are the mean \pm SD of 5 separate experiments.

3.5 Discussion and conclusion

The dramatic increase in the use of nanoparticles (NPs) in medicine has raised questions about the potential toxicity of such materials. Unfortunately, not enough is known about how the novel properties of NPs correlate with the interactions that may take place at the nano/bio interface.

Recent results show that seemingly small changes in NP chemistry can cause significant differences in potency and safety, making thorough characterization critical for the use of NPs in medicine. For example, the difference in electrostatic potential between the stationary layer of fluid surrounding the nanoparticles and the bulk fluid (zeta potential) is an important physicochemical property that has proven to be critical in modulating cytotoxicity effects of nanoparticles [23]. For instance, it is proposed that nanoparticle cytotoxicity could be modulated by controlling the electrostatic interaction between nanoparticles and cellular targets [24]. The effect that structure has on toxicity becomes even more complex if we consider that essential biological functions, such as cellular uptake, can be influenced by the nature of the surface coating on nanomaterials that may be purposely introduced (such as dextran) [25] or modified by the biological environment through adsorption of proteins and other biomolecules [26].

Polyethylenimine (PEI) is an efficient non-viral gene delivery vector readily taken up by cells through endocytosis and escapes endosomal degradation by the proton-sponge effect because of its cationic nature [27][28]. However, the major drawback of PEI is its high cell toxicity [29]. Several strategies have been previously studied to reduce the toxicity of this cationic material, and to some extent, also maintain its transfection performance at the same time. These strategies include the use of degradable cross-linkages, synthesis of more linear polymers such as linear PEI,

grafting PEI polymers with hydrophobic moieties, and incorporating liposomal ingredients with cationic polymers to form polysomes [30]. However, an effective and convenient strategy to lower PEI general toxicity remains an unmet need.

Recent studies on PEI have showed that primary and secondary amines increased toxicity, while tertiary amines reduced toxicity [29][31]. Since the amino groups on the polymeric backbone are responsible for condensing DNA and for the proton-sponge effect, modifications of the amino groups have been explored to further improve PEI tolerability. In this work, we have modified the amino groups in polymer backbone by acetylation with acetic anhydride to alter the protonation behavior of the polymer. We demonstrated that acetylated PEI-NPs may represent a valid alternative to PEI-NPs for drug delivery. Despite having a reduced surface charge, acetylated PEI-NPs still forms nanoparticles with a positive zeta potential. The positive charge as well as the enhanced lipophilicity facilitates both their association with the cell membrane and their uptake, which explains the little difference that we demonstrated in the cell uptake of control and acetylated copolymers. As expected, the toxicity of the polymers was reduced by the modifications as shown in Fig. 3 (A and B). These data fit very well with literature, where several modifications of branched PEI led to decreased charge and lower toxicity of the polymer [32]

While it appears that partial acetylation does not affect nanoparticle uptake, and biocompatibility profile, the genotoxicity and ROS production of the two nanoparticulates were strongly dependent by the degree of PEI acetylation.

By definition, genotoxic agents damage DNA, with resulting loss of DNA integrity, mutagenesis, and chromosomal aberrations. Nanoparticles as a group are known to induce genotoxic effects by a variety of mechanisms (Singh et al., 2009) including (1) direct inter-action with DNA; (2) impairment of the cellular transcription and

translation machinery; and (3) inducement of DNA point mutations or/and single- or double-strand breaks via ROS generation. While the first two mechanisms seem to be related with the genotoxicity of quantum dots, due to their ability to enter the nucleus and to localize mainly in perinuclear region, DNA damage caused by ROS seems to be relevant for the genotoxicity of PEI nanoparticles. An increased ROS production results in an oxidative stress when cells fail to compensate for the increased ROS and consequently fail to maintain or restore normal physiological redox-regulated functions, leading to toxicological outcomes, such as DNA damage and expression of inflammatory cytokines. The expression of inflammatory cytokines is determined through transcriptional activation of the gene promoters by redox-sensitive mitogen-activated protein (MAP) kinase and the transcription factor nuclear factor kappa-B (NF- κ B) signaling cascades (Tier 2). Following this concept, we conducted an integrated series of cellular screening assays in presence of PEI-NPs or AcPEI-NPs to quantify (i) ROS production, (ii) cytokine expression, and (iii) DNA damage.

Interestingly, our studies evidenced that the intracellular level of ROS generation and DNA damage were significantly reduced using AcPEI-NPs in comparison with PEI-NPs.

Overall, the substantial reduction in NP-induced cell toxicity and significant decrease in genotoxicity can be achieved especially in nanomedicine applications of NPs. This will be clinically valuable if the therapeutical application of NPs is intended for management of tough-to-treat disease conditions (e.g. cancer) using high dose levels or repeated dosing for which low carrier toxicity is essential.

Acknowledgments

This work was supported by grants from Ministry of Education, University and Research (MIUR) for Research Programs of National Interest (PRIN) Contract no. 1407/Ric/2008.

3.6 References

- [1] Place, E.S., Evans, N.D., Stevens, M.M., 2009. Complexity in biomaterials for tissue engineering. *Nature Materials* 8, 457–470.
- [2] Woo, K.M., Chen, V.J., Ma, P.X., 2003. Nano-fibrous scaffolding architecture selectively enhances protein adsorption contributing to cell attachment. *Journal of Biomedical Materials Research Part A* 67, 531–537.
- [3] Nel, A., Xia, T., Madler, L., Li, N., 2006. Toxic potential of materials at the nanolevel. *Science* 311, 622–627.
- [4] Lanone, S., Boczkowski, J., 2006. Biomedical applications and potential health risks of nanomaterials: molecular mechanisms. *Current Molecular Medicine* 6, 651–663.
- [5] Omid, Y., Hollins, A.J., Benboubetra, M., Drayton, R., Benter, I.F., Akhtar, S., 2003. Toxicogenomics of non-viral vectors for gene therapy: a microarray study of lipofectin- and oligofectamine-induced gene expression changes in human epithelial cells. *Journal of Drug Targeting* 11, 311–323.
- [6] Regnstrom, K., Ragnarsson, E.G., Fryknas, M., Koping-Hoggard, M., Artursson, P., 2006. Gene expression profiles in mouse lung tissue after administration of two cationic polymers used for nonviral gene delivery. *Pharmaceutical Research* 23, 475–482.
- [7] Card, J.W., Magnuson, B.A., 2011. A method to assess the quality of studies that examine the toxicity of engineered nanomaterials. *International Journal of Toxicology* 29, 402–410.
- [8] Nimesh, S., Aggarwal, A., Kumar, P., Singh, Y., Gupta, K.C., Chandra, R., 2006. Influence of acyl chain length on transfection mediated by acylated PEI nanoparticles. *International Journal of Pharmaceutics* 337, 265–274.
- [9] Habeeb, A.F.S.A., 1966. Determination of free amino groups in proteins by trinitrobenzenesulfonic acid. *Analytical Biochemistry* 14, 328–336.
- [10] Li, J., Feng, L., Fan, L., Zha, Y., Guo, L., Zhang, Q., Chen, J., Pang, Z., Wang, Y., Jiang, X., Yang, V.C., Wen, L., 2011. Targeting the brain with PEG-PLGA nanoparticles modified with phage displayed peptides. *Biomaterials* 32, 4943–4950.
- [11] Hu, K., Shi, Y., Jiang, W., Han, J., Huang, S., Jiang, X., 2011. Lactoferrin conjugated PEG-PLGA nanoparticles for brain delivery: preparation, characterization and efficacy in Parkinson's disease. *International Journal of Pharmaceutics* 415, 273–283.
- [12] Haase, A., Rott, S., Manton, A., Graf, P., Plendl, J., Thunemann, A.F., Meier, W.P., Taubert, A., Luch, A., Reiser, G., 2012. Effects of silver nanoparticles on primary mixed neural cell cultures: uptake, oxidative stress and acute calcium responses. *Toxicological Sciences* 126, 457–468.

- [13] Zumbansen, M., Altrogge, L.M., Spottke, N.U., Spicker, S., Offizier, S.M., Domzalski, S.B., St Amand, A.L., Toell, A., Leake, D., Mueller-Hartmann, H.A., 2010. First siRNA library screening in hard-to-transfect HUVEC cells. *Journal of RNAi and Gene Silencing* 6, 354–360.
- [14] Karlsson, H.L., 2010. The comet assay in nanotoxicology research. *Analytical and Bioanalytical Chemistry* 398, 651–666.
- [15] Collins, A.R., Duthie, S.J., Dobson, V.L., 1993. Direct enzymic detection of endogenous oxidative base damage in human lymphocyte DNA. *Carcinogenesis* 14, 1733–1735.
- [16] Kahlert, S., Schonfeld, P., Reiser, G., 2005. The Refsum disease marker phytanic acid, a branched chain fatty acid, affects Ca²⁺ homeostasis and mitochondria, and reduces cell viability in rat hippocampal astrocytes. *Neurobiology of Disease* 18, 110–118.
- [17] Gabrielson, N.P., Pack, D.W., 2006. Acetylation of polyethylenimine enhances gene delivery via weakened polymer/DNA interactions. *Biomacromolecules* 7, 2427–2435.
- [18] Sharma, V., Singh, S.K., Anderson, D., Tobin, D.J., Dhawan, A., 2011. Zinc oxide nanoparticle induced genotoxicity in primary human epidermal keratinocytes. *Journal of Nanoscience and Nanotechnology* 11, 3782–3788.
- [19] Strober, W., 2001. Trypan blue exclusion test of cell viability. *Current Protocols in Immunology*, Appendix 3, Appendix 3B.
- [20] Kumari, M., Mukherjee, A., Chandrasekaran, N., 2009. Genotoxicity of silver nanoparticles in *Allium cepa*. *Science of the Total Environment* 407, 5243–5246.
- [21] Rank, J., Jensen, A.G., Skov, B., Pedersen, L.H., Jensen, K., 1993. Genotoxicity testing of the herbicide Roundup and its active ingredient glyphosate isopropylamine using the mouse bone marrow micronucleus test, *Salmonella* mutagenicity test, and *Allium* anaphase-telophase test. *Mutation Research* 300, 29–36.
- [22] Singh, N., Manshian, B., Jenkins, G.J., Griffiths, S.M., Williams, P.M., Maffei, T.G., Wright, C.J., Doak, S.H., 2009. NanoGenotoxicology: the DNA damaging potential of engineered nanomaterials. *Biomaterials* 30, 3891–3914.
- [23] Sayes, C., Ivanov, I., 2010. Comparative study of predictive computational models for nanoparticle-induced cytotoxicity. *Risk Analysis* 30, 1723–1734.
- [24] Feris, K., Otto, C., Tinker, J., Wingett, D., Punnoose, A., Thurber, A., Kongara, M., Sabetian, M., Quinn, B., Hanna, C., Pink, D., 2010. Electrostatic interactions affect nanoparticle-mediated toxicity to gram-negative bacterium *Pseudomonas aeruginosa* PAO1. *Langmuir* 26, 4429–4436.

- [25] Kunzmann, A., Andersson, B., Vogt, C., Feliu, N., Ye, F., Gabrielsson, S., Toprak, M.S., Buerki-Thurnherr, T., Laurent, S., Vahter, M., Krug, H., Muhammed, M., Scheynius, A., Fadeel, B., 2011. Efficient internalization of silica-coated iron oxide nanoparticles of different sizes by primary human macrophages and dendritic cells. *Toxicology and Applied Pharmacology* 253, 81–93.
- [26] Monopoli, M.P., Walczyk, D., Campbell, A., Elia, G., Lynch, I., Bombelli, F.B., Dawson, K.A., 2011. Physical–chemical aspects of protein corona: relevance to in vitro and in vivo biological impacts of nanoparticles. *Journal of the American Chemical Society* 133, 2525–2534.
- [27] Boussif, O., Lezoualc’h, F., Zanta, M.A., Mergny, M.D., Scherman, D., Demeneix, B., Behr, J.-P., 1995. A versatile vector for gene and oligonucleotide transfer into cells in culture and in vivo: polyethylenimine. *Proceedings of the National Academy of Sciences of the United States of America* 92, 7297–7301.
- [28] Akin, A., Mini, T., Klibanov, A.M., Langer, R., 2005. Exploring polyethylenimine-mediated DNA transfection and the proton sponge hypothesis. *Journal of Gene Medicine* 7, 657–663.
- [29] Fischer, D., Li, Y., Ahlemeyer, B., Krieglstein, J., Kissel, T., 2003. In vitro cytotoxicity testing of polycations: influence of polymer structure on cell viability and hemolysis. *Biomaterials* 24, 1121–1131.
- [30] Dehshahri, A., Oskuee, R.K., Shier, W.T., Hatefi, A., Ramezani, M., 2009. Gene transfer efficiency of high primary amine content, hydrophobic, alkyl-oligoamine derivatives of polyethylenimine. *Biomaterials* 30, 4187–4194.
- [31] Mintzer, M.A., Simanek, E.E., 2009. Nonviral vectors for gene delivery. *Chemical Reviews* 109, 259–302.
- [32] Lv, H., Zhang, S., Wang, B., Cui, S., Yan, J., 2006. Toxicity of cationic lipids and cationic polymers in gene delivery. *Journal of Controlled Release* 114, 100–109.
- [33] Thomas, M., Klibanov, A.M., 2002. Enhancing polyethylenimine’s delivery of plasmid DNA into mammalian cells. *Proceedings of the National Academy of Sciences of the United States of America* 99, 14640–14645.

4 Enhanced gene silencing through human serum albumin-mediated delivery of polyethylenimine-siRNA polyplexes

Elena Nicoli^{1,2}, M. Isabel Syga^{2,3}, Michela Bosetti¹, V. Prasad Shastri^{2,3}

¹Dipartimento di Scienze del Farmaco, University of Eastern Piedmont, Novara, Italy; ²Institute for Macromolecular Chemistry, University of Freiburg, Germany; ³BIOSS–Centre for Biological Signalling Studies, University of Freiburg, Germany

Submitted to PLOS ONE, under peer review

4.1 Summary

Small interfering RNA (siRNA) targeted therapeutics (STT) offers a compelling alternative to tradition medications for treatment of genetic diseases by providing a means to silence the expression of specific aberrant proteins, through interference at the expression level. The perceived advantage of siRNA therapy is its ability to target, through synthetic antisense oligonucleotides, any part of the genome. Although STT provides a high level of specificity, it is also hindered by poor intracellular uptake, limited blood stability, high degradability and non-specific immune stimulation. Since serum proteins has been considered as useful vehicles for targeting tumors, in this study we investigated the effect of incorporation of human serum albumin (HSA) in branched polyethylenimine (bPEI)-siRNA polyplexes in their internalization in epithelial and endothelial cells. We observed that introduction

of HSA preserves the capacity of bPEI to complex with siRNA and protect it against extracellular endonucleases, while affording significantly improved internalization and silencing efficiency, compared to bPEI-siRNA polyplexes in endothelial and metastatic breast cancer epithelial cells. Furthermore, the uptake of the HSA-bPEI-siRNA ternary polyplexes occurred primarily through a caveolae-mediated endocytosis, thus providing evidence for a clear role for HSA in polyplex internalization. These results provide further impetus to explore the role of serum proteins in delivery of siRNA.

4.2 Introduction

Gene therapy is a therapeutic approach that aims to treat otherwise incurable diseases, like viral infections, hereditary disorders and cancer by replacing defective genes and the function of aberrant proteins, through gene incorporation in plasmids or viral vectors for nuclear delivery [1]. Non-viral systems are however widely preferred, in order to reduce cellular toxicity, risk of casual gene insertion in the genome and mutagenesis. More recently the discovery of endogenous mechanisms involved in regulating gene expression, through antisense oligonucleotides, opened a new approach of gene therapy, i.e., targeting a specific gene for silencing in cells. RNA interference (RNAi) is a mechanism triggered in the cell cytoplasm by exogenous small interfering RNA (siRNA) and endogenous microRNA (miRNA), causing the blockade of protein translation, by specific mRNA sequence matching [1][2]. The design of synthetic siRNA sequences of 21-25 bp, is nowadays employed for specific gene knockdown, with increasing number of RNAi-based drugs in clinical trials [3][4].

The delivery of siRNA includes a lot of challenges, regarding *in vivo* injection and intracellular uptake: siRNA sequences are large and negatively charged and do not spontaneously cross the cell membrane. Furthermore, high degradability from extracellular nucleases, poor bloodstream circulation, renal clearance and difficulties to traverse the endothelial barrier to reach a target tissue are the major issues to be considered [5][2].

The condensation of siRNA with linear or branched cationic polymers, with linear or branched structure, is widely used as a packaging and delivery strategy, which ensures protection from degradation while promoting non-specific endocytosis and intracellular escape from endosomes [5][6]. Polycations although commonly used for condensation and delivery of siRNA *in vivo*, show an inverse relationship between backbone charge density and toxicity [7].

The first cationic polymer-siRNA formulation, to enter clinical trial in 2008, was based on cyclodextrin based nanoparticles containing siRNA (CALAA-01) with incorporation of transferrin (Tf), as a targeting ligand for tumors [4]. Transferrin transports iron in the bloodstream and malignant cells up-regulate the expression of the Tf-receptor [8].

Serum proteins have been recently discovered to serve as endogenous targeting ligand and for increasing nanoparticles circulation, after injection [3][9]. In Kim *et al.*, have reported that apolipoprotein A-I, a component of the high density lipoprotein (HDL), can be assembled with liposomes to address siRNA delivery to the liver, through specific receptor-mediated internalization in hepatocytes [10]. Therefore, identifying other possible endogenous targeting molecules in circulation can provide new insights and opportunities in siRNA delivery. Albumin, which is the most abundant protein with physiological function of transporting fatty acids, has been explored extensively for the delivery of therapeutic molecules. Most notable is

the enhanced delivery and efficiency of paclitaxel when delivered as an albumin conjugated nanoparticle, Abraxane®[9]. Additionally, albumin has been demonstrated to accumulate in tumors by the enhanced permeability and retention (EPR) effect and a specific trans-endothelial transportation, and is a promising candidate as a carrier for anti-cancer drugs [11][12]. Work to date on using albumin as a carrier for gene delivery, has focused on the covalent modification of the protein to synthesize cationized albumin (CA) which has then been used for the complexation of oligonucleotides [13].

Encouraged by these findings, in this study, we explored the role of native unmodified human serum albumin (HSA) in mediating the delivery of siRNA in endothelial and breast cancer metastatic cells. Branched polyethylenimine (bPEI), the most routinely of commonly used cationic polymer for nucleic acids delivery, was complexed with siRNA and HSA was added subsequently for electrostatic incorporation via bPEI [14][15]. HSA-bPEI-siRNA ternary complexes significantly improved internalization and silencing efficiency, compared to bPEI-siRNA polyplexes. The presence of free albumin interfered with the internalization, clearly suggesting an important role of HSA in mediating the increased transfection. The HSA participation in the intracellular trafficking was further elucidated by uptake mechanism studies.

4.3 Materials and Methods

Materials

TurboGFP Stealth RNAi™ siRNA sequence was designed to target TurboGFP mRNA, with the on-line program BLOCK-iT™ RNAi Designer

(<http://rnaidesigner.lifetechnologies.com/>). TurboGFP Stealth RNAi™ siRNA was used for the characterization studies of the complexes and the silencing experiments. Sense sequence: *GAUAACGAUCUGGAUGGCAGCUUCA*, antisense sequence: *UGAAGCUGCCAUCCAGAUCGUUAUC*.

BLOCK-iT AlexaFluor 555 control siRNA (Invitrogen, Germany) was used for all the uptake and mechanism studies. Branched polyethylenimine (MW 25 kDa) and Human serum albumin were purchased from Sigma-Aldrich (Germany). Lipofectamine2000 was purchased from Invitrogen (Germany).

Cell culture

Human primary pulmonary microvascular endothelial cells (HPMEC) and human breast adenocarcinoma cell line (MDA-MB-231) were used for all the siRNA transfection studies. MDA-MB-231 cells were provided by the Centre for Biological Signalling Studies (BIOSS) and were genotyped and verified at Labor für DNA Analytik (Freiburg, Germany), while HPMEC were purchased from ScienCell (Provitro, Germany).

MDA-MB-231 were grown in Dulbecco's modified Eagle's Medium (DMEM) (Invitrogen, Germany) supplemented with 10% FBS (Invitrogen, Germany) and 1% penicillin/streptomycin/amphotericin B solution (Pan Biotech, Germany) and HPMEC were cultured in Endothelial Cell Medium (ECM), supplemented with 5% fetal bovine serum (FBS), 1% endothelial cell growth supplement (ECGS) and 1% penicillin/streptomycin/amphotericin B solution (ScienCell, US/Provitro, Germany). Cells were cultured in a humidified incubator containing 5% CO₂ at 37°C.

TurboGFP expressing cells were obtained by TurboGFP stable transfection in MDA-MB-231 and HPMEC, carried by lentiviral transfection of non-silencing control

pGIPZ vector (Thermo Scientific, Germany). MDA-MB-231 and HPMEC were seeded in 6 well-plates at the concentration of 7.0×10^4 cells/well and transfected with the lentiviral solution in complete medium for 24 hours. Puromycin (Sigma-Aldrich, Germany) was added at the concentration of $4 \mu\text{g/ml}$ after 48 hours, to select the successfully transfected population.

Synthesis of the complexes

The ternary complexes were prepared in DNase-RNase free water (GIBCO, Germany). SiRNA was mixed with branched polyethylenimine 25kDa (bPEI) at nitrogen/phosphate groups ratio (N/P ratio) of 10 and incubated at room temperature for 20 minutes. The reaction was performed with a fixed siRNA concentration of $22 \mu\text{g/ml}$ BLOCK-iT Alexa Fluor 555 control siRNA (~13.8 kDa) or $26 \mu\text{g/ml}$ of Stealth RNAi™ TurboGFP siRNA sequence (~16.5 kDa). Human serum albumin 67kDa (HSA) was added at a final concentrations of $0,125 \text{ mg/ml}$, for further 30 minutes. bPEI solution and HSA solution were prepared in DNase-RNase free water and filtered with a $0.22 \mu\text{m}$ cellulose acetate filter (Corning, NY).

Lypofectamine 2000 (Invitrogen, Germany) was used as a positive control, for the silencing experiments. The lipoplexes were prepared with the same siRNA concentration used for HSA-bPEI-siRNA ternary complexes and bPEI-siRNA polyplexes ($26 \mu\text{g/ml}$), following the protocol guide from Invitrogen, in relation to the surface area and in relation to cell density ($2.8 \mu\text{l}$).

Gel Retardation assay and RNase protection assay

RNase protection assay was performed incubating the samples with 17µg/ml of RNase solution (Sigma-Aldrich, Germany) for 30 minutes. Gel retardation assay and RNase protection assay were performed loading 10 µl aliquot of the sample, together with 2µl of loading buffer (Invitrogen, Germany) on a 4% agarose gel, prepared in 1X Tris-boric acid-EDTA (TBE) buffer. The Electrophoresis was conducted in TBE buffer at 100V for 1 hour. Gel bands were stained with Gel red nucleic acid stain (Biotium, US) for 30 minutes and visualized under UV Fusion FX7 (PeqLab). 100bp and 10bp DNA ladder (Invitrogen, Germany) were run in the gel to confirm siRNA integrity.

Determination of Size and Zeta Potential

The mean complexes size, polydispersity index value and zeta potential were measured by DelsaNano C particle analyzer (Beckman Coulter). The complexes were diluted 1:3 with distilled DNase-RNase free water. Morphology and size of the complexes were furthermore studied by Transmission Electron Microscopy (TEM), using Zeiss LEO 912 Omega transmission electron microscope, at an accelerating voltage of 120 kV. The prepared samples was settled in CF-400-Cu square mesh copper grids (Electron Microscopy Sciences, USA) and stained with 2 % uranyl acetate solution. ImageJ software was used to create a statistic of the size of the complexes.

Microscopy transfection studies

Cell microscopy studies were performed in 8-well chambers (Sarstedt, Germany). 1.5×10^4 cells were seeded 24 hours before the experiment in 300 µl of complete

medium. Alexa Fluor 555 siRNA-labeled complexes were incubated at 37°C for two hours. The cells were washed 3 times with Phosphate Buffered Saline *PBS* (GIBCO, Germany) and then were fixed in 4% formaldehyde solution and stained with DAPI using Vectashield Mounting Medium (Vector Laboratories, Burlingame). Images were acquired in multichannel acquisition with Axio Observer Z1 (Zeiss), with 63X oil immersion objective.

Fluorescence activating sorter (FACS) transfection studies

Quantitative siRNA internalization in cells was studied measuring the mean fluorescence value for cell, following the uptake of siRNA-labeled complexes in MDA-MB-231 and HPMEC. Cells were seeded in 24-well plate at a concentration of 1.0×10^5 in complete medium, 24 hours before the experiment. Cells were then transfected with the complexes for 4 hours in 500 μ l of serum free medium. Subsequently, cells were washed with PBS and detached with trypsin from each well. Complete medium with 10% FBS was used to block trypsin action. The cells were centrifuged at 800 rpm 5 minutes and the pellet was resuspended in PBS 2% FBS. The fluorescent signal was detected with FACS Gallios (Beckman Coulter) with FL2 channel (excitation laser:488 nm; emission filter: 575 nm) and the data were analyzed with Flowing software 2 (Perttu Terho). The histograms in Figure 3b and Figure 6 were generated using FlowJo software. Statistics were carried using the student t-test module in Excel for paired datasets, assuming a two-tailed distribution and equal variance between data sets (homoscedastic). A p value of < 0.05 was considered statistically significant.

FACS silencing experiments

Silencing experiments were conducted with MDA-MB-231 and HPMEC expressing TurboGFP. Cells were seeded in 24-well plate at a concentration of 1.0×10^5 in complete medium, 24 hours before the experiment. Cells were transfected with the complexes for 4 hours in 500 μ l of serum free medium. The medium was replaced with complete medium, containing FBS, for 72 hours. Cells were then washed with PBS and detached with trypsin from each well. Complete medium with 10% FBS was used to block trypsin action. The cells were centrifuged at 800 rpm 5 minutes and the pellet was resuspended in PBS 2% FBS. The fluorescent signal was detected with FACS Gallios (Beckman Coulter) with FL1 channel (excitation laser: 488 nm; emission filter 525 nm) and the data were analyzed with Flowing software 2 (Perttu Terho). Lypofectamine2000 (Invitrogen) was used as a positive control. The histograms in Figure 4 were generated using FlowJo software. Statistics were carried using the student t-test module in Excel for paired datasets, assuming a two-tailed distribution and equal variance between data sets (homoscedastic). A p value of < 0.05 was considered statistically significant.

Cell Viability Assay

To test the cytotoxicity of the different formulations, an 3-(4,5-Dimethylthiazol-2yl)2,5-diphenyl-2H-tetrazoliumbromide (MTT) (Sigma, Germany) assay was executed after the incubation with the complexes. Cells were seeded in a 24-well plate 24 hours prior to the experiment. The cells were transfected with the complexes for 4 hours in serum free medium. Then the serum free medium was replaced with complete medium for 72 hours, testing the cell viability at the same time point of the knockdown efficiency. Cells were then washed with PBS and 200 μ l of a solution of MTT (0.25 mg/ml in RPMI without phenol red) was added and incubated for 3 h at

37°C. The MTT solution was removed, 200 µl of DMSO were added to each well and the absorbance at 550 nm was measured using a Synergy HT plate reader (BioTek).

Uptake mechanism studies

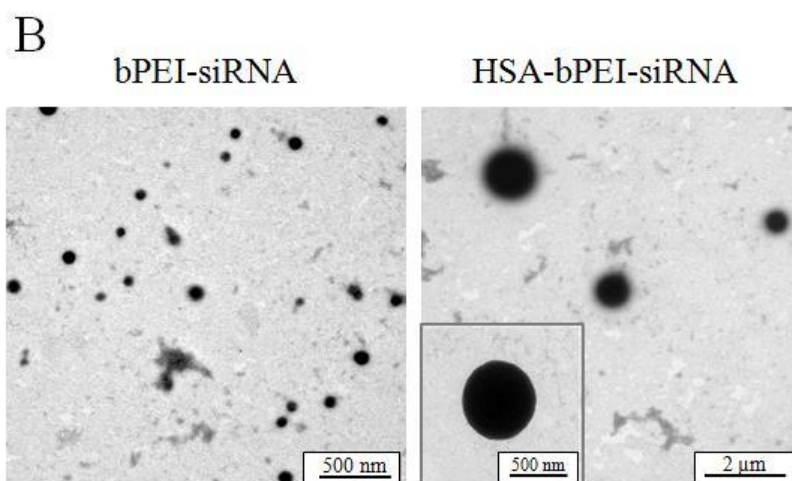
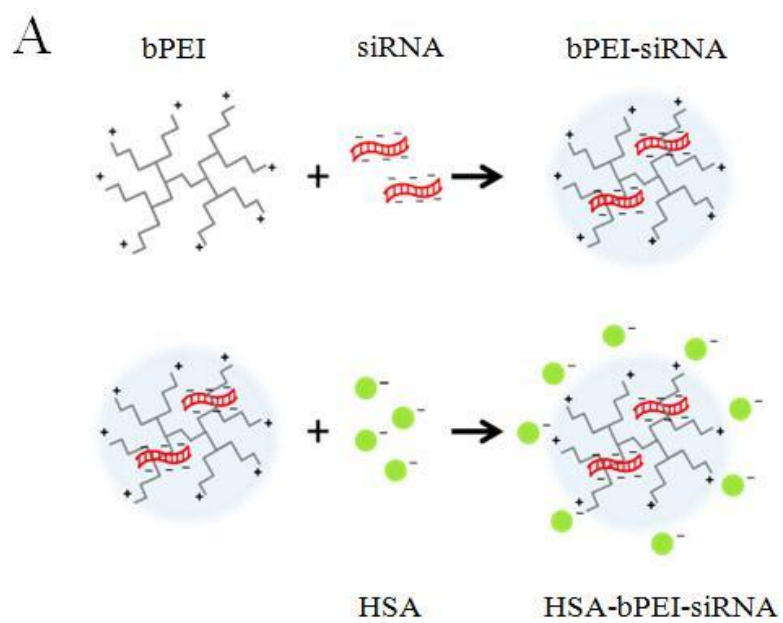
Colocalization studies with selective markers of endocytosis were conducted in both cell lines. Alexa-Fluor 647 labeled transferrin (50µg/ml) and Cholera toxin b (3.5µg/ml) (Invitrogen, Germany) were used as intracellular markers of clathrin-mediated endocytosis and caveolae-mediated endocytosis. Alexa-Fluor 555 siRNA-labeled complexes were transfected for 2 hours in cells and transferrin (Tf) or cholera toxin b (CTB) were subsequently added for 30 minutes. Inhibition studies were performed with specific inhibitors: Chlorpromazine (2µg/ml for MDA-MB-231 and 5µg/ml for HPMEC), Filipin III (5µg/ml) and Nystatin (20µg/ml). All the inhibitors were purchased from Sigma-Aldrich. Cells were pre-treated for 20 minutes with each inhibitor, in serum free medium, and then incubated with the siRNA-labeled complexes for 2 hours, without removing the inhibitors. Cells were then trypsinized and collected for FACS fluorescence detection. The chosen concentrations of each inhibitor were previously tested for cell viability with MTT test (S3).

4.4 Results and discussion

Characterization of HSA-bPEI-siRNA ternary complex.

Due to the negatively charged backbone, delivery of siRNA to cells requires it to be packaged as a complex with a polycation. Typically, PEI (linear or branched) is the

polycation of choice. This complexation is important to ensure the stability of the siRNA through RNAses and to promote the entry of siRNA into cells. The ternary complexes were formed using branched polyethylenimine (bPEI) and HSA was introduced as an aqueous solution at pH 7, where it is negatively charged, thereby capable of interacting with the positive charged amino groups of PEI (Figure 1a). The introduction of HSA to bPEI-siRNA complex induced only modest changes in zeta (ζ)-potential. However, the size of the complexes dramatically increased. This was also confirmed by TEM (Figure 1b, Table1). This increase in size could be due to either aggregation of smaller polyplexes or reorganization of the PEI-siRNA complexes, in presence of albumin, to a more thermodynamically stable structure. We first ascertained if the addition of albumin would impact the capacity of siRNA to complex with bPEI. Gel Retardation assay showed total siRNA incorporation by the complexes (Figure 1c) and the ability to protect the siRNA against extracellular endonucleases was verified by RNase Protection assay (Figure 1d). HSA adsorption on nanocomplexes surface did not alter the ability of siRNA condensation and RNase cleavage protection, which are characteristic of the bPEI-siRNA system [16].



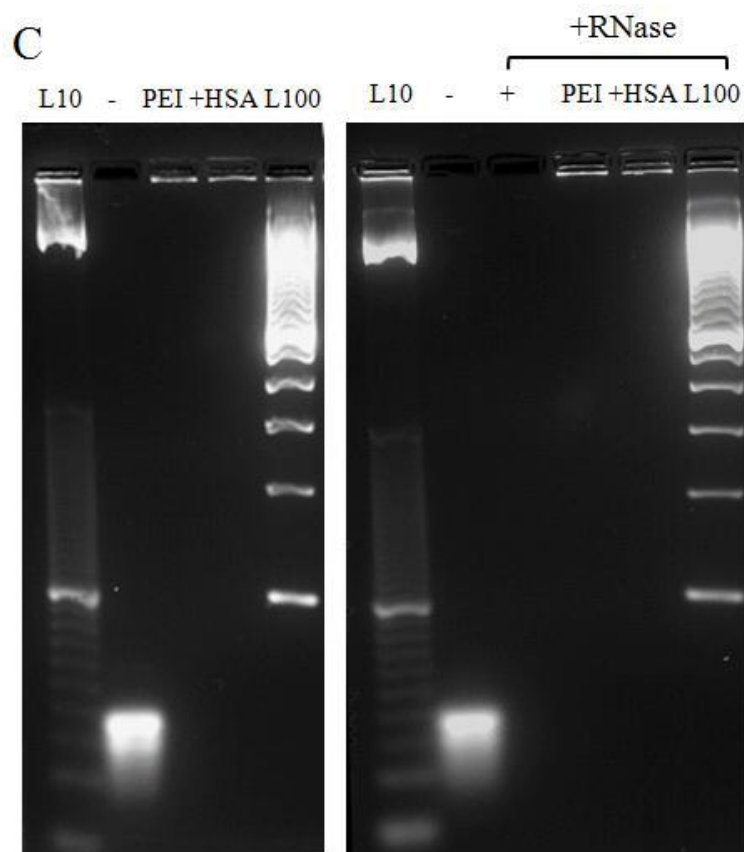


Figure1. Characterization of HSA-bPEI-siRNA complexes. A) Schematic representation of the two steps formulation protocol, where bPEI-siRNA native interaction was preserved and HSA was used for interacting with the positive charged amino-groups of bPEI. B) Transmission electron microscopy (TEM) images showing the increase in size upon addition of HSA. C) Gel retardation assay, demonstrating siRNA complexation on the top of the gel. From left, 10 base pair ladder (L10); free siRNA (-); PEI-siRNA (PEI); HSA-PEI-siRNA (+HSA); 100 base pair ladder (L100). D) RNase protection assay, indicating efficient siRNA protection from RNase degradation. Complexes are unaltered on the top of the gel, while free RNA is completely degraded. From left, 10 base pair ladder (L10); free siRNA (-); samples incubated with RNase: free siRNA (+), PEI-siRNA (PEI) and HSA-PEI-siRNA (+HSA); 100 base pair ladder (L100).

Table1. Size - zeta potential characterization and polydispersity index value (n=12)

	Size (nm) TEM	Size (nm) DLS	PDI	ζ -potential (mV)
PEI-siRNA	84 ± 17	103 ± 12	0.2	+ 2.4 ± 4
HSA-PEI-siRNA	842 ± 230	959 ± 170	0.2	- 4.5 ± 5

HSA colocalizes with siRNA in cells and increases transfection efficiency.

To investigate the cell uptake efficiency of the developed system and to understand the role of HSA in mediating siRNA delivery, we performed the transfection studies in metastatic human breast cancer cells (MDA-MB-231) and human pulmonary microvascular endothelial cells (HPMEC).

These cells were chosen as vasculature is important for tumor survival and lung is the prominent organ for epithelial tumor metastasis [17][18]. Additionally, endothelial cells and metastatic breast cancer cells have been shown to actively take up albumin [19][20].

To ascertain the role of HSA in the internalization of siRNA, a colocalization study was undertaken, in MDA-MB-231, with fluorescently labeled siRNA. Fluorescence microscopy revealed that HSA colocalizes with siRNA, therefore, clearly shown that HSA participates in the transcellular uptake of siRNA complexes and their trafficking in the cytosol (Figure2).

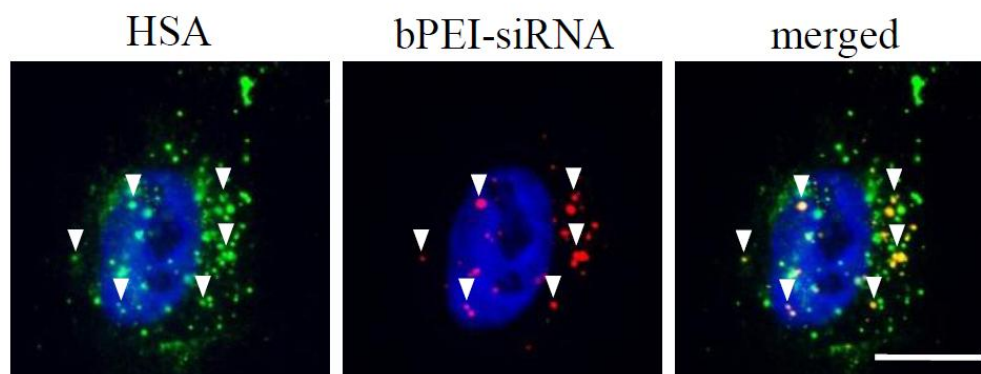
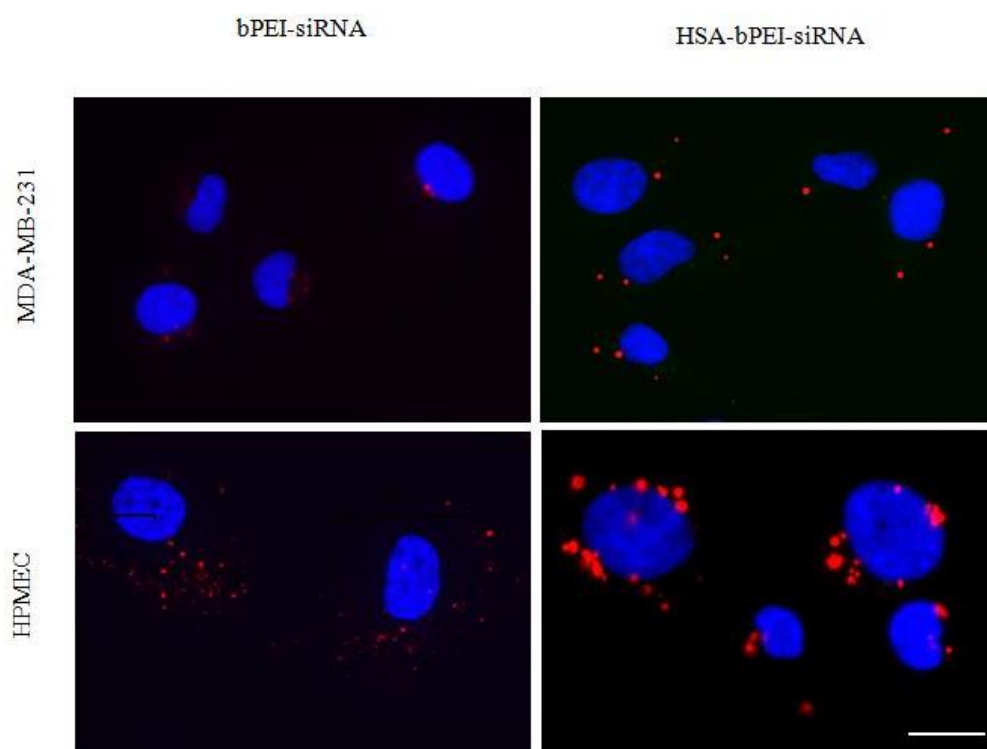


Figure 2. Colocalization of HSA and bPEI-siRNA polyplexes in MDA-MB-231 cells. Fluorescence microscopy revealed that Alexa-fluor 488 labeled HSA and Alexa-fluor 555 siRNA access in the same intracellular trafficking. (DAPI nuclear stain, blue; Alexa-fluor 555 siRNA labeled complexes, red; Alexa-fluor 488 labeled HSA, green). White arrows indicate points of colocalization. Scale bar: 20 μ m.

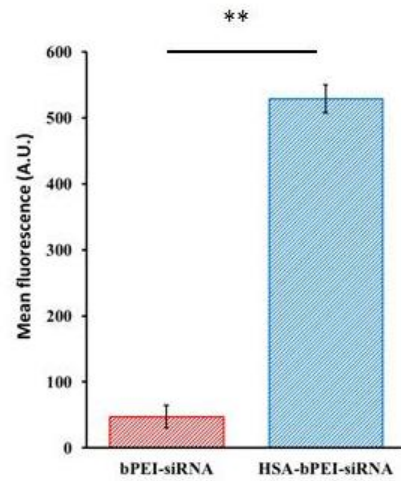
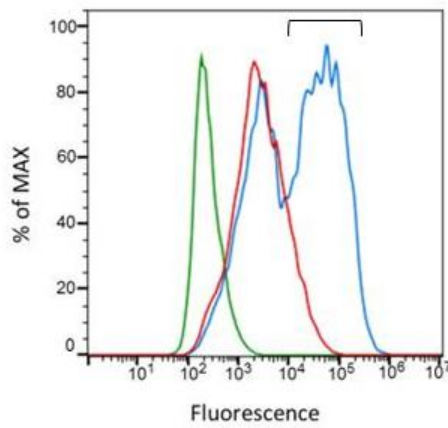
The quantification of HSA-bPEI-siRNA complex internalization was first evaluated in MDA-MB-231 and HPMEC and compared with bPEI-siRNA polyplexes, using flow cytometry (FACS). Alexa dye labeled siRNA formulations were used for the study. To eliminate the interference from the transfection medium, uptake studies were conducted in serum free medium. Fluorescence micrographs of transfected cells are shown (Figure 3a). FACS analysis showed that the ternary complexes were taken up to a significantly greater extent in comparison to bPEI-siRNA polyplexes. The uptake efficiency was about 11 fold greater, in MDA-MB-231, and about 6 fold greater, in HPMEC, over bPEI-siRNA control. In contrast to HPMEC, where a single gaussian distribution was observed, in MDA-MB-231 cancer cells a bimodal distribution was observed, with about 55% of the population showing higher internalization and the remaining population having similar uptake efficiency of bPEI-siRNA (Figure 3b).

A



B

MDA-MB-231



HPMEC

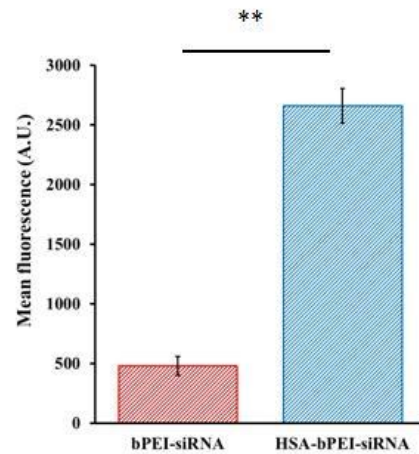
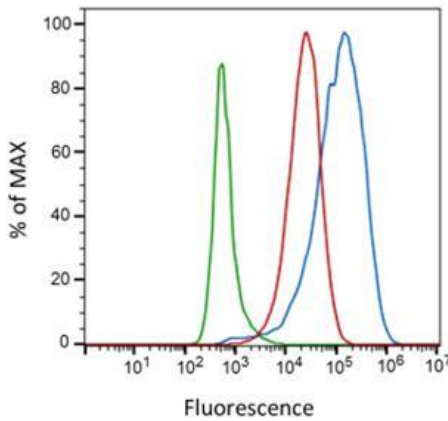


Figure 3. Uptake of HSA-bPEI-siRNA and PEI-siRNA complexes in MDA-MB-231 cells and HPMECs. A) Representative fluorescence micrographs showing siRNA labeled complexes in cells (DAPI nuclear stain, blue; Alexa-fluor 555 siRNA labeled complexes, red) Scale bar: 20 μ m. B) FACS quantitative measurements, expressed as mean fluorescence value for cell, revealed increased uptake by HSA-bPEI-siRNA complexes, compared to bPEI-siRNA control, in both cell lines. Results are shown as mean \pm SD (n=3). MDA-MB-231 cells ** p<0.001, HPMECs **p<0.005.

Ogris *et al.*, have reported that the conjugation of PEI with transferrin (Tf) could enhance gene delivery to tumors. Despite the formation of complexes up to micrometer size, they observed increased cell uptake and gene expression [21]. In this study, the large HSA-bPEI-siRNA complexes also showed higher uptake. It is possible that a loose association of smaller polyplexes occur and this could be the reason of the higher efficiency. Further evidence in support of the role of HSA, in transporting or facilitating siRNA internalization, was obtained by carrying out transfection in presence of serum, where albumin is the most dominant protein. Interestingly, the transfection efficiency of the ternary complex was diminished (S1). This could be due to competition between free albumin and albumin associated with bPEI-siRNA for the same transporter on the cell surface.

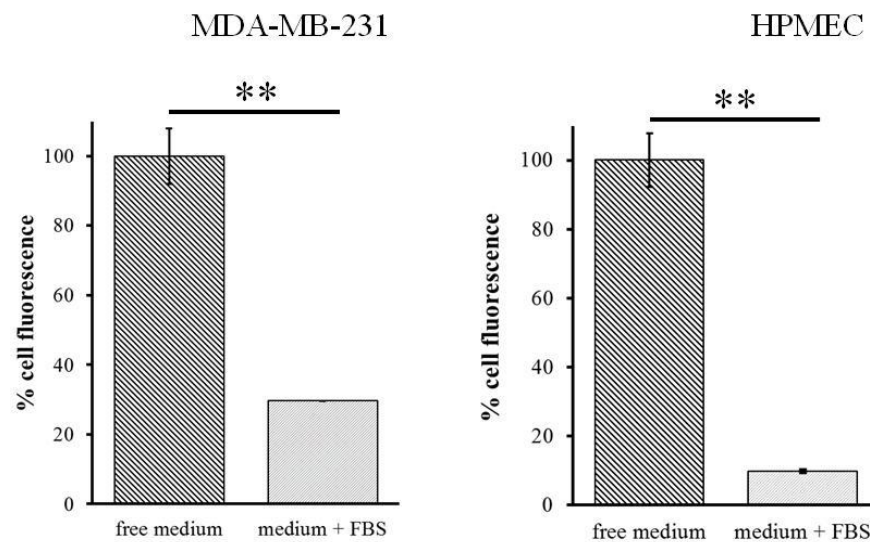
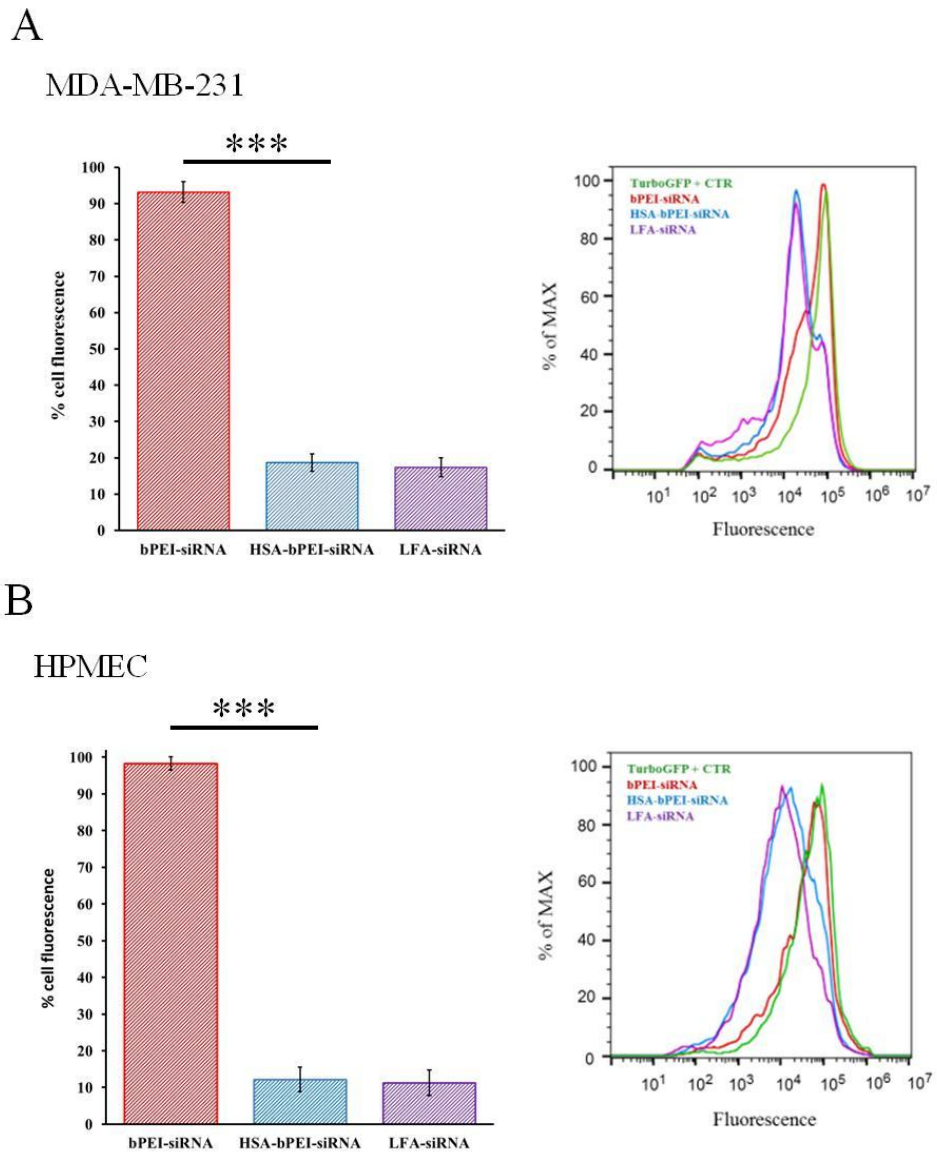


Figure S1. Uptake study comparing HSA-bPEI-siRNA uptake in transfection medium with and without fetal bovine serum (FBS).

HSA increases gene silencing in MDA-MB-231 and HPMEC

To see if the increased uptake efficiency translates into higher availability of free siRNA, a gene silencing study was undertaken using cell lines expressing TurboGFP. In accordance with the higher internalization, HSA-bPEI-siRNA showed about 12 and 53 times more silencing than bPEI-siRNA, in MDA-MB-231 and HPMEC, respectively, and was comparable with Lipofectamine, as seen by the reduced TurboGFP fluorescence in cells transfected with the ternary complex. Similar results were also obtained in HPMEC, indicating that HSA complexation with bPEI-siRNA presents a general strategy for improving the efficiency in siRNA delivery. The lack of any appreciable gene silencing using bPEI-siRNA may be attributed to poor siRNA internalization. In MDA-MB-231, $62 \pm 1.4\%$ of the cell population was efficiently silenced with HSA-bPEI-siRNA complexes, with cell fluorescence reduction of $81 \pm 2.4\%$ (Figure 4a). For HPMEC, $69 \pm 2.0\%$ of cells showed efficient knockdown, having fluorescence reduction of $88 \pm 3.3\%$ for HSA-bPEI-siRNA (Figure 4b). Lipofectamine2000-siRNA showed similar results, in terms of effectively silenced population and knockdown efficiency. The contribution of differences in cell viability, in the observed higher transfection efficiency with the ternary system, can be eliminated, as cells exposed to HSA-bPEI-siRNA and bPEI-siRNA complexes showed comparable viability in MTT assay (S2).



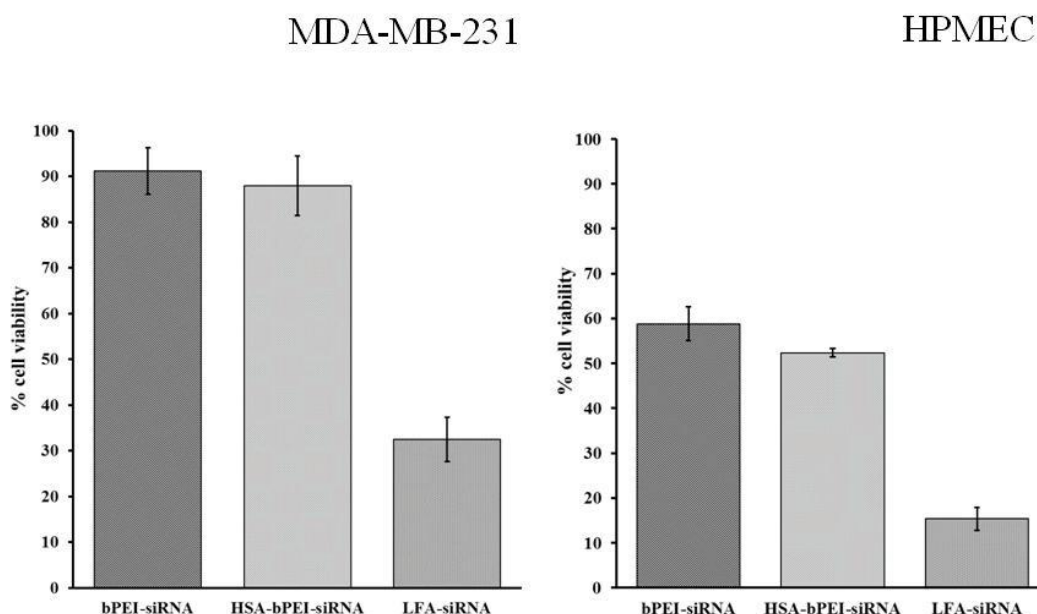


Figure S2. MTT test showing cell viability after transfection.

Uptake Mechanism of HSA-bPEI-siRNA complexes

In order to understand which uptake mechanism mediates the higher siRNA delivery efficiency of HSA-bPEI-siRNA, the involvement of clathrin-mediated endocytosis and caveolae-mediated endocytosis was elucidated. The size of the complexes influences their entry in cells and their intracellular trafficking. Previous studies have demonstrated that nanospheres with diameter lower than 200 nm were preferentially internalized by clathrin mediated pathway, while particles higher than 500 nm followed the activation of caveolae or “caveosomes”, derived from multiple caveolae assemblies on the cellular surface [22][23].

We investigated the uptake inhibition of siRNA-labeled complexes in presence of Chlorpromazine (CPZ), a known inhibitor of the clathrin pathway, and Nystatin

(Nyst) and Filipin III (Fil III), both cholesterol depletors, that block the formation of caveolae. The inhibitors concentrations were chosen so as to have minimal impact on cell viability (S3).

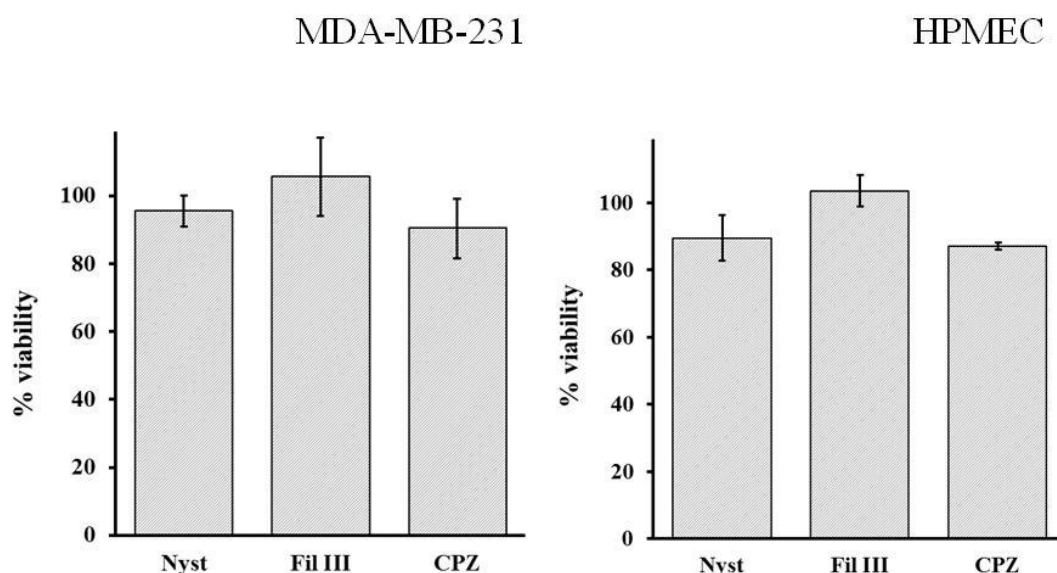
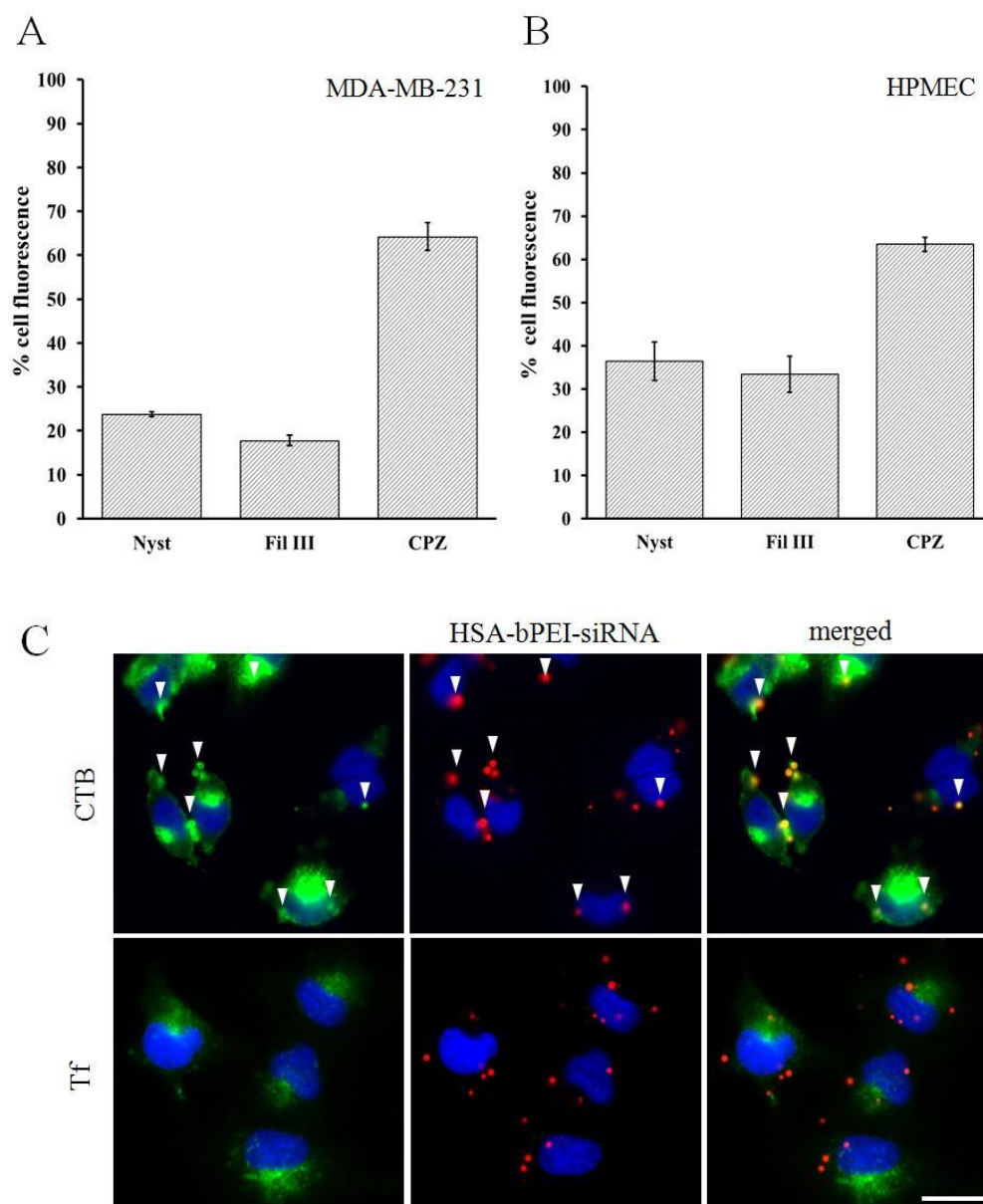


Figure S3. MTT test showing cell viability after incubation with inhibitors, at the concentrations used.

We observed that the ternary complexes are primarily taken up by the caveolae uptake mechanism in both cells, which this uptake pathway was more pronounced in MDA-MB-231. The uptake through clathrin mediated endocytosis was around 30% in MDA-MB-231 and HPMEC (Figure 5a, 5b). Colocalization with cholera toxin b (CTB) in fluorescence microscopy further confirmed the intracellular trafficking through caveolae (Figure 5c, 5d).



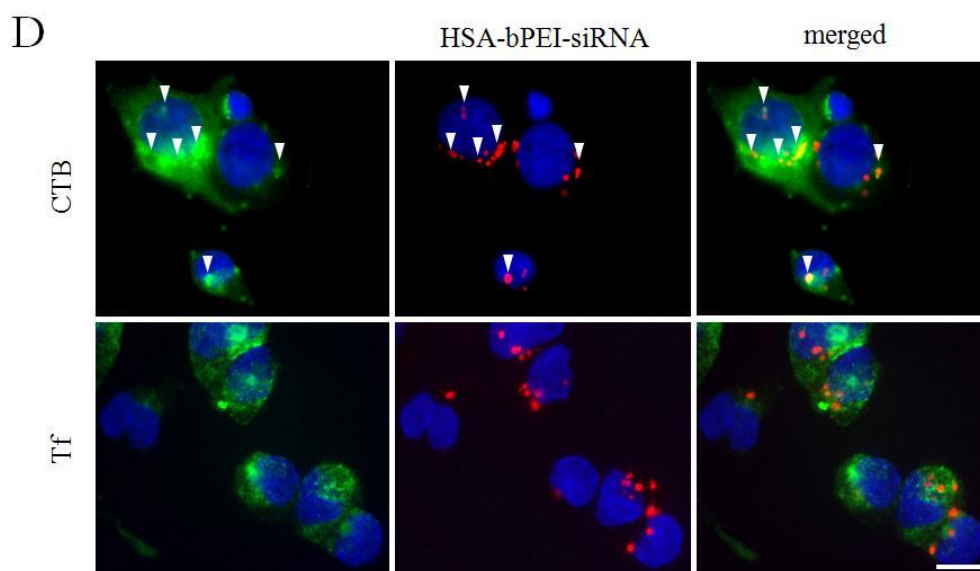


Figure 5. Uptake mechanism study of HSA-bPEI-siRNA complexes in MDA-MB-231 cells and HPMECs. The uptake inhibition was quantified in presence of Nystatin (Nyst), Filipin III (Fil III) and Chlorpromazine (CPZ). Fluorescence reduction was evaluated in FACS. A) Inhibition in MDA-MB-231 cells; B) Inhibition in HPMECs. Results are shown as mean \pm SD (n=3). From the study, partial involvement of clathrin-mediated pathway was observed, with around 30% inhibition by CPZ, and low colocalization with Tf. Predominant activation of caveolae-mediated endocytosis resulted in the internalization of HSA-bPEI-siRNA complexes, in both cell lines. Colocalization study in fluorescence microscopy with uptake markers cholera toxin b (CTB), marker of caveolae-mediated pathway, and transferrin (Tf), marker of clathrin-mediated pathway, is shown in C) MDA-MB-231 cells; D) Colocalization results in HPMEC. White arrows indicate points of colocalization. Scale bar: 20 μ m.

It is well known that endothelial cells have high expression of caveolae [24]. Also multidrug resistant (MDR) cancer cells have been shown to significantly overexpress caveolae [25]. Since we have shown that the particles appear to be taken through caveolae mediated endocytosis, the higher efficiency could maybe due to the fact that this pathway is able to bypass lysosomal degradation [26][22].

Gp60, a protein that is associated with caveolae complexes has been shown to aid in the transport of albumin across endothelial and epithelial barriers [27][20].

Therefore, the specific role of gp60 in enhancing the uptake efficiency of the ternary complex needs to be investigated further.

To further elaborate the role of albumin in the uptake of HSA-bPEI-siRNA complexes, we substituted HSA with bovine serum albumin (BSA) and we made an interesting observation, that the uptake efficiency was diminished by over 2 fold in both cell lines. Although HSA and BSA yielded complexes comparable in size, they showed different uptake profiles (Figure 6) and this clearly shows that human albumin confers specificity in the uptake in human cells. Similarly, it has been postulated that the higher efficiency observed when paclitaxel is covalently linked to HSA (Abraxane®) is due to the active uptake of albumin, through the gp60 receptor [19].

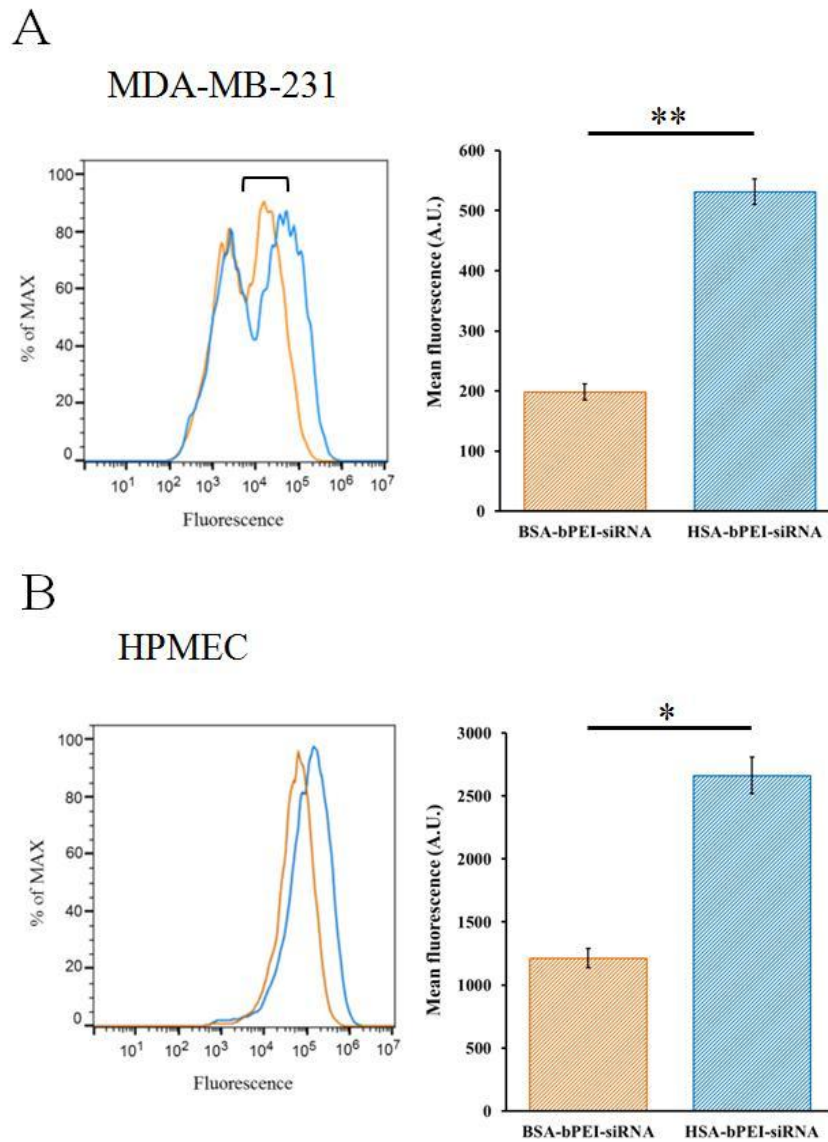


Figure 6. Uptake efficiency comparing complexes formed with BSA and HSA. Uptake efficiency was evaluated by FACS. (A) Study in MDA-MB-231 cells, $**p < 0.005$; (B) Study in HPMECs, $*p < 0.01$. Results are shown as mean \pm SD ($n=3$). Complexes formed with BSA showed reduced internalization compared with HSA, confirming the role of HSA in improving siRNA delivery in both cell lines.

4.5 Conclusion

In this study, we evaluated the role of native HSA in mediating the uptake and silencing of siRNA, towards cells expressing TurboGFP. It was observed that the presence of albumin on the exterior of the bPEI-siRNA polyplexes dramatically improve uptake and gene silencing in both human endothelial and tumor epithelial cells. Inhibition studies suggest a role for caveolae mediated endocytosis in the uptake of the ternary complexes. This is extremely promising for the delivery of siRNA for in vitro studies.

Acknowledgements

The authors thank Dr. Ralf Thomann for the transmission electron microscopy, Esther Kohler for assistance with cell culture, Shengnan Xiang for technical advice regarding inhibition studies and FACS analysis. This work was funded by the 5th INTERREG Upper Rhine Program (Project A21: NANO@MATRIX), the excellence initiative of the German Federal and State Governments (Grant EXC 294; Centre for Biological Signalling Studies, BIOSS), and the University of Freiburg. EN stay at the University of Freiburg was supported by a stipend from the Scuola di Alta Formazione, which is supported by the Compagnia di San Paolo and the University of Eastern Piedmont, Novara.

4.6 References

- [1] T. P. O'Connor and R. G. Crystal, "Genetic medicines: treatment strategies for hereditary disorders.," *Nat. Rev. Genet.*, vol. 7, no. 4, pp. 261–76, Apr. 2006.
- [2] R. L. Kanasty, K. a Whitehead, A. J. Vegas, and D. G. Anderson, "Action and reaction: the biological response to siRNA and its delivery vehicles.," *Mol. Ther.*, vol. 20, no. 3, pp. 513–24, Mar. 2012.
- [3] R. Kanasty, J. R. Dorkin, A. Vegas, and D. Anderson, "Delivery materials for siRNA therapeutics.," *Nat. Mater.*, vol. 12, no. 11, pp. 967–77, Nov. 2013.
- [4] J. E. Zuckerman, I. Gritli, a. Tolcher, J. D. Heidel, D. Lim, R. Morgan, B. Chmielowski, a. Ribas, M. E. Davis, and Y. Yen, "Correlating animal and human phase Ia/Ib clinical data with CALAA-01, a targeted, polymer-based nanoparticle containing siRNA," *Proc. Natl. Acad. Sci.*, vol. 111, no. 31, Jul. 2014.
- [5] K. a Whitehead, R. Langer, and D. G. Anderson, "Knocking down barriers: advances in siRNA delivery.," *Nat. Rev. Drug Discov.*, vol. 8, no. 2, pp. 129–38, Feb. 2009.
- [6] A. Aigner, "Gene silencing through RNA interference (RNAi) in vivo: strategies based on the direct application of siRNAs.," *J. Biotechnol.*, vol. 124, no. 1, pp. 12–25, Jun. 2006.
- [7] A. Malek, O. Merkel, L. Fink, F. Czubayko, T. Kissel, and A. Aigner, "In vivo pharmacokinetics, tissue distribution and underlying mechanisms of various PEI(-PEG)/siRNA complexes.," *Toxicol. Appl. Pharmacol.*, vol. 236, no. 1, pp. 97–108, Apr. 2009.
- [8] K. C. Gatter, G. Brownt, I. A. N. S. Trowbridget, and D. Y. Mason, "Transferrin receptors in human tissues : their distribution and possible clinical relevance," *J Clin Pathol*, vol. 36, pp. 539–545, 1983.
- [9] F. Kratz and U. Beyer, "Serum Proteins as Drug Carriers of Anticancer Agents : A Review," *Inf. Heathcare*, vol. 5, no. 4, pp. 281–299, 1998.
- [10] S. I. Kim, D. Shin, H. Lee, B.-Y. Ahn, Y. Yoon, and M. Kim, "Targeted delivery of siRNA against hepatitis C virus by apolipoprotein A-I-bound cationic liposomes.," *J. Hepatol.*, vol. 50, no. 3, pp. 479–88, Mar. 2009.
- [11] F. Kratz, "Albumin as a drug carrier: design of prodrugs, drug conjugates and nanoparticles.," *J. Control. Release*, vol. 132, no. 3, pp. 171–83, Dec. 2008.

- [12] O. Access and A. B. Malik, "Targeting Endothelial Cell Surface Receptors: Novel Mechanisms of Microvascular Endothelial Barrier Transport," *J. Med. Sci.*, vol. 2, pp. 13–17, 2009.
- [13] J. Han, Q. Wang, Z. Zhang, T. Gong, and X. Sun, "Cationic bovine serum albumin based self-assembled nanoparticles as siRNA delivery vector for treating lung metastatic cancer.," *Small*, vol. 10, no. 3, pp. 524–35, Feb. 2014.
- [14] J.-H. Kang, Y. Tachibana, S. Obika, M. Harada-Shiba, and T. Yamaoka, "Efficient reduction of serum cholesterol by combining a liver-targeted gene delivery system with chemically modified apolipoprotein B siRNA.," *J. Control. Release*, vol. 163, no. 2, pp. 119–24, Oct. 2012.
- [15] T. Pan, Z.-D. Xiao, and P.-M. Huang, "Characterize the interaction between polyethylenimine and serum albumin using surface plasmon resonance and fluorescence method," *J. Lumin.*, vol. 129, no. 7, pp. 741–745, Jul. 2009.
- [16] A. Kwok and S. L. Hart, "Comparative structural and functional studies of nanoparticle formulations for DNA and siRNA delivery.," *Nanomedicine*, vol. 7, no. 2, pp. 210–9, Apr. 2011.
- [17] J. Folkman, "Angiogenesis: an organizing principle for drug discovery?," *Nat. Rev. Cancer*, vol. 6, no. April, pp. 273–286, 2007.
- [18] D. X. Nguyen, P. D. Bos, and J. Massagué, "Metastasis: from dissemination to organ-specific colonization.," *Nat. Rev. Cancer*, vol. 9, no. 4, pp. 274–84, Apr. 2009.
- [19] N. Desai, V. Trieu, B. Damascelli, and P. Soon-shiong, "SPARC Expression Correlates with Tumor Response to Albumin-Bound Paclitaxel in Head and Neck Cancer Patients," *Transl. Oncol.*, vol. 2, no. 2, pp. 59–64, 2009.
- [20] Jane E. Scnitzer and Phil Oh, "Antibodies to SPARC inhibit albumin binding endothelium to SPARC , gp60 , and microvascular," *Am. J. Physiol.*, vol. 263, no. 6, pp. 1872–9, 1992.
- [21] M. Ogris, P. Steinlein, S. Carotta, S. Brunner, and E. Wagner, "DNA/polyethylenimine transfection particles: influence of ligands, polymer size, and PEGylation on internalization and gene expression.," *AAPS PharmSci*, vol. 3, no. 3, p. E21, Jan. 2001.
- [22] J. Rejman, V. Oberle, I. S. Zuhorn, and D. Hoekstra, "Size-dependent internalization of particles via the pathways of clathrin- and caveolae-mediated endocytosis.," *Biochem. J.*, vol. 377, no. Pt 1, pp. 159–69, Jan. 2004.
- [23] M. Lundqvist, J. Stigler, G. Elia, I. Lynch, T. Cedervall, and K. a Dawson, "Nanoparticle size and surface properties determine the protein corona with possible implications for biological impacts.," *Proc. Natl. Acad. Sci. U. S. A.*, vol. 105, no. 38, pp. 14265–70, Sep. 2008.

- [24] J. Voigt, J. Christensen, and V. P. Shastri, "Differential uptake of nanoparticles by endothelial cells through polyelectrolytes with affinity for caveolae," *Proc. Natl. Acad. Sci. U. S. A.*, vol. 111, no. 8, pp. 2942–7, Feb. 2014.
- [25] Y. Lavie, G. Fiucci, and M. Liscovitch, "Upregulation of caveolin in multidrug resistant cancer cells: functional implications," *Adv. Drug Deliv. Rev.*, vol. 49, no. 3, pp. 317–23, Jul. 2001.
- [26] J. Rejman, A. Bragonzi, and M. Conese, "Role of clathrin- and caveolae-mediated endocytosis in gene transfer mediated by lipo- and polyplexes," *Mol. Ther.*, vol. 12, no. 3, pp. 468–74, Oct. 2005.
- [27] C. Tirupathi, "Gp60 Activation Mediates Albumin Transcytosis in Endothelial Cells by Tyrosine Kinase-dependent Pathway," *J. Biol. Chem.*, vol. 272, no. 41, pp. 25968–25975, Oct. 1997.

5 Biocompatible cationic nanoparticles for gene delivery in bone tissue engineering: uptake trafficking, localization and activity in human primary osteoblasts

Bosetti Michela¹, Nicoli Elena¹, Calarco Anna³, Peluso Gianfranco³, Fusaro Luca², Cannas Mario²

¹Dipartimento di Scienze del Farmaco, University of Eastern Piedmont, Novara, Italy; ²Dipartimento di Scienze della Salute, University of Eastern Piedmont, Novara, Italy; ³Institute of Protein Biochemistry, CNR, Naples, Italy

Unpublished results: in progress for Tissue Engineering

5.1 Summary

Polyethylenimine (PEI) is a synthetic cationic polymer that resulted particularly efficient in condensing nucleic acids and in mediating their intracellular uptake [1]. The high density of amino groups allows the formation of nano-scale polyplexes with nucleic acids and electrostatic interactions with the cellular membrane, but the major limitation of PEI applicability *in vivo* is the cytotoxicity, associated with the high positive charge [2][3]. In our previous work we presented the possibility to reduce PEI toxicity by partial acetylation of primary amino groups in PEI backbone, creating a more suitable delivery agent for *in vivo* application. In particular, the acetylation of 50% of the amino groups of PEI (AcPEI), forming AcPEI based nanoparticles by co-polymerization with PLGA (AcPEI-NPs), did not affect the

uptake and gene delivery efficiency of nanoparticles in endothelial cells, but reduced the genotoxic and immunotoxic effect, observed with PEI-NPs [4]. In this work, we considered the application of AcPEI-NPs in bone regeneration and we investigated their uptake efficiency in human primary osteoblasts (hOB) and the impact on cellular differentiation and mineralization, for future utilization in the delivery of genes or small interference RNA (siRNA). We obtained that AcPEI-NPs are internalized by hOB similarly to non-acetylated PEI-NPs, in a concentration and time dependent manner. Furthermore, AcPEI-NPs resulted to not activate cell death, neither by necrosis or apoptosis process. Investigating the effect of NPs on osteoblast activity, we observed that AcPEI-NP, free of the delivery agent, significantly increase alkaline phosphatase (ALP) activity, compared to PEI-NPs and non-transfected hOB. Extensive study on the expression of late differentiation marker and mineralization activation, did not confirm osteogenesis that can be improved with nucleic acids delivery for gene therapy.

5.2 Introduction

Over the last decade, gene therapy has captured the scientific interest with the purpose to modify gene expression, delivering foreign genes or inhibiting the expression of aberrant proteins expression, for treating hereditary disorders [5]. The challenge of applying genetic medicine in tissue engineering consists in the possibility to regenerate diseased organs or tissues, by the use of genetically corrected undifferentiated cells, in order to direct the regeneration versus normal tissues [6]. Somatic stem cells conserve the capacity of self-renewal and differentiation in cell types of the tissue of origin, under appropriate stimuli. Therefore, the sophisticate development of non-viral gene delivery vectors has been

accompanied with the possibility to transplant genetically modified cells expanded in vitro, or, alternatively, to immobilize growth factors genes in a scaffold matrix, with the aim of acting on local multipotent cells. Tissue regeneration is strictly regulated by the action of growth factors and cytokines and, nowadays, the delivery of signalling molecules has been overcome by a more effective growth factors gene delivery, which counteract the short half-life of signalling proteins and the overall cost needed for reaching a biological effect [7]. *Short interfering RNA* (siRNA) has been also delivered to cells for activating or down-regulating specific downstream pathways [8].

Nanotechnology has enabled, so far, the development of lipid and polymer-based nanoscale devices that, conjugated with nucleic acids, can act as "Trojan horse" vectors, directed to a specific tissue at a distant site from the injection [9]. Prerequisite for injectable devices is nanoparticles stability, effective genetic material condensation, good cellular uptake, tolerance from the immune system and absence of cytotoxicity. In our previous work, we developed acetylated PEI-NPs (AcPEI-NPs), a compelling alternative strategy to PEI-NPs for major biocompatibility and similar transfection efficiency [4]. In this work, we considered the application of AcPEI-NPs in bone regeneration and we investigated their internalization efficiency in human primary osteoblasts and the impact on cellular differentiation and mineralization, for future therapeutic utilization. Cell therapy is a promising alternative to bone autografts, to afford every year more than 500,000 surgical interventions for bone fractures, and bone injuries of surgical, degenerative or traumatic causes [7]. A recent study has developed cationic PEI-pDNA (encoding PDGF-B) complexes, incorporated in a collagen scaffold, to induce osteogenesis. The expression of PDGF-B in bone marrow stromal cells significantly improve cell proliferation and new bone formation [10]. With the purpose of increasing the safety

of PEI delivery system for bone regeneration, we studied AcPEI-NPs internalization in hOB and the effects on cell viability and activity. From our results, we observed that PEI acetylation did not alter the uptake efficiency of NPs, as demonstrated in comparison with PEI-NPs. Deep studies in the uptake mechanism, showed an activation of endocytosis, by non specific clathrin and caveolae mediated pathways and colocalization studies demonstrated the incorporation in endosomes, without final accumulation in lysosomes. This results, together with the absence of cytotoxicity post-transfection, render AcPEI-NPs a promising candidate for gene therapy in bone regeneration. Furthermore, investigations on hOB activity, after transfection with NPs, have suggested a role of PEI acetylation in promoting the early stage of osteoblast differentiation, inducing increased alkaline phosphatase (ALP) activity. Future studies will be focused on the incorporation of therapeutic plasmid genes or small interference RNA (siRNA) for improving bone osteogenesis.

5.3 Materials and methods

Materials

Branched PEI (MW, 25 kDa) and poly(vinyl-alcohol) (PVA) were obtained from Sigma Aldrich (Milan, Italy). D,L-Lactide/Glycolide copolymer (PLGA, PURASORB®, inherent viscosity 0.20 dl/g) was a generous gift from PURAC (Gorinchem, The Netherlands). Details of the synthesis of the PEI-PLGA copolymer, as well its physicochemical properties were previously described [4]. Briefly, copolymer of branched PEI (PEI) or acetylated PEI (AcPEI) with PLGA were prepared using a two-step procedure. First, PLGA was activated by DCC and NHS and, afterwards, the copolymerization was conducted at a PLGA:PEI molar ratio of

3:1. The synthesis of PLGA-PEI copolymer was confirmed by using ^1H NMR analysis.

Acetylated PEI (AcPEI) was obtained as described by N.P. Gabrielson and D.W. Pack, 2006 [11]. To determine the extent of acetylation, each polymer was dissolved in D_2O and ^1H NMR spectra were acquired on a Varian Unity 400 with a 5-mm probe. The extent of primary and secondary amine acetylation was determined by peak integration, using the formula reported by Nathan P. Gabrielson and Daniel W. Pack [11]. Nanoparticles based on PLGA-PEI and AcPEI-PLGA copolymerization were prepared directly from the reaction solution by a simple emulsion procedure. The reaction was stopped after 3 h by ice cooling, and 2 mL of chloroform solution were homogenized with 20 mL of 0.5% PVA aqueous solution by means of an ultrasonic processor. The nanoparticles suspension was stirred at 200 rpm rate for 24 h for chloroform evaporation. The obtained nanospheres were collected by centrifugation in a high speed centrifuge at 16000 rpm for 15 min, carefully washed to remove unreacted PEI with a water/methanol mixture, and then freeze dried. Nanoparticles were stored at 4°C and characterized as previously described [4].

Fluorescent nanoparticles were obtained dissolving 6 mg of Coumarin 6 in aqueous solution, finally added to polymer solution before homogenization.

Before incubation with cells, the nanoparticles were suspended in culture media containing 2% penicillin-streptomycin at a concentration of 10 mg/ml, subjected to sonication in ice for 20 minutes at maximum setting in continuous mode (Branson Sonifier), and sterilized by filtration using $0.45\ \mu\text{m}$ gauge filters (Sartorius Stedim Biotech GmbH, Goettingen, Germany). Nanoparticles eventually entrapped in the filter have been recovered by washing the filter with an equal volume of media, obtaining a final solution of nanoparticles of 5 mg/ml that has been used as stock solution for all *in vitro* tests.

Cell culture

Primary osteoblasts were grown from explants of human trabecular bone fragments from knee joints, isolated during surgery interventions (kindly provided by the Orthopedic Institute, Major Caritas Hospital, Novara, Italy). The osteoblasts (hOB) were cultured in Iscove's modified Dulbecco's medium supplemented with 10% fetal calf serum (Hyclone, USA), 2 mM L-glutamine, and antibiotics for 2–3 weeks. Cells cultured from up of three passages were used for all experiments.

Cellular uptake

After 24 hours of adhesion, cells were incubated for 1 hour with fluorescent labeled nanoparticles at different concentrations, ranging from 10 to 300 $\mu\text{g/ml}$, in order to study the kinetic of uptake. Besides, at fixed concentration of nanoparticles (300 $\mu\text{g/ml}$) time dependent uptake was tested, over a time course ranging from 5 min to 1 hour (37°C, 5% CO_2). After nanoparticles incubation, the cells were washed and detached by trypsinization, centrifuged and resuspended in a 0.4% trypan blue (TB) solution in PBS, to quench the extracellular Coumarin 6 fluorescence [12]. This assay is based on the observation that TB dye, quenching the Coumarin fluorescence of a extracellular particles causes red fluoresce, whereas internalized particles will release green fluorescence. Cells were then centrifuged, the TB solution was removed, the cell pellet was resuspended in PBS, and each sample was analyzed on a laser scanning cytometer FACS Calibur (Beckton Dickinson, NJ, USA), for green and red fluorescence. 10,000 cells were measured in each sample. Furthermore, time-lapse fluorescent microscopy was conducted to confirm the internalization time. Fluorescent and Phase images of viable cells were acquired with Leica DM 2500 microscope system from Leica (Leica Microsystem, Milano, Italy) that included an aqueous immersion objective 63x and an incubation enclosure around on the

microscope stage. This system maintained normal cell culture conditions (37°C, 5% CO₂ atmosphere, 100% relative humidity) and acquired images on a specific region regularly (every 5 min in this study). Human osteoblasts were incubated with the studied nanoparticles at a concentration of 300 µg/ml, throughout 1 hour of experiment. The fluorescence was detected through a BP 515-560 nm excitation filter and images have been acquired using a Leica Q550FW camera and analyzed using Qwin Image Analysis software (Leica, Heidelberg, Germany). Fluorescence images were processed digitally for background fluorescence correction from nanoparticles that remained suspended in the media solutions. Uneven fluorescence excitation was corrected by normalizing all images by a flat field image that was generated by imaging a spatially homogeneous glass filter of 475 nm. Correction for background fluorescence was a simple background intensity subtraction, where the fluorescence intensity attributed to background was determined from cell-free areas (as determined by phase contrast images) within each region of interest. The background fluorescence varied during the different experiments, so the background fluorescence intensity was determined at each point. The total intensity over the whole image was then summed to yield a measurement of the relative accumulation of nanoparticles by cells within the region of interest.

Inhibition studies

To explore different mechanisms of nanoparticles interaction with human osteoblasts and trafficking across the plasma membrane, uptake of PEI-NPs and Ac-PEI-NPs was studied under different blocking conditions (Table 1).

Table 1. Inhibitors and concentrations used for uptake mechanism studies.

Pathway	Inhibitor	Mechanism
Energy dependent processes	4°C	Blocks energy dependent processes
Energy dependent processes	Colchicine (15mM)	Inhibit endocytic processes
Endocytosis	Filipin (1,25 µg/ml)	Specifically inhibits caveolin-mediated endocytosis
Endocytosis	Chlorpromazine (25µM)	Specifically inhibits clathrin-mediated endocytosis

In all cases, cells were incubated with the different inhibitors for 30 min before the addition of the NPs, and then co-incubated with the NPs for 1 h. Untreated cells were used as negative control and cells incubated with NPs at 37°C, without the incubation with inhibitors, as positive control. The fluorescence associated with the Coumarin-NPs inside the cells was measured in a SpectraMAX®M5 multidetection microplate reader at an excitation wavelength of 480 nm and an emission wavelength of 529 nm. Results were expressed as relative fluorescence units (RFU). Each assay was performed five times in triplicate.

Intracellular localization of nanoparticles

After 1 hour of time lapse microscopy, cells were fixed for 30 min with 4% formaldehyde solution in PBS at room temperature, then washed with PBS and stained with the antibodies for RAB5 and LAMP1, to evidence endosomal and/or lysosomal colocalization. Briefly, cells were incubated ON at 4°C with primary antibodies: LAMP1 (20 µg/ml) and RAB5 (2 µg/ml) (Abcam, Cambridge, UK); after PBS washings cells were incubated 1 hour at room temperature with, respectively the Texas Red anti-mouse (Vector Lab, CA USA) secondary antibody used at 3 µg/ml and the IRIS 5-goat anti-mouse (Cyanine Tecnologies, Torino, Italy) secondary antibody used at 2 µg/ml. Dried cells were mounted with an anti-photobleaching

medium (Vector) and observed at confocal microscopy (Leica DM IRE2) at 40x magnification. Images have been acquired after excitation with Argon laser at 488 nm, a Helium-Neon-Green laser excitation at 543 nm and a Helium-Neon-Red laser excitation at 633 nm. Coumarin 6 labeled nanoparticles were shown as green spots at 510 nm emission; Texas RED positive RAB at 620 nm emission and IRIS positive LAMP at 680 nm emission. Images were recorded separately in each fluorescence channel and merged afterwards.

Cytotoxicity tests

Necrosis was evaluated through the quantification of the activity of lactate dehydrogenase (LDH) in culture media of cells cultured 6 hours, 1 day, 3 and 5 days with samples at a final concentration of 300 µg/ml using a detection kit from Roche (Roche Applied Science, Basel, Switzerland). Released LDH catalyzed the oxidation of lactate to pyruvate with simultaneous reduction of NAD⁺ to NADH. The rate of NAD⁺ reduction was directly proportional to LDH activity in the cell medium and was measured as an increase in absorbance at 340 nm. The activity of the LDH enzyme rises when cells are damaged: the LDH activity induced by samples was compared to the effect induced by a toxic agent Triton X100 0.05% in phosphate-buffer saline (PBS) and to non stimulated negative control (CTR-). 5 replicates for each studied concentration were prepared for *in vitro* tests.

Apoptosis has been studied by Western Blot. After exposure to nanoparticles (PEI-NPs and AcPEI-NPs) at 5, 50, and 300 µg/ml for 24 h, cells were lysed in hot buffer (50% H₂O, 25% SDS10%, 25% Tris-HCl pH 6.8), and 20 µg of total proteins in sample buffer (5% β-mercaptoethanol, 0.5% bromophenol blue) were used for SDS-PAGE. Blotted proteins were blocked with 5% free fat dried milk in PBS pH 7.4, for 1 h at room temperature, and incubated overnight with primary antibodies (Bax, Bcl-

2, tubulin and caspase 9, from Calbiochem, Darmstadt, Germany) at a ratio of 1:500 in PBS. After washing 3 times with PBS solution with Tween 20 0.1%, membranes were incubated with secondary anti-mouse or anti-rabbit antibody conjugated with peroxidase (PerkinElmer, Shelton, CT-USA) for 1 h at room temperature. Protein bands were visualized using enhanced chemiluminescence substrate (PerkinElmer) detection reagents in a chemisensitive visualizer (VersaDoc, BioRad, Italy). Tests were performed in triplicate for each experimental condition.

Alkaline phosphatase activity

Alkaline phosphatase activity (APA), was determined by an assay based on the hydrolysis of p-nitrophenylphosphate to p-nitrophenol. hOB seeded in 24-well culture dishes at 2×10^4 cells/well were collected after treatment with three different concentrations of nanoparticles (5, 50 and 300 $\mu\text{g/ml}$), rinsed three times with PBS and lysed with 60 μl of a hot solution composed by 75% H_2O , 2.5% SDS, 10% 25% Tris-HCl pH 6.8. To 50 μl of this solution, 50 μl of substrate (1mM paranitrophenyl-phosphate in 1 M diethanolamine + 1 mM MgCl_2 pH 9.8 all from Sigma) were added. The mixture was incubated 30 min at 37°C and measured on a Bio-Rad micro-plate photo-spectrometer reader at 405 nm (Bio-Rad, Milan, Italy) and results (n=3) expressed in μM p-nitrophenol. Results were normalized per microgram of cell protein. Protein content was measured in cell lysate by Bicinchoninic Acid (BCA) protein assay reagent kit (Pierce Biotechnology, Rockford, IL, USA).

Collagen estimation

hOB collagen synthesis was quantified by a picrosirius dye staining. Cells were previously observed in light microscopy for detecting the presence of collagen, afterwards the samples were eluted with 0.1N NaOH and the absorbance quantified at $\lambda = 540$ nm in a Model 450 microplate reader (Bio–Rad). The collagen concentration of each sample was calculated from the ratio between the absorbance of the samples and a standard curve of collagen at known concentrations. The curve was obtained as follows: calf skin type I collagen (Sigma) was dissolved overnight in 0.2% acetic acid (Sigma) at a concentration of 1 mg/ml. The solution was then diluted from 4 to 0.5 $\mu\text{g}/50$ μL to obtain a standard curve. The 50 μl of collagen standard were plated into a microtiter plate and incubated at 37°C for 16 h (humidified) and then 24 h at 37°C (dry). Wells were washed three times with 200 μL of distilled water, filled with 100 μL of 0.1% Sirius Red F3BA (BDH, Milano, Italy) in saturated picric acid (Sigma) (w/v) and stained for 1 h at room temperature. The plates were washed five times with 200 μL of 10 mM HCl for 10 s per wash and the collagen bound stain was eluted with 200 μL of 0.1M NaOH for 5 min, and read at $\lambda = 540$ nm in a Model 450 microplate reader (Bio–Rad). Data were reported as mean \pm standard deviation of four experiments.

Mineralization

For mineralization assay, cells were seeded at 2×10^4 cells/well in 24-well culture plates. Cells were cultured in growth medium for 1 day and then the medium was changed to calcification medium, containing 10 mM β -glycerophosphate (Sigma) and 50 $\mu\text{g}/\text{ml}$ L-ascorbic acid (Sigma). Samples were treated with nanoparticles at the concentration of 50, 100 and 300 $\mu\text{g}/\text{ml}$. The medium supplemented of nanoparticles was replaced twice a week. As negative control we have used cells

cultured in calcification medium, and as positive control cells cultured in calcification medium stimulated with 10 mM dexamethasone (DEX). On day 24, hOB monolayers were tested for mineralization by calcein staining. Cells were treated overnight at 5% CO₂/95% air at 37°C with culture medium containing 5 µg/ml calcein, then cells were washed 2 times with PBS and examined microscopically using a BP 515-560 excitation filter. Measurement of mineralized nodules formed in culture was determined by acquiring 8 random calcein fluorescence images in fields of 1.0912 µm² in each experiment, which has been repeated 4 times (n=32). Images have been acquired using a Leica Q550FW camera and analyzed using Qwin Image Analysis software (Leica, Heidelberg, Germany).

Osteogenic marker expression by Real Time PCR

Cells were plated at a density of 1x10⁵ cells/well in 6 multiwell plates and cultured for 7 and 21 days with nanoparticles used at 300 µg/ml. Total RNA was isolated using a commercial kit, RNeasy mini kit (Qiagen, Hilden, Germany), according to the manufacturer's instructions. Total RNA was quantified using Nanodrop 2000c spectrophotometer (Thermo Scientific, Wilmington, USA), and 200 ng of total RNA were reverse transcribed (RT) using High-Capacity cDNA Archive Kit in a final volume of 40 µl (Applied Biosystems, Foster City, CA, USA), as described by the manufacturer. The RT thermal cycle was 25°C for 10 min, 37°C for 120 min, 85°C for 5 min and kept at 4°C.

Real-time RT-PCR is considered the gold standard for mRNA quantitative evaluation. mRNA levels were measured by real-time RT-PCR based on TaqMan methodology, using CFX96 Real-Time System C 1000 Thermal Cycler (BioRad, Milano, Italia). Real-time data analysis was performed with BioRad CFX Manager 2.1 software. A reference gene was identified for GAPDH stable expression. Primers

and probe for osteopontin (OPN), osteocalcin (OCN) and receptor activator of NF- κ B ligand (RANKL) mRNA were provided by TaqMan gene expression assay (Applied Biosystems).

Amplification reactions were performed with SSOFast Probes Supermix with ROX (BioRad), using 5 μ l of cDNA in a final volume of 20 μ l. Primers and probes were added to the reaction mixture according to the manufacturer's directions. All reactions were performed in duplicate. Conditions for quantitative real-time PCR were: 2 min denaturing step at 95°C and then 40 cycles of 15 s at 95°C and 1 min at 60°C. Primer specific cloned PCR-products served as positive controls for the PCR, while water was used as negative control. Every set of experiments was carried out with cDNA of the same sample to exactly compare the expression of the different genes of interest. Target gene expression was normalized to GAPDH mRNA expression. Relative differential gene expression was calculated according to [13].

Statistical Analysis

Statistical analysis of data was carried out using the SPSS for Windows software. Multiple comparison of data was performed using one-way analysis of variance (ANOVA), Bonferroni t-test was applied to evaluate differences in the trend of the measured parameters. p value was obtained from the ANOVA table and the conventional 0.05 level was considered to reflect statistical significance.

5.4 Results

Cell uptake, trafficking and intracellular localization of AcPEI-NPs in hOB

AcPEI-NPs were firstly tested for internalization efficiency in human primary osteoblasts (hOB). We investigated the cellular uptake in presence of either AcPEI-NPs and PEI-NPs and we observed that the uptake efficiency was not altered by the acetylation of PEI, as shown in confocal micrographs (Figures 1A and 1B). Although the reduction in zeta-potential, compared with PEI-NPs [4], AcPEI-NPs retained a net positive charge that ensured good transfection efficiency in hOB. The kinetic of hOB internalization with Coumarin-6 loaded nanoparticles, resulted, quantification, concentration and time dependent by flow cytometry (FACS) quantification. We tested 5 different PEI-NPs and AcPEI-NPs concentrations (10 μ g/ml, 25 μ g/ml, 50 μ g/ml, 100 μ g/ml, 300 μ g/ml), showing that the increased uptake was directly proportional to the increased concentration (Figure 1C). In time-laps microscopy we verified that higher nanocomplexes concentration, 300 μ g/ml, reflected faster uptake (2-5 minutes) then lower concentration, 10 μ g/ml, (15-30 minutes). Nanoparticles fluorescent signal, at fixed concentration of 300 μ g/ml, was visible inside the cells as nano-sized dots, within 5 minutes, and increased proportionally into the first 15 minutes, reaching slowly a saturation point at 60 minutes. The whole process can be visualized in a video clip provided as Additional file 1 and confirmed by FACS analysis (Figure1E).

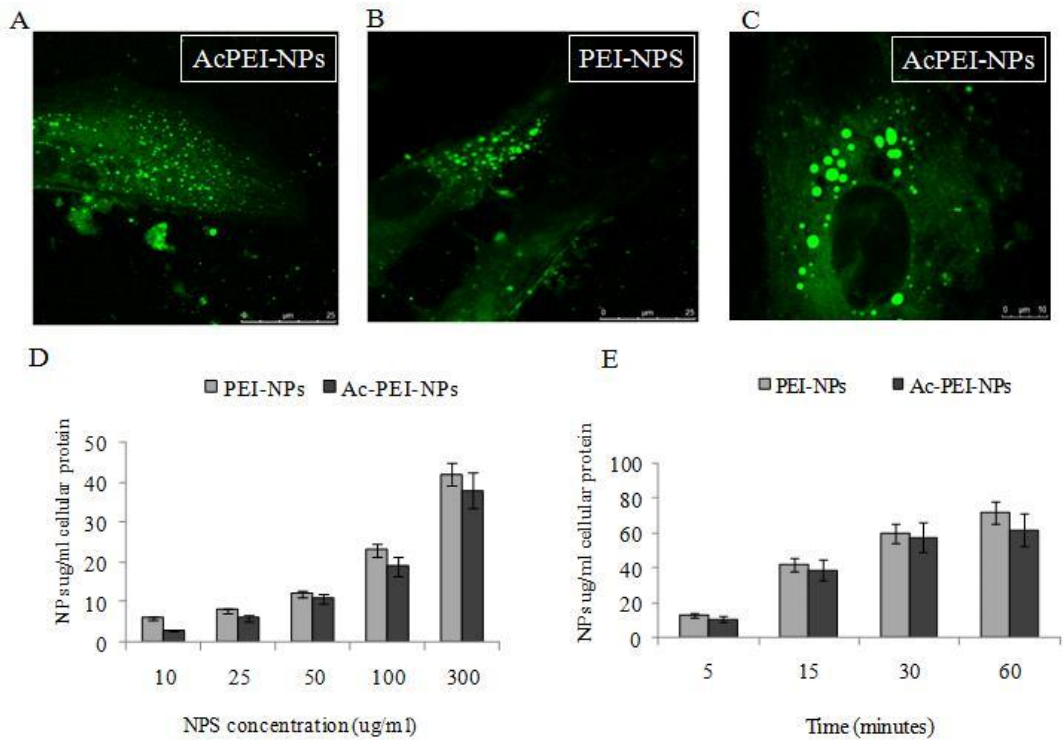


Figure 1. Uptake of Coumarin 6 labeled NPs (1h). PEI-NPs and AcPEI-NPs confocal micrographs showed similar uptake efficiency in human primary osteoblasts, respectively in A and B. Figure 1C shows higher magnification 63x, zoomed 2,5x, of cytoplasmic AcPEI-NPs. Representative images of four replicates are shown. D,E) FACS analysis results, evidencing the kinetic of AcPEI-NPs in comparison with PEI-NPs: *left*, based on the increase in concentrations, *right*, based on different time-points.

Uptake mechanism studies were then developed, in order to understand the intracellular trafficking of AcPEI-NPs. The narrow NPs size profile (105 \pm 1.5 SD) and the hydrophilic composition suggested a role of endocytosis, an energy dependent mechanism. Considering the fast internalization, the inhibition studies were performed with AcPEI-NPs concentration of 300 μ g/ml, with specific inhibitors pre-treatment of clathrin-mediated endocytosis and caveolae-mediated endocytosis

(Figure2). Cell incubation at 4 °C reduced AcPEI-NPs uptake of ~80%, confirming the involvement of an energy dependent process, since low temperature decrease membrane flexibility and selectively block energy dependent processes [14][15]. To understand in details the pathway involved, hOB were incubated with Chlorpromazine (Cpz) a clathrin-mediated endocytosis inhibitor [16] and Filipin III (F III) an inhibitor of caveolae formation [17]. Cpz and F III reduced by ca. 70% and 50%, respectively, intracellular relative fluorescence unit (RFU), and as shown in the quantitative histogram in Figure 2, a synergic inhibitory effect of ~ 95% was observed, when cells were incubated with both Cpz an F III.

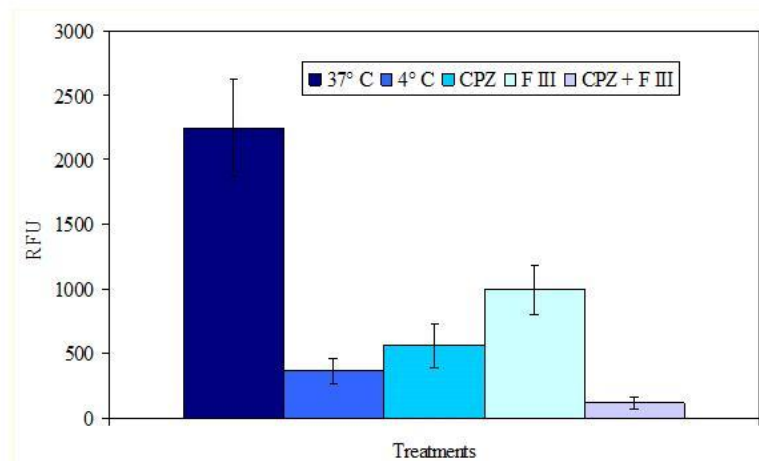
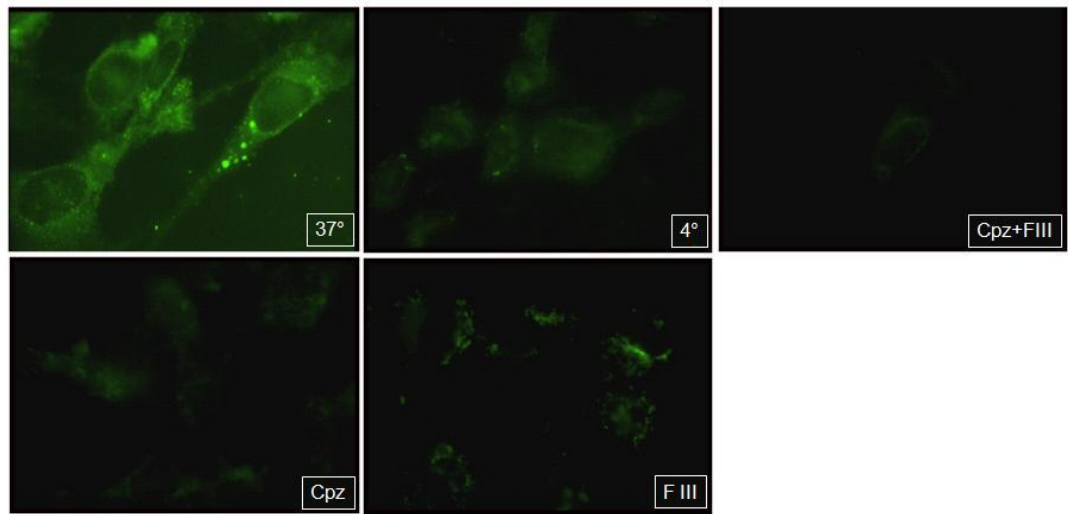


Figure 2. Inhibition studies of AcPEI-Cumarin6-loaded NPs. The uptake was evaluated by densitometry quantification of cell fluorescence in fluorescence microscopy, following inhibitors incubation. Low temperature (4 °C) significantly decreased NPs internalization in human primary osteoblasts, demonstrating the activation of an energy dependent process. Specific inhibitors Chlorpromazine (CPZ) and Filipin III (F III), significantly reduced fluorescent AcPEI-NPs intracellular detection, revealing the activation of both clathrin-dependent and caveolae-dependent endocytosis.

Being aware of the activation of endocytosis in AcPEI-NPs uptake, intracellular localization with specific markers of early endosomes, RAB5 and lysosomes LAMP1 were performed in confocal microscopy by immune-fluorescence assay. Confocal micrographs showed, after transfection of 1 hour, that AcPEI-NPs co-localize with early endosomes (Figure 3A), but not with lysosomes (Figure 3B), confirming an initial incorporation in endosomes, mediated by endocytosis, that in both clathrin-mediated pathway and caveolae-mediated pathway does not conclude in lysosomal degradation. Considering that the final target destination of gene/siRNA delivery is, respectively, nuclear and cytoplasm targeting, endosomes escape is successfully reached by our system. This result is an important conclusive step, that suggest the conserved ability of AcPEI to activate at intracellular level the proton sponge effect and this can explain the maintained successful GFP gene delivery, obtained in our previous work, in endothelial cells.

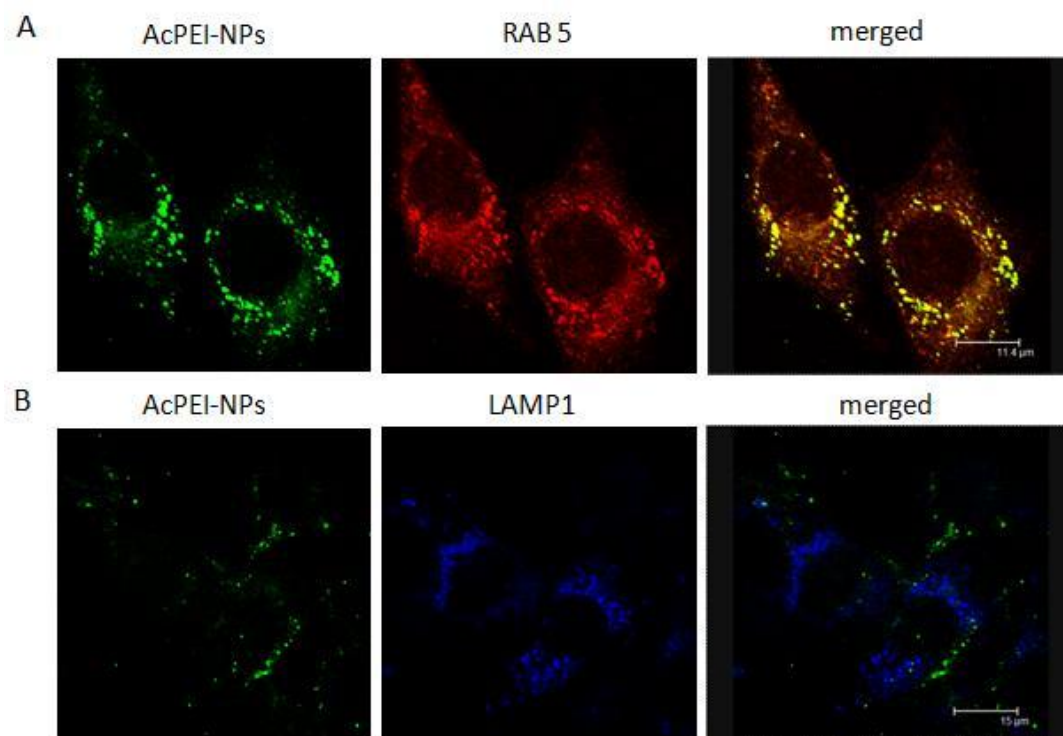


Figure 3. A, B - Confocal microscopy images showing colocalization of AcPEI Coumarin 6 loaded nanoparticles (green) with early endosomes RAB₅⁺(red) and lysosomes LAMP⁺ (blue). Important colocalization with endosomes is shown in A as yellow colocalized dots, while no accumulation in lysosomes has been observed in B.

Cytotoxicity of AcPEI-NPs in hOB

Cell biocompatibility, following nanoparticles transfection, was evaluated in terms of necrosis or apoptosis activation. Lactate dehydrogenase (LDH) activity in cell supernatant revealed that AcPEI, at the highest concentration used (300 μg/ml) does not affect cell membrane integrity and cell viability after long term incubation (5 days), showing levels of LDH activity comparable to the untreated control. Also PEI-NPs did not show any signal of necrosis in cells, as shown in Figure 4.

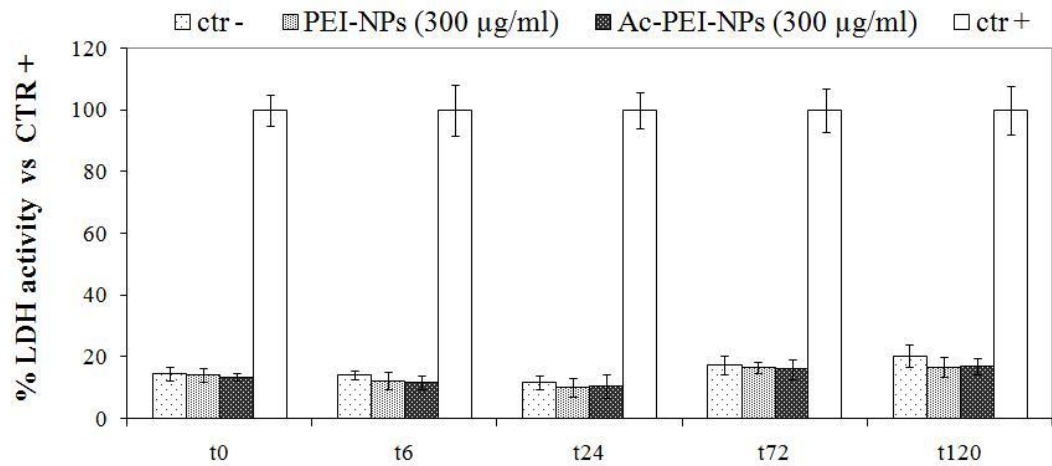


Figure 4. LDH assay of hOB after 6, 24, 72 and 120 hours of exposure to 300 µg/ml of PEI-NPs and AcPEI-NPs. Non transfected control cells were tested in parallel to the treated groups. The results are expressed as percentage of LDH activity values obtained with the positive control, treated with TritonX100 surfactant 0,05%. The results showed at all the time points tested low levels of LDH release from hOB, indicating membrane integrity. The percentage values are representative of mean \pm SD of 5 separate experiments. *Statistically significant compared to control $p < 0.05$.

Likewise, in order to exclude the activation of the programmed cell death (apoptosis), Western blot analyses were performed to quantify the expression of Bax family proteins and Bcl-2 protein levels, calculating the ratio of pro-apoptotic and anti-apoptotic signals in the cells. Caspase9 activation was also tested, knowing that the induction of the stress signalling pathways JNK/SAPK causes release of citochrome C and formation of apoptotic bodies, through the cleavage of the pro-enzyme of caspase-9 into the active form. Figure 5A shows Bax / Bcl-2 ratio that resulted comparable to untreated control for cells treated with AcPEI-NPs, while a little increase in pro-apoptotic balance was observed with 300µg/ml of PEI-NPs. Figure 4B reveals that both nanoparticle formulations do not induce a significant

activation of caspase 9, compared to the positive control stimulated with hydrogen peroxide (H₂O₂).

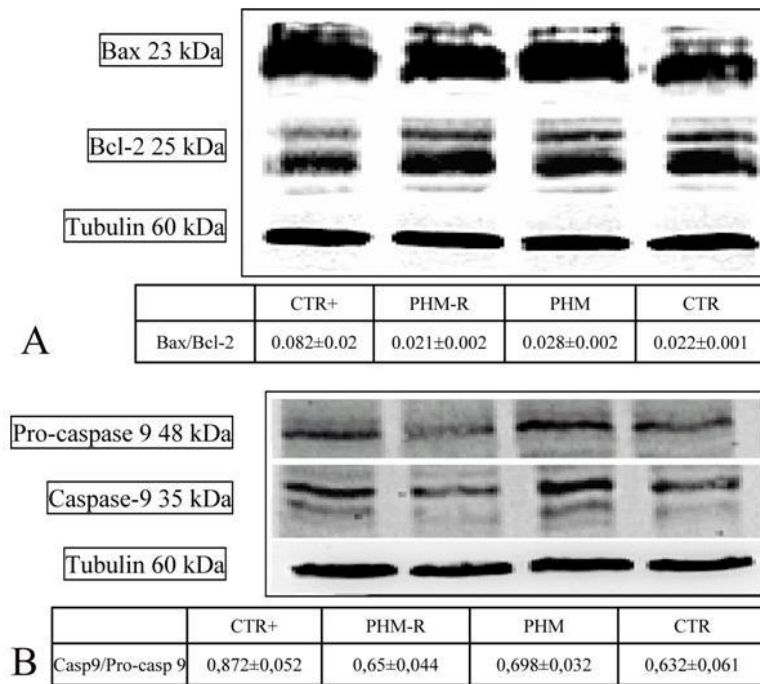


Figure 4. Western blot analysis of Bax and Bcl-2 (A) and of pro-caspase 9 and caspase 9 (C) on untreated cells (CTR), cells treated with H₂O₂, (CTR+) and nanoparticles PEI-NPs and AcPEI-NPs, at the concentration of 300µg/ml. The images are representative of experiments performed in triplicates. B, D) Densitometry measurements were normalized with endogenous tubulin protein expression and indicated as Bax/Bcl2 and pro-caspase9/caspase9 mean values ± SD. No pro-apoptotic index was observed with AcPEI-NPs, while a little increase in the pro-apoptotic balance was observed with PEI-NPs, *statistically significant compared to control p<0.05.

Effects of AcPEI-NPs on hOB differentiation

The impact of AcPEI-NPs on hOB differentiation was investigated by measuring the activity of alkaline phosphatase (ALP), collagen synthesis, mineralization and expression of differentiation markers, like osteopontin (OP), osteocalcin (OC) and

nuclear factor-kappaB ligand (RANKL).

We analyzed first the activity of ALP, that resulted increased, compared to untreated control, at longer incubation time ≥ 8 days, with AcPEI-NPs at concentrations ≥ 50 $\mu\text{g/ml}$. From day 8 to day 24 after transfection, the statistical relevance between AcPEI-NPs at 300 $\mu\text{g/ml}$ and PEI-NPs 300 $\mu\text{g/ml}$ increased (Figure 6). Alkaline phosphatase activity is greatly enhanced in proliferating osteoblasts during bone formation and it is considered an early marker of osteoblast differentiation. ALP interacts with bone collagen matrix and processes pro-collagen to collagen to finally lead to matrix mineralization in vitro [18][19].

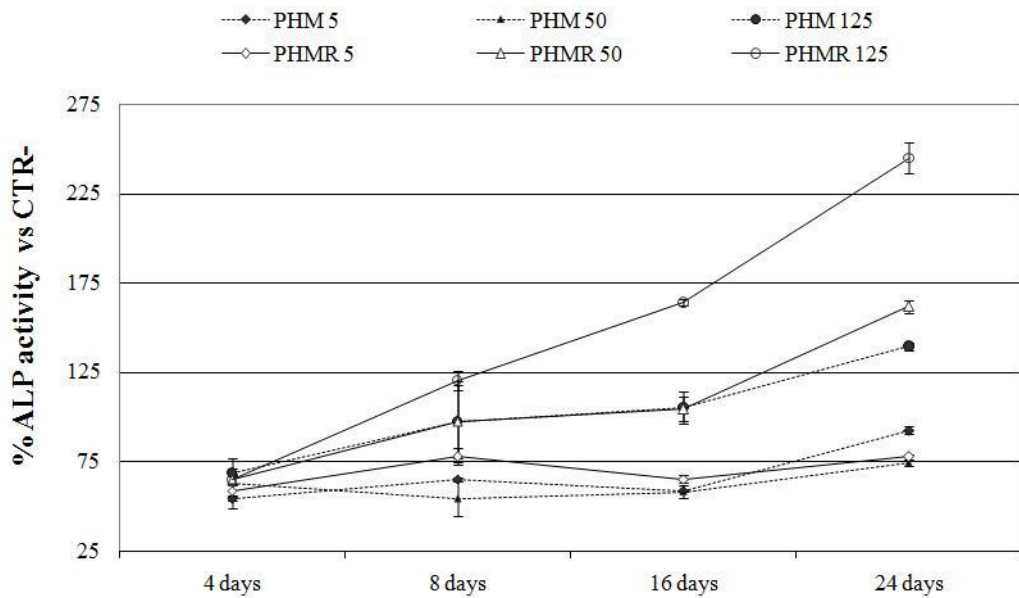


Figure 6 – ALP activity at different time-points and different concentrations of AcPEI-NPs and PEI-NPs. Results are expressed as percentage of p-nitrophenol activity of the negative control, represented by cells without NPs treatment. The calculated value resulted the average of three experiments (mean \pm SD) performed in duplicate for each NPs concentration (5, 50, 300 $\mu\text{g/ml}$) and for each incubation time (4, 8, 16 and 24 days).

Collagen I (COLI) matrix production is another marker of the early stage of osteoblast differentiation and COLI synthesis was, therefore, tested by Sirius red staining, by light microscopy for qualitative evaluation and by spectrophotometry for quantitative measurement. Cells were stimulated for 3 days with PEI-NPs and Ac-PEI-NPs (300 $\mu\text{g/ml}$) and vitamin D₃ (1,25(OH)₂D₃) 10⁻⁸M was used as positive control. 1,25(OH)₂D₃ induced wide areas of bone collagen matrix formation in light microscopy (Figure 7A), compared to the small areas shown in untreated negative control (Figure 7B). The plates stimulated with NPs showed a collagen synthesis comparable to the negative control, with no significant differences between the two NPs formulations (Figure 7C and 7D). The samples, after the elution of the dye, were quantified with the spectrophotometer and the absorbance values confirmed the absence of significant COLI synthesis by NPs (Figure 7E).

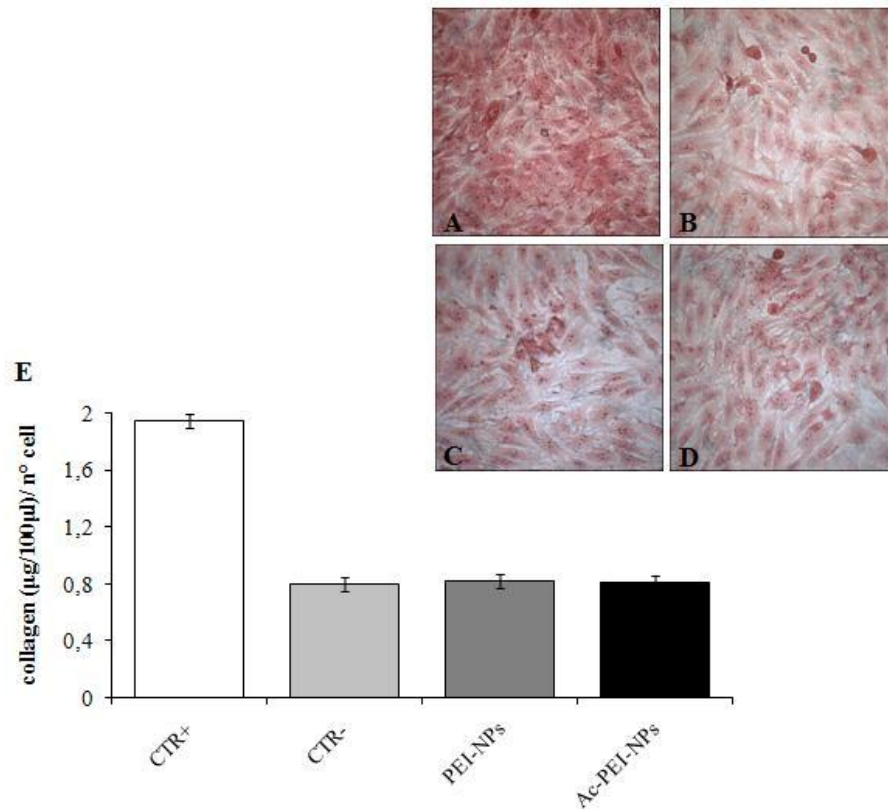


Figure 7. Light microscopy images of hOB stained with Sirius Red. (A) positive control stimulated with $1,25(\text{OH})_2\text{D}_3$ (CTR+); (B) untreated negative control (CTR-), (C) cell stimulated with PEI-NPs or (D) Ac-PEI-NPs. (E) Ratio of quantitative evaluation of Sirius Red staining, normalized for cell density. $1,25(\text{OH})_2\text{D}_3$ resulted significantly increase collagen matrix production $*p < 0.05$, respect to PEI-NPs and Ac-PEI-NPs, which showed comparable collagen production of untreated control.

Latest stages of hOB differentiation were tested in terms of mineralization and specific differentiative markers expression. The effect of NPs in inducing mineralization was measured after NPs incubation of 21 days and results are reported in Figure 8 as percentage of mineralization normalized to negative control, that was considered as 100%. Dexamethasone, a synthetic glucocorticoid involved in the

formation of mineralized bone nodules *in vitro* [20], was used as positive control in the experiment and both nanoparticles have shown comparable calcified matrix of untreated cells.

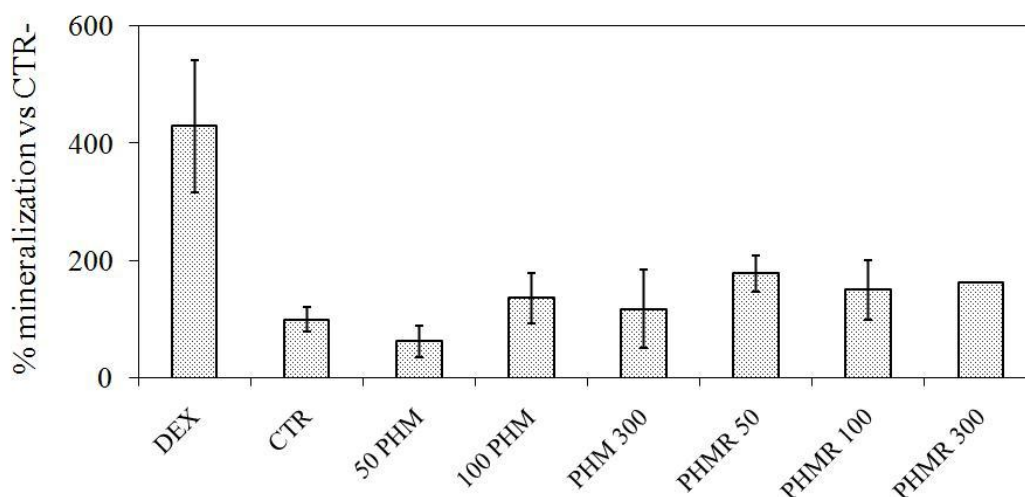


Figure 8. – Quantitative measurements of osteoblast mineralization *in vitro*. Confluent human osteoblasts, cultured with ascorbic acid and β -glycerolphosphate, were treated with different concentrations of the tested nanoparticles PEI-NPs or AcPEI-NPs for 21 days. The formation of mineralized nodules was detected on cells by calcein staining. Photomicrographs were obtained by a digital Leica camera connected to the fluorescence microscope and quantitative analysis of mineralized nodules was performed by measuring the surface of mineralization areas on a computer-assisted image analyzer. Results represent the average \pm standard deviation (SD) of three independent experiments. * $p < 0.01$ vs. negative control.

In order to complete the differentiation studies, real-time PCR was performed to investigate the expression of osteopontin (OPN), a marker for middle stage differentiation, and the expression of osteocalcin (OC), a marker for late stage differentiation. Experiment was conducted at the time-point of 8 days, with hOB treated with PEI-NPs or Ac-PEI-NPs (300 $\mu\text{g/ml}$) and dexamethasone as positive

control (Figure 9). We obtained, accordingly with the mineralization studies, statistically relevant mRNA levels of OPN in cells treated with $1,25(\text{OH})_2\text{D}_3$, ~ 4 times more than the negative control. Nevertheless, the expression of OPN, increased also in cells treated with both NPs types, showing two times higher mRNA than untreated control, without significant differences between the two formulations.

Considering the expression of OC, a protein involved in bone mineralization and calcium homeostasis in the final stage of differentiation, only $1,25(\text{OH})_2\text{D}_3$ demonstrated ability in increasing mRNA expression level, 293 times higher than the negative control (Figure 9B). From our study, therefore, PEI-NPs and Ac-PEI-NPs did not activate the expression of OC.

For last, but not less important, we evaluated the mRNA expression level of RANKL, protein belonging to the superfamily of cytokines, inducing maturation, differentiation and activation of osteoclasts. This protein is produced by mature osteoblasts and induce the differentiation of osteoclasts by a signal transduction pathway, activated by the contact between the secreted RANK-L protein and the receptor on the membrane of osteoclasts. Real time PCR showed that AcPEI-NPs, do not induce RANKL expression, despite a little activation, ~ 2 fold over control, was induced after transfection with PEI-NPs. Cell stimulation with $1,25(\text{OH})_2\text{D}_3$ confirmed that osteoblasts differentiation is accompanied by activation of osteoclasts, showing RANKL mRNA expression levels 16.7 times higher than the negative control, which can interfere with bone regeneration, causing bone disruption (Figure 9).

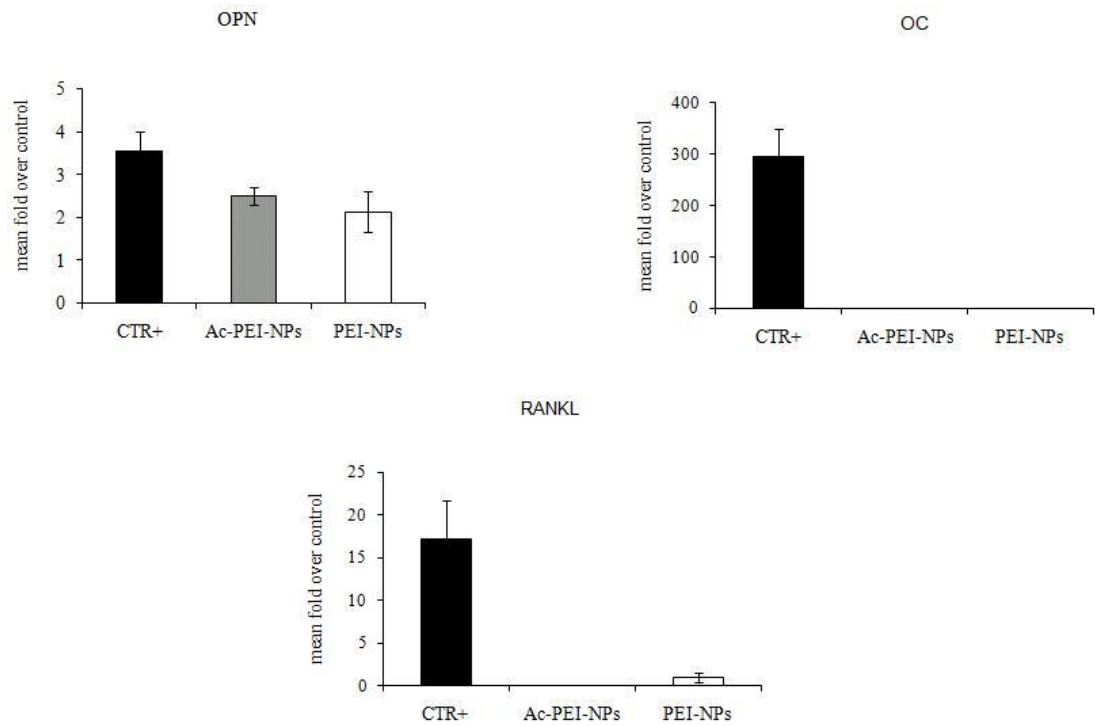


Figure 9. - Real time PCR expression of osteopontin (OPN), osteocalcin (OC) and RANKL in hOB stimulated with PEI-NPs and Ac-PEI-NPs. The results are shown as mRNA quantification level, expressed as fold over untreated control, for the markers of differentiation tested: A) OPN; B) OC; C) RANKL. 1,25(OH)2D3 has been used as positive control.

5.5 References

- [1] A. Kwok and S. L. Hart, “Comparative structural and functional studies of nanoparticle formulations for DNA and siRNA delivery,” *Nanomedicine*, vol. 7, no. 2, pp. 210–9, Apr. 2011.
- [2] V. Kafil and Y. Omid, “Cytotoxic impacts of linear and branched polyethylenimine nanostructures in A431 cells,” *Bioimpacts*, vol. 1, no. 1, pp. 23–30, Jan. 2011.
- [3] L. Parhamifar, A. K. Larsen, a. C. Hunter, T. L. Andresen, and S. M. Moghimi, “Polycation cytotoxicity: a delicate matter for nucleic acid therapy—focus on polyethylenimine,” *Soft Matter*, vol. 6, no. 17, p. 4001, 2010.
- [4] A. Calarco, M. Bosetti, S. Margarucci, L. Fusaro, E. Nicolì, O. Petillo, M. Cannas, U. Galderisi, and G. Peluso, “The genotoxicity of PEI-based nanoparticles is reduced by acetylation of polyethylenimine amines in human primary cells,” *Toxicol. Lett.*, vol. 218, no. 1, pp. 10–7, Mar. 2013.
- [5] S. Misra, “Human gene therapy: a brief overview of the genetic revolution,” *J. Assoc. Physicians India*, vol. 61, no. 2, pp. 127–33, Feb. 2013.
- [6] T. P. O’Connor and R. G. Crystal, “Genetic medicines: treatment strategies for hereditary disorders,” *Nat. Rev. Genet.*, vol. 7, no. 4, pp. 261–76, Apr. 2006.
- [7] T. N. Vo, F. K. Kasper, and A. G. Mikos, “Strategies for controlled delivery of growth factors and cells for bone regeneration,” *Adv. Drug Deliv. Rev.*, vol. 64, no. 12, pp. 1292–309, Sep. 2012.
- [8] C. N. Rios, R. J. Skoracki, and A. B. Mathur, “GNAS1 and PHD2 short-interfering RNA support bone regeneration in vitro and in an in vivo sheep model,” *Clin. Orthop. Relat. Res.*, vol. 470, no. 9, pp. 2541–53, Sep. 2012.
- [9] W. Wang, W. Li, N. Ma, and G. Steinhoff, “Non-Viral Gene Delivery Methods,” *Curr. Pharm. Biotechnol.*, vol. 14, no. 1, pp. 46–60, Jan. 2013.
- [10] S. Elangovan, S. R. D’Mello, L. Hong, R. D. Ross, C. Allamargot, D. V Dawson, C. M. Stanford, G. K. Johnson, D. R. Sumner, and A. K. Salem, “The enhancement of bone regeneration by gene activated matrix encoding for platelet derived growth factor,” *Biomaterials*, vol. 35, no. 2, pp. 737–47, Jan. 2014.
- [11] Gabrielson, N.P., Pack, D.W., 2006. Acetylation of polyethylenimine enhances gene delivery via weakened polymer/DNA interactions. *Biomacromolecules* 7, 2427–2435.

- [12] Hu, K., Shi, Y., Jiang, W., Han, J., Huang, S., Jiang, X., 2011. Lactoferrin conjugated PEG-PLGA nanoparticles for brain delivery: preparation, characterization and efficacy in Parkinson's disease. *International Journal of Pharmaceutics* 415, 273–283.
- [13] K. J. Livak and T. D. Schmittgen, "Analysis of relative gene expression data using real-time quantitative PCR and the 2(-Delta Delta C(T)) Method.," *Methods*, vol. 25, no. 4, pp. 402–8, Dec. 2001.
- [14] Kessner S, Krause A, Rothe U, Bendas G, Investigations of the cellular uptake of E-Selectin-targeted immunoliposomes by activated human endothelial cells. *Biochim Biophys Acta* 2001; 1514:177-90
- [15] Piasek A, Thyberg J. Effects of colchicine on endocytosis of horseradish peroxidase by rat peritoneal macrophages. *J cell Sci* 1980; 45:59-71.
- [16] Schnitzer JE, Oh P, Pinney E, Allard J. Filipin-sensitive caveolae mediated transport in endothelium: reduced transcytosis, scavenger endocytosis and capillary permeability of select macromolecules. *J Cell Biol* 1994; 127:1217-32
- [17] Wang LH, Rothberg KG, Anderson RG. Mis-assembly of clathrin lattices on endosomes reveals a regulatory switch for coated pit formation. *J Cell Biol* 1993; 123:1107-17.
- [18] E. E. Golub and K. Boesze-Battaglia, "The role of alkaline phosphatase in mineralization," *Curr. Opin. Orthop.*, vol. 18, no. 5, pp. 444–448, Sep. 2007.
- [19] Y. Sugawara, K. Suzuki, M. Koshikawa, M. Ando, and J. Iida, "Necessity of Enzymatic Activity of Alkaline Phosphatase for Mineralization of Osteoblastic Cells," *Jpn. J. Pharmacol.*, vol. 88, no. 3, pp. 262–269, 2002.
- [20] Y. Mikami, K. Omoteyama, S. Kato, and M. Takagi, "Inductive effects of dexamethasone on the mineralization and the osteoblastic gene expressions in mature osteoblast-like ROS17/2.8 cells.," *Biochem. Biophys. Res. Commun.*, vol. 362, no. 2, pp. 368–73, Oct. 2007.

6 Conclusions

Gene therapy, through the delivery of foreign genes or antisense oligonucleotides to inhibit the expression of an endogenous protein, is a promising approach and in some cases the only alternative to cure hereditary monogenic diseases, viral infections and cancer. This work was focused in improving polyethylenimine (PEI)-based nanocarriers, considering the unique capability of PEI in nucleic acids complexation and delivery to cells, avoiding lysosomal degradation. The polymer structure, rich in positive charged amino groups, allows the efficient electrostatic interactions with the phosphate groups of DNA/siRNA and regulate the attraction to the cellular membrane for nanoparticles internalization. The disadvantage of PEI, as widely known, is the cellular cytotoxicity that is also linked to the high density of positive charges and the non biodegradability, limiting its utilization *in vivo* for aggregation with erythrocytes and serum proteins and immune system activation. The genotoxicity of nanomaterials is often neglected, but of fundamental importance for the large use of nanomaterials in cosmetic products, orthopedic implants and drugs and nucleic acids delivery systems. Although the extensive use of PEI as gene delivery agent, the genotoxicity of the polymer has not been deeply investigated so far. In our work we conducted an extensive study of the toxicity of PEI nanoparticles, focusing on cytotoxicity, genotoxicity and immunotoxicity, being aware of DNA aberrations and mutations that can lead to carcinogenesis. The genotoxic effect of PEI resulted particularly relevant with induction of DNA fragmentation and oxidization of DNA bases, sister chromatide exchange and micronuclei formation. Revising the literature, it is known that nanoparticles can cause direct or indirect DNA damage. Direct contact with the genome is mainly

regulated by the nuclear pore sizes and nanoparticles of 100 nm are considered too big to cause a direct alteration of the genome. Rather, an indirect DNA damage mediated by oxidative stress in cells was investigated. Radical oxygen species (ROS) are known to cause indirect DNA strand breaks, sister chromatid exchange and mutations, thereby the observed increase in the production of radical oxygen species (ROS) by cells transfected with PEI-NPs suggested a role of ROS in mediating genotoxicity. Immune system activation resulted negligible considering the release of pro-inflammatory cytokines, but peripheral monocytes, activated by the exposure with PEI-NPs, resulted enhancing the levels of ROS, which can contribute to the oxidative stress in cells. In order to improve PEI gene delivery system, we firstly developed an alternative nanoparticles formulation, preserving the copolymerization with PLGA, where PEI backbone was modified with acetylation of 50% of the amino groups. The new formulation AcPEI-NPs resulted a compelling alternative of PEI-NPs, able to reduce cytotoxicity, genotoxicity and immunotoxicity of unmodified PEI, maintaining unaltered transfection and gene expression efficiency in cells. AcPEI, from our study, formed nanoparticles of comparable size of unmodified PEI and the reduction in zeta potential did not affect the capacity of condensing plasmid into polyplexes and the uptake efficiency in endothelial cells and osteoblasts. Moreover, gene delivery efficiency, evaluated through GFP expression in endothelial cells, resulted increased with AcPEI-NPs.

The uptake mechanism in cells was studied in order to understand the intracellular trafficking of NPs. Specific inhibition of NPs uptake at 4°C indicated the activation of endocytosis, and inhibition studies with specific inhibitors demonstrated the involvement of either clathrin mediated pathway and caveolae mediated pathway. Intracellular trafficking of nanoparticles is an important feature to establish: for instance, involvement of endosomes requires nanoparticles escape from these

structures in the cytoplasm for gene therapy purpose. More in details in our study, AcPEI-NPs colocalized with early endosomes, but absence of accumulation in lysosomes was observed. This evidence could be correlated with unaltered ability of PEI to activate the “proton sponge” effect that leads to endosomes escape. After having demonstrated the higher biocompatibility of AcPEI-NPs with conserved capacity of cellular transfection, we investigated the possibility to utilize AcPEI-NPs to transfect human primary osteoblasts for future application in gene and siRNA delivery, to promote bone regeneration and/or inhibiting ossification of blood vessels *in vivo*. In particular, we tested in comparison the effect of AcPEI-NPs and PEI-NPs on osteoblast differentiation and mineralization, to evaluate a possible effect of PEI acetylation. We observed that AcPEI-NPs significantly improved ALP activity, early marker of osteoblast differentiation, rather than PEI-NPs, but further investigations demonstrated that the latest stages of the differentiation process are not induced by nude NPs. Future applications, a part the delivery of known growth factors genes, as BMPs for bone regeneration, are directed to inhibit the calcification of vasculature that occurs in diseased conditions, as atherosclerosis. The idea is to develop with AcPEI-NPs a novel therapeutic approach to prevent, stabilize or reverse ectopic arterial calcifications, based on specific siRNA delivery directed to cells of the vasculature wall (such as smooth muscle and endothelial cells). The nanoparticles will be tested with traditional cell culture assay *in vitro* and atherosclerotic dynamic model *ex vivo*.

We created, subsequently, a second nano-formulation based on bPEI, trying to improve the targeting and the efficiency of the system in the delivery of siRNA. Serum proteins have been recently discovered to serve as endogenous targeting ligand and for increasing nanoparticles circulation, after injection. For example,

apolipoprotein A-I, a component of the high density lipoprotein (HDL), can be assembled with liposomes to address siRNA delivery to the liver, through specific receptor-mediated internalization in hepatocytes.

In this study, we have considered a possible use of human serum albumin (HSA) to complex with pre-formed bPEI-siRNA complexes, to improve the targeting to tumors, for anti-cancer application. Evidences have demonstrated that albumin accumulates in tumors by the enhanced permeability and retention (EPR) effect and a specific trans-endothelial transportation, and is a promising candidate as a carrier for anti-cancer drugs. Abraxane®, an albumin conjugated nanoparticle have already demonstrated the role of albumin in enhancing delivery and efficiency of paclitaxel in breast metastatic cancer *in vivo*.

In our system, electrostatic forces regulated the interaction of HSA with the polyplexes, forming a ternary complex. The incorporation of HSA resulted clear for the dramatic increase in size of the complexes, about 10 times more of the 80-90 nm of bPEI-siRNA polyplexes, but despite of the submicron size, the ternary complex resulted more efficient in siRNA uptake and gene silencing in endothelial and epithelial breast cancer tumor cells. Smooth association of smaller polyplexes, mediated by albumin, is a possible reason of the increased amount of intracellular siRNA, resulted important for activating the RNAi mechanism. From our study, it is evidenced an important correlation between uptake efficiency and Turbo-GFP silencing in cells. HSA-bPEI-siRNA complexes, being internalized by cells more efficiently than bPEI-siRNA, resulted able to activate the RNA interference (RNAi) pathway. The low gene silencing of unmodified polyplexes can be attributed to the inefficient siRNA internalization.

The study of the uptake mechanism of the complexes was conducted with special inhibitors of clathrin and caveolae mediated endocytosis and revealed a major

activation of caveolae mediated pathway, the same pathway involved in albumin uptake in endothelial cells. Speculations of Abraxane® effectiveness suggested a specific receptor caveolae-mediated mechanism, enhanced by albumin in tumor microenvironment, but the mechanism is still partly unclear. From literature, gp60 receptor, in caveolae structures, has been demonstrated to mediate albumin transcytosis through endothelial cells and the extracellular protein SPARC seems to be involved in the uptake in tumor cells. Our study clarified that also breast metastatic cancer cells internalized the complexes by caveolae, giving that MDR cells and endothelial cells are known to overexpress caveolae. To investigate more in detail a specific role of HSA in the uptake of the ternary complex, we carried out studies in presence of excess of albumin, as in FBS complete medium, and BSA resulted competing with the internalization of the complexes. Furthermore, the substitution of HSA with BSA in the ternary complex, in serum-free medium transfection, reduced the efficiency of uptake.

The role of HSA in improving the efficiency of PEI-siRNA polyplexes is therefore clear and the system resulted a promising strategy for the delivery of siRNA for *in vitro* studies. The knockdown efficiency, similar to lipoplexes formed with Lipofectamine2000, was exceeded by HSA-bPEI-siRNA increase in cell viability after transfection. However, no contribution in cell viability was conferred to PEI-siRNA polyplexes, despite the high difference in siRNA delivery.

Therefore, HSA-PEI-siRNA polyplexes resulted to be an efficient transfection agent in epithelial cancer cells and endothelial cells, but the application *in vivo* could be limited by the uptake competition with HSA and the big size profile of the complexes.

Further studies could be direct to elucidate the role of albumin as targeting molecule, investigating, for example, the involvement of the receptor gp60 in the uptake of the

ternary complex, being aware that HSA could also offer the advantage of immune tolerance and increased bloodstream circulation half-life to nanocomplexes.

Concluding, this thesis offers some line of research, from reduction of cytotoxicity to improvement of cell targeting of nanocarriers, and some interesting results that can encourage further studies in optimizing DNA/siRNA delivery systems to be utilized for gene therapy.

List of publications

M. Bosetti, L. Fusaro, **E. Nicolì**, A. Borrone, S. Aprile, M. Cannas “PLLA-modified scaffolds for osteoinduction and osteoconduction”, *J Biomed Mater Res A*. Oct;102(10):3531-9 (2014).

M. Bosetti, L. Fusaro, A. Borrone, **E. Nicolì**, M. Cannas "Injectable bone-graft substitute for in vivo tissue regeneration" *Italian Journal of Anatomy and Embriology* 118(2):33 (2013).

M. Bosetti, M. Sabbatini, L. Fusaro, **E. Nicolì**, M. Cannas. “Effects and differentiation activity of IGF-I, IGF-II, insulin and preptin on human primary bone cells” *Growth Factors*, 31(2):57-65 (2013).

A. Calarco, M. Bosetti, S. Margarucci, L. Fusaro, **E. Nicolì**, O. Petillo, M. Cannas, U. Galderisi, G. Peluso, “The genotoxicity of PEI-based nanoparticles is reduced by acetylation of polyethylenimine amines in human primary cells” *Toxicology Letters*, 218:10-17 (2013).

Publications in progress:

Elena Nicolì, M. Isabel Syga, V. Prasad Shastri. “Human serum albumin (HSA) increases siRNA delivery efficiency by complexation with polyethylenimine-siRNA polyplexes”. *PLOS ONE*, Submitted November 2014.

M. I. Syga, **E. Nicolì**, E. Kohler, V. Prasad Shastri. “Albumin-based ternary polyplexes enhanced gene delivery into epithelial cells by formation sequence”. In progress to *PLOS ONE*.

M. Bosetti, M Sabbatini, **E. Nicolì**, A. Borrone, L. Fusaro, M. Cannas “A flow perfusion bioreactor maintain ex vivo human tissue viability: an alternative model to animals to study biocompatibility” in progress for Cells Tissues Organs

Bosetti Michela, **Nicolì Elena**, Calarco Anna, Peluso Gianfranco, Fusaro Luca, Cannas Mario. “Biocompatible cationic nanoparticles for gene delivery in bone tissue engineering: uptake trafficking, localization and activity in human primary osteoblasts” in progress for Tissue Engineering.

Nele Teske, **Elena Nicolì**, V. Prasad Shastri. “Heparin-functionalized polyester nanoparticles for cancer cell targeting”.

Conferences:

Elena Nicolì, V. Prasad Shastri.

“Albumin-polyethylenimine-siRNA nanocomplexes for improving siRNA delivery efficiency”. 26.05.14-30.05.14 E-MRS 2014 SPRING MEETING, Lille (France). Abstract book p.N-14.

Bosetti, L. Fusaro, A. Borrone, **E. Nicolì**, M. Cannas “PLLA-modified scaffolds for osteoinduction and osteoconduction”. 20.09.13-22.09.13. 67° Meeting of the Italian Society of Anatomy and Histology, Brescia.

E. Nicolì, M. Bosetti, F. Boccafoschi, A. Calarco, L. Fusaro, G. Peluso, M. Cannas. “Nanotoxicity of PEI-based nanoparticles is reduced by acetylation of polyethylenimine amines in human primary cells”. 18.06.12-20.06.12 National Congress of Biomaterials 2012 (SIB), Lecce (Italy). Abstract book p.40.

Acknowledgements

I would like to gratefully thank my PhD advisor Prof.ssa Michela Bosetti for the possibility to undertake my PhD in the University of Eastern Piedmont, Novara, Italy, for believing me, for revising my thesis and for the working experience I made in the laboratory of Human Anatomy. I am grateful to Compagnia San Paolo for supporting my PhD fellowship and the University of Eastern Piedmont, Prof. Bosetti e Prof. Rizzi for the possibility to spend large part of my PhD in the Institute of Macromolecular Chemistry, Hermann-Staudinger-Haus, University of Freiburg, Germany.

I am thankful to Prof. Shastri for having welcomed me in his laboratory and for being my second advisor, giving me the possibility to develop my own project, supporting my work and following me in the paper writing step by step, with important teachings.

Furthermore, I want to thank technicians, PhD students and Post-docs part of the “Shastri lab” for being a great team to work and for the help in the laboratory. In particular special thanks to Jon Christensen, mentor and teacher of the Bio-Lab, Julia Voigt, Esther Kohler, Shengnan Xiang, Surya Lamichhane, Neha Arya and Nele Teske for sharing working experience with me, inspiring scientific discussions and being good friends.

In the end, I am thankful to my family, in particular my parents Amedeo Nicolì and Laura Pernisco, for being always present with their support, and my sister Valentina Nicolì and my friends Amanda Passadore, Alessandra Ilaria Borra, Alessia Borrone,

Charlotte Häming, Ruth Weber and Anja Lüttmann for being with me during this important and constructive experience.